

Forschungszentrum Karlsruhe
Technik und Umwelt

Wissenschaftliche Berichte
FZKA 5616

Mechanisms for Two Phase Flow in Porous Media

G. Weber

Institut für Angewandte Informatik

Juli 1995

Forschungszentrum Karlsruhe

Technik und Umwelt

Wissenschaftliche Berichte

FZKA 5616

**Mechanisms for Two Phase Flow
in Porous Media**

G. Weber

Institut für Angewandte Informatik

Forschungszentrum Karlsruhe GmbH, Karlsruhe

1995

Als Manuskript gedruckt
Für diesen Bericht behalten wir uns alle Rechte vor

Forschungszentrum Karlsruhe GmbH
Postfach 3640, 76021 Karlsruhe

ISSN 0947-8620

www.fzka.de

A B S T R A C T
=====

For a better understanding of transport mechanisms in soil for a system with two phases of immiscible liquids the physics of porous media gives again important contributions. In this report, the considerations mainly concentrate on horizontal transport. Our approach is based on the similarity solution of the transport equation which reduces a given nonlinear partial differential equation (PDE) to an ordinary differential equation (ODE). It can be seen, how dimensionless similarity solutions of the ODE depend, in addition to the similarity variable, on two parameters:

- the capillary number N_c , giving the ratio of capillary forces and viscous forces, and
- the ratio of the viscosities of the two liquid phases.

It is shown, under which conditions different mechanisms of transport are to be expected, such as

- a completely stable displacement or
- an unstable displacement, related to viscous fingering (DLA, Diffusion Limited Aggregation) or to capillary fingering (IP, Invasion Percolation).

These mechanisms are also strongly dependent on certain critical exponents (characteristic for DLA or IP). These relations are discussed in our report. Again, for some regions of saturation, mechanisms of displacement are either clearly dominated

- by imbibition (e.g. water pushing oil) or
- by drain (e.g. oil pushing water).

Some of the results are also transformed again from the similarity solution of the ODE to a solution of the PDE (with space- and time coordinates). It is seen, that even with this somewhat simplified approach, we obtain a considerable spectrum of mechanisms.

Transportmechanismen für 2-Phasensysteme in Porösen Medien

K U R Z F A S S U N G

Zu einem besseren Verständnis der Transportmechanismen im Boden für ein System aus zwei Phasen mit nichtmischbaren Flüssigkeiten ist die Physik Poröser Medien auch hier von großer Bedeutung. Im vorliegenden Bericht wird insbesondere horizontaler Transport untersucht. Unser Vorgehen basiert auf einer Ähnlichkeitslösung der Transportgleichung, wobei eine nichtlineare partielle Differentialgleichung (PDG) zu einer gewöhnlichen Differentialgleichung (DGL) reduziert wird. Es zeigt sich dabei, wie eine dimensionslose Ähnlichkeitslösung der gewöhnlichen DGL, neben der Ähnlichkeitsvariablen von zwei Parametern abhängt:

- der Kapillarzah N_c , die das Verhältnis von kapillaren Kräften und viskosen Kräften angibt, und
- dem Verhältnis der Viskositäten der beiden flüssigen Phasen.

Es wird gezeigt, unter welchen Bedingungen verschiedene Transportmechanismen zu erwarten sind, nämlich

- eine völlig stabile Verdrängung oder
- eine instabile Verdrängung, die zum viskosen Fingern gehört, (DLA, Diffusion Limited Aggregation) oder die zum kapillaren Fingern gehört (IP, Invasions-Perkolation).

Diese Mechanismen hängen eng mit bestimmten kritischen Exponenten zusammen (die für DLA oder IP und Perkolation charakteristisch sind). Diese Beziehungen werden in unserem Bericht diskutiert.

Weiterhin gibt es in verschiedenen Bereichen der Sättigung bestimmte Verdrängungsmechanismen, die entweder klar mit

- Imbibition (e.g. Wasser verdrängt Öl) oder
- Drainage (e.g. Öl verdrängt Wasser) zusammenhängen.

Einige unserer Resultate werden auch wieder von der Ähnlichkeitslösung der gewöhnlichen DGL zu einer normalen Lösung der PDG zurücktransformiert (mit Raum- und Zeitkoordinaten). Man sieht hier, daß bereits mit vereinfachten Modellen ein reiches Spektrum von Mechanismen auftritt.

MECHANISMS FOR TWO PHASE FLOW IN POROUS MEDIA

CONTENTS

<u>1. Transport of two phases in a porous medium</u>	7
1.1 Introduction	7
1.2 Modelling by physics of porous media	7
1.3 Basic steps for a 1-dimensional displacement	7
1.4 Interpretation of the solution	8
1.5 Structure of the report	8
1.6 A few remarks on application	10
<u>2. 2-dimensional Flow</u>	11
2.1 A model of the Hele-Shaw-Cell	11
2.2 Dimensionless quantities	12
2.3 Steady state solutions and fingers	15
2.4 Capillary number	17
<u>3 Different types of transport</u>	22
3.1 Criteria for different mechanisms	22
3.2 Formation of viscous fingers	25
3.3 A phase diagram showing different mechanisms	30
<u>4. Evaluation of two phase flow in a porous medium</u>	33
4.1 Basic equations	33
4.2 Continuity equations	34
4.3 Continuity and Darcy-law	35
4.4 Dimensionless considerations	37

4.5 Similarity variables	39
4.6 Analytic solution	41
4.7 Further results related to simliarity transform	42
<u>5. A first characteristics for transport</u>	43
5.1 Introduction	43
5.2 Figures and tables	43
5.3 Interpretation of the results	44
5.4 Some 3-dimensional representations for $f(c_i, N_c)$	45
<u>6. A further characteristic for transport</u>	60
6.1 Continuity equations and flux	60
6.2 Interpretation of flux curve $J(S; t, N_c)$	62
6.3 Some details of J_s -flux curve	65
6.4 Interpretation of various conditions of flow	66
6.5 Figures and tables	73
6.6 Interpretation of the results	73
<u>7. Change from similarity solution to saturation</u>	86
7.1 Introduction	86
7.2 The transformation of the similarity solution	86
7.3 Figures and tables for saturation $S(x, t)$	87
7.4 Limits of similarity solution (short time behavior)	88
<u>8. Solutions for different parameters</u>	106
8.1 Introduction	106
8.2 Exponents m, n larger than 1	106

8.3 Exponents m, n smaller than 1	107
8.4 Considerations for parameters	108
<u>CONCLUSIONS</u>	123
<u>APPENDICES</u>	
<u>A1 Similarity methods for partial differential equations</u>	125
A1.1 Introduction	125
A1.2 Similarity method	125
A1.3 Steps for similarity solution	125
<u>A2 From continuity equation to similarity solution</u>	128
A2.1 Introduction	128
A2.2 A generalized interpretation of fractional flow	128
A2.3 Transformation of the continuity equation	129
<u>A3 Transitions between different mechanisms</u>	131
A3.1 Basic considerations for transitions	131
A3.2 A classification of transitions	131
A3.3 Critical exponents for percolation	133
A3.4 Introduction of correlation length	133
A3.5 Calculation of correlation length	135
A3.6 A line which includes the cluster: the hull	136
A3.7 Some considerations of porous media	136
A3.8 Boundaries for mechanisms	142
A3.9 Generalization and some limits of the model	144

<u>A4 Relations of permeability and saturation</u>	149
A4.1 Introduction	149
A4.2 A few concepts from percolation	149
A4.3 Mass and fractal dimension D_f	149
A4.4 Saturation and polynomial laws	151
A4.5 Relation to permeability	152
<u>A5 Remarks on programs for analytic solutions</u>	153
A5.1 Introduction	153
A5.2 Similarity solution and flux curve	154
<u>A6 Check of the behavior of the similarity solution</u>	157
A6.1 Analytic form of the similarity solution	157
A6.2 Partial derivative with regard to x	158
A6.3 Partial derivative with regard to nc	158
REFERENCES	160

1. Transport of two Phases in a Porous Medium

=====

1.1 Introduction

The main topic of this report is a better understanding of the behavior of a system of two phases in a porous medium. Since the knowledge of the behavior of such systems (e.g. of oil and water in soil) is of importance for the ecology in a country with fast increasing industry, this type of research gives an important insight.

For the understanding of such a 2-phase system in soil, the physics of porous media will give important contributions. An important step to the understanding of such systems is the scientific research on mechanisms of transport which will be detailed now.

1.2 Modelling by Physics of Porous Media

By means of some basic concepts of the physics of porous media a transport equation is obtained (nonlinear partial differential equation (PDE)), with coefficients which are in general not constant).

This equation describes the displacement of a liquid (defender) by another liquid (invader) in a porous medium. It is known, that frequently modelling by porous media is successful for analyzing the transport of contaminants in soil.

For our purpose, it is useful, to divide the problem into two subproblems:

- (a) Simple porous media with a 1-dimensional displacement.
- (b) More complex porous media (which are closer to reality but require a PDE with nonconstant coefficients and boundary conditions related to a 2- or 3-dimensional displacement.

We mainly concentrate on subproblrm (a) in this report.

1.3 Basic steps for a 1-dimensional displacement

(1) Choice of model

Using the transport equation mentioned for (a) (which is a PDE), we describe a 1-dimensional transport. It will occur in this case that the flow is directed in only one direction, without significant contributions to transport in directions which are orthogonal to the abszissa x .

(2) Method of solution

Now, the mathematical model (the PDE) will be tranformed to a nondimensional representation. From this, a suitable similarity transformation reduces the PDE to an ODE (ordinary differential equation). As can be seen, this "similarity solution" will show the main physical properties of the 1-dimensional displacement.

1.4 Interpretation of the solution

Having this similarity solution, already certain criteria can be obtained, which closely can be related to regions of parameters where certain mechanisms occur, i.e. mechanisms of displacement in the porous medium. In our similarity solution, we have still two parameters:

- the (reduced) ratio of viscosities
- the (reduced) ratio of viscous forces and capillary forces: the capillary number.

Criteria

Certain criteria regarding these parameters show, whether we have

- (2a) a completely stable displacement,
- (2b) a displacement which can be characterized as Invasion Percolation,
- (2c) a displacement which can be characterized as Diffusion Limited Aggregation (DLA).

Note this:

Case (2a) produces a stable type of behavior.

Case (2b) produces an instable type of behavior, Invasion Percolation, (having relations to percolation, but differences from usual percolation).

Case (2c) will have a different type of instability (DLA) (also having relations to fingering).

It has to be noted, that case (2a) is completely stable, but cases (2b), (2c) are also related to some methods known from the field of phase transitions (critical states, renormalization, fixed scale transformation).

1.5 Structure of the report

We start in sect. 2 with some considerations of a Hele-Shaw Cell, also introducing the capillary number N_c (i.e. ratio of the capillary forces to viscous forces). Then different mechanisms for transport are considered in sect. 3. In sect. 4 a PDE (based on continuity equation and Darcy-law) is considered, using a nondimensional representation and a similarity solution (reduced saturation is obtained. Then in sect. 5 and 6 different characteristics for transport are given. In sect. 7 from the similarity solution a transformation from a similarity solution to a usual solution (saturation) is obtained. Finally, in sect. 8, some different versions of an ODE (also with the same type of similarity solution) are discussed. In the Appendices, some problems are discussed, such as more details on the similarity solution, and a discussion of transitions between different mechanisms, with a representation of parameters (such as permeability) by power laws, and discussion of some computer programs used for this research. Note that the main steps of this research are shown in Fig. 1-1.

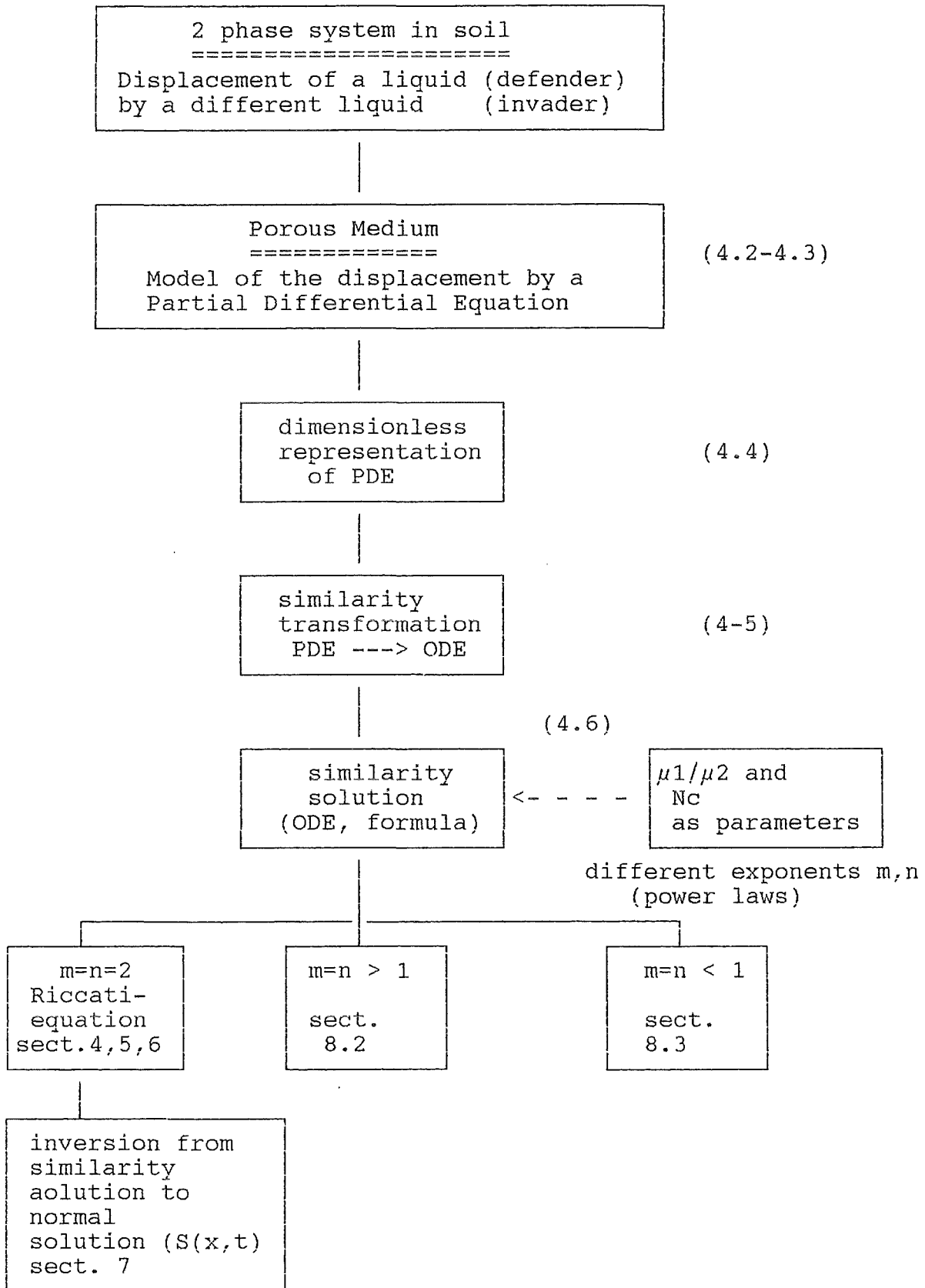


Fig. 1-1 Main issues of the method for two phase systems

1.6 A few remarks on application

It seems quite clear from the various considerations in this report, that the method can be applied for various systems of two phases. Let us note two things: From experiments and from the physics of porous media it follows, that for mechanisms of displacement (such as for oil and water) capillary forces and viscosities are responsible. Related to some experiments in the physics of porous media and for different types of soils a study is possible which can describe the behavior of some liquids which are likely to give a two phase system in soil. This understanding of mechanisms will contribute to planning of ecology and also as a decision help for ecological engineering.

2. 2-dimensional Flow

It may be noted, that a considerable number of phenomena, also for two phases can be seen already by a significantly simplified approach: The consideration of a 2-dimensional flow. For this

- experiments,
- simulations, and
- analytic evaluations

are possible for modelling.

2.1 A Model of the Hele-Shaw-Cell

For modelling a flow in 2 dimensions frequently a Hele-Shaw-Cell can be used (see Fig. 2-1). It can be seen that this type of cell is a pair of plain and parallel glass plates, with a narrow gap between the plates, (e.g. of gap thickness of more or less 1 mm), which has a considerable width and length (say, e.g. 10 cm), and an input or output for liquids, which may according to different requirements be at one end of the cell or in the middle of the cell.

We assume, that along the top and bottom plate (Fig. 2-2) the flow velocity v vanishes. With these boundary conditions, we obtain

$$v_{||} = \frac{3}{2} * \left(1 - \frac{4*z^2}{b^2} \right) * v_{||}(x,y) \quad (2-1)$$

with $v_{||}$ denoting the mean velocity having only components in the x-y plane. We assume, that

$$v = 0 \quad \text{for } z = \pm b/2,$$

i.e. at the top and bottom plate.

For a flow which has only negligible changes of $|v|$ in time, $(d|v|/dt) = 0$, the general Navier-Stokes equation reduces to the following expressions (2-2):

$$\mu * \nabla^2 v = \text{grad } p \quad (2-2)$$

Substituting equ. (2-2) into (2-1) we obtain [Lamb]

$$v_{||} = - \frac{b^2}{12*\mu} * \text{grad } p \quad (2-3a)$$

It should be noted, that (2-3a) is for the case of the Hele-Shaw model equivalent to Darcy's law. In this case, Darcy's law is not only a phenomenological law, but could be derived from the basic equation of hydromechanics (2-2a) and a few assumptions which are reasonable. When we replace $(b^2/12)$ by the permeability K we obtain the usual form of Darcy's law, which is definitely valid for a porous medium:

$$v = - \frac{K}{\mu} * \text{grad } p \quad (2-3b)$$

Now it is useful to introduce a dimensionless formalism, which will be closely related to a number of characteristic quantities as used for transport phenomena with two phases in porous media and for transport in soils.

2.2 Dimensionless quantities

We consider the two phase flow in a Hele-Shaw cell with a constant average velocity. We have a displacement of a viscous fluid by a non-viscous fluid (or a fluid with low viscosity), e.g. air. Inside the viscous fluid clearly Darcy's law holds. Thus the flow will be uniform, at least when sufficiently distant from the interface (between displacing fluid and displaced fluid). If the viscous fluid is incompressible, we simply have

$$\nabla^2 p = 0 \quad (2-4)$$

In the x-direction we have

$$p \text{ ----> } - \frac{12*\mu}{b^2} v_{\infty} * x \quad (\text{for } x \text{ ----> } \infty) \quad (2-5)$$

However, at the interface, conservation of fluids means that the phase boundary moves according to

$$n * \nabla p = \frac{12*\mu}{b} * v_n \quad (2-6)$$

where v_n is the normal velocity of the interface. Moreover at the impermeable sidewalls of the cell,

$$y = \pm a \text{ we have } \frac{\partial p}{\partial y} = 0 .$$

It is also important to note, that the pressure p is related to the surface tension and to the curvature as follows:

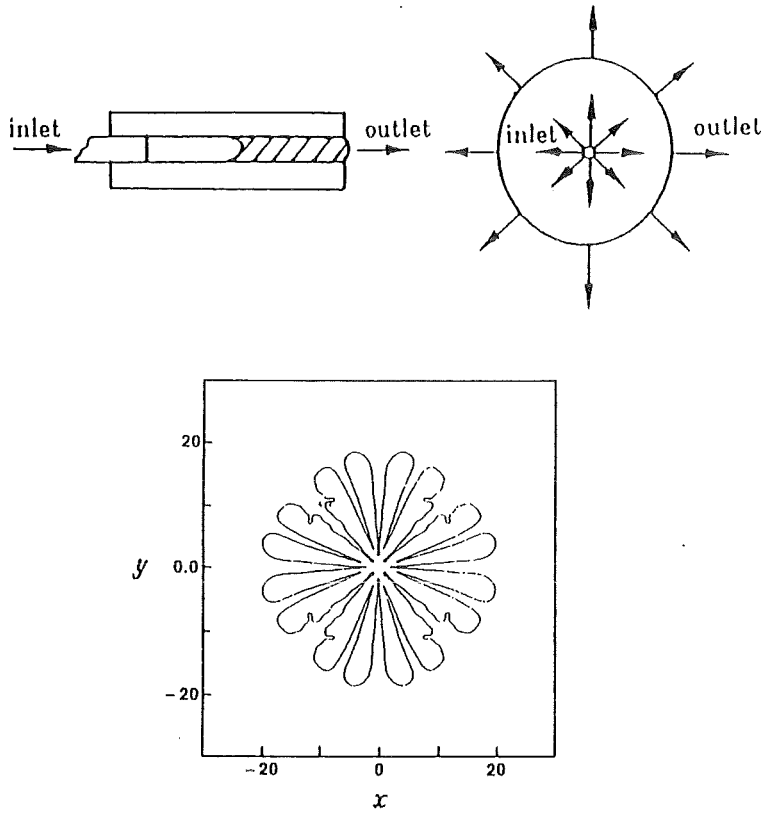


Fig. 2-1 Hele-Shaw-cell (schematic)

- (a) inlet (left), outlet (right)
- (b) inlet (center), outlet (outside)
- (c) fingering in a Hele-Shaw-cell

$$p = p_{\text{air}} + \gamma * K \quad (2-7)$$

The following variables are dimensionless:

ϕ is called reduced pressure p ,

$\bar{\gamma}$ is called reduced surface tension γ .

We introduce these DIMENSIONLESS VARIABLES as follows:
 =====

$\phi = \frac{b^2}{12 * \mu * v_{\infty} * a} * p \quad (2-8a)$
$\bar{\gamma} = \frac{\gamma}{12 * \mu * v_{\infty}} * (b/a)^2 \quad (2-8b)$

Here

a represents the half-channel width of the Hele-Shaw cell

b gives the gap between top and bottom plate.

γ is the surface tension

v_{∞} is the velocity at a place sufficiently distant from the interface.

It will be interesting to note the relation of the dimensionless variable of (2-8b) to the capillary number Nc as shown in section (2.3). Next we introduce a system of equations, analogous to (2-4), (2-5), (2-6), referring to the uniform flow (on the basis of the Saffman-Taylor model):

$$\nabla^2 \phi = 0 \quad (2-9)$$

$$n * \nabla \phi = v n \quad (2-10)$$

$$\phi(x_{int}) = \bar{\gamma} * K \quad (2-11)$$

Here we have as boundary conditions

$$\phi \sim x \quad \text{for large } x \quad (2-12)$$

and
$$\frac{\partial \phi}{\partial y} = 0 \quad \text{at } y = \pm 1$$

This system the evolution equations for the Saffman-Taylor model. Now it can be seen, that the pattern generation in this model is due to morphological instabilities (which are also of a certain similarity to instabilities as encountered for solidification which occurs in dendritic growth (see [Kessler])).

2.3 Steady state solutions and fingers

We note here that for the Saffman-Taylor model (equ. (2.9), (2-10). (2-11)) some analytic solutions of a stationary type exist. They describe the shape of the interface of a displacing liquid and a displaced liquid (e.g. air and water, or a liquid with low viscosity and a liquid with high viscosity). This is not the place to discuss the methods related to these solutions in detail (but see, e.g. [Kessler]). But let us note that from

$$n^*v = n^*\nabla\phi \tag{2-13}$$

which is equivalent to (2-10) of the Saffman-Taylor model we can introduce a new parameter λ , where $1/\lambda$ is equal to the speed. Thus we obtain (in a suitable coordinate system)

$$\frac{y^*n}{\lambda} = \frac{1}{\lambda} * \frac{\partial y}{\partial s} \tag{2-14}$$

where s is the arc length (which is measured in the direction of the flow). Using a second function ψ (which has properties similar to ϕ) we can, using some formalism, obtain a solution which consists of a Fourier series:

$$x = \frac{2}{\pi^*(1-\lambda)} \sum_{n=0}^{\infty} \frac{(-1)^n}{n} * \cos(n*\pi*y/\lambda) \tag{2-15a}$$

This can be rewritten as follows:

$$x = \frac{1-\lambda}{\pi} * \ln \frac{1 + \cos(\pi*y/\lambda)}{2} \tag{2-15b}$$

A graphic representation of (2-15b) shows the interface between two liquids, which is a "Saffman-Taylor-finger" (See Fig. 2-2). It is important to note that comparing the shape of (2-15b) with an experimental finger (as shown in Fig. 2-3) produced by air displacing water (see [Kessler]) it can be seen that the two interfaces correspond quite closely.

Note: In some different cases solutions are only available by simulation or by rather involved analytical methods. The Saffman-Taylor model will be sufficient to give some insight to our problems.

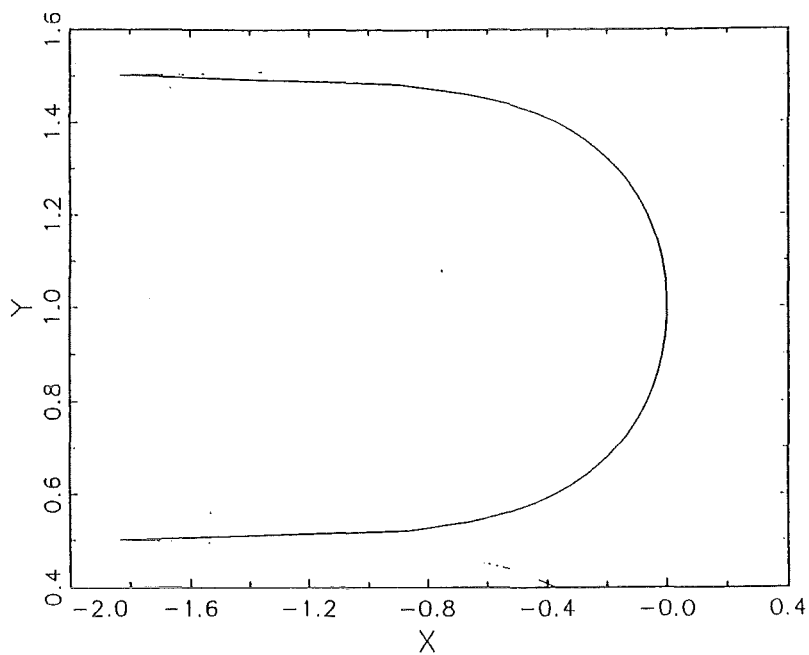


Fig. 2-2 Saffman-Taylor finger model

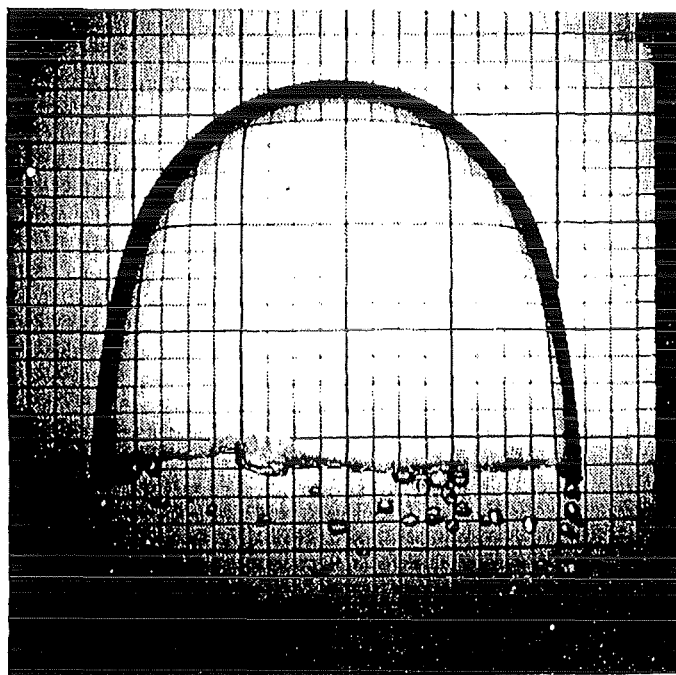


Fig. 2-3 Finger: Air displacing water

2.4 Capillary Number

Now the capillary number N_c will be introduced, which is one of the most interesting characteristics for physics of porous media. The capillary number is also widely used to describe the transport of fluids in soils.

We consider here a disordered porous medium containing two viscous, immiscible, incompressible Newtonian liquids which are in contact. For instance, when a liquid with lower viscosity displaces a liquid with higher viscosity (such as water displacing oil) it may be very interesting to know which of two types of forces

- capillary forces or
- viscous forces

is stronger. As will be seen in this section, also for Hele-Shaw cells a capillary number can be defined.

We assume, that the porous medium under consideration is two - dimensional, and can be schematically modeled as shown in Fig. 2-5. A porous medium can e.g. be characterized by two quantities;

- R pore radius and
- r typical radius of a throat,

where usually $r \ll R$ holds (throats are usually smaller than pores). Now we introduce on the basis of this model and a few formulas from hydrodynamics these characteristics:

capillary pressure P_{cap}

$$\Delta P_{cap} \sim \frac{\gamma}{r} \quad (2-16)$$

where

- γ surface tension,
- r throat radius.

Based on the law of Hagen-Poiseuille for stationary flow we obtain as viscous pressure drop ΔP_{visc}

$$\Delta P_{visc} \sim \frac{\mu * Q * R}{4r} \quad (2-17)$$

where

- μ viscosity
- Q flow rate
- R radius of pore
- r throat radius.

It is possible to obtain the ratio P_{cap}/P_{visc} to replace one of the quantities, Q (flow rate) by introducing

n_1 = average number of pores/throat combinations per unit area

(e.g. $n_1 = 2$).

We can write for the average velocity (Darcy-velocity)

$$v \sim n_1 * Q$$

and for the porosity θ related to R :

$$\theta \sim n_1 * R^2$$

Thus we can write for the ratio of viscous pressure and capillary pressure:

$$\frac{\Delta P_{visc}}{\Delta P_{cap}} \sim \frac{\mu * v}{\gamma} * \left(\frac{R}{r} \right)^3 * \frac{1}{\theta} \quad (2-18)$$

We can define the CAPILLARY NUMBER N_c which is clearly related to the ratio of viscous pressure and capillary pressure:

$$N_c = \frac{\mu * v}{\gamma} \quad (2-19)$$

We call also c_g the geometry related constant:

$$c_g = * \left(\frac{r}{F} \right)^3$$

Thus we can write for N_c

$$N_c \sim c_g * \frac{\Delta P_{visc}}{\Delta P_{cap}} \quad (2-20)$$

We can compare the capillary number N_c with the constant $1/\bar{\gamma}$ as introduced in equ.(2-8b) for Hele-Shaw model. If we separate from $1/\bar{\gamma}$ the factors due to Hele-Shaw geometry we immediately see that

$$\begin{aligned} \bar{\gamma} &= \frac{\gamma}{\mu * v} * \frac{(b/a)^2}{12} \\ &= \frac{\gamma}{\mu * v} * CHS \end{aligned} \quad (2-21)$$

where CHS refers to Hele-Shaw geometry.

Thus we can relate

$$N_c = \frac{CHS}{\gamma} \quad (2-22)$$

This means (while μ and v are constant):

Surface tension γ	Capillary Number N_c	$\bar{\gamma}$ - factor
INCREASING	DECREASING	INCREASING
DECREASING	INCREASING	DECREASING

Examples

 In Fig.2-4 a number of simulations are shown for a Hele-Shaw cell, which are related to stepwise decreasing surface tensions. It can be seen that instability and ramification increases with decreasing surface tension.

Relation to critical exponents

 It is also possible to explain the behavior of the capillary number as related to Fractal Dimensions and critical exponents, as useful for percolation, invasion percolation and diffusion limited aggregation (DLA, as discussed in Appendix A3 and A4).

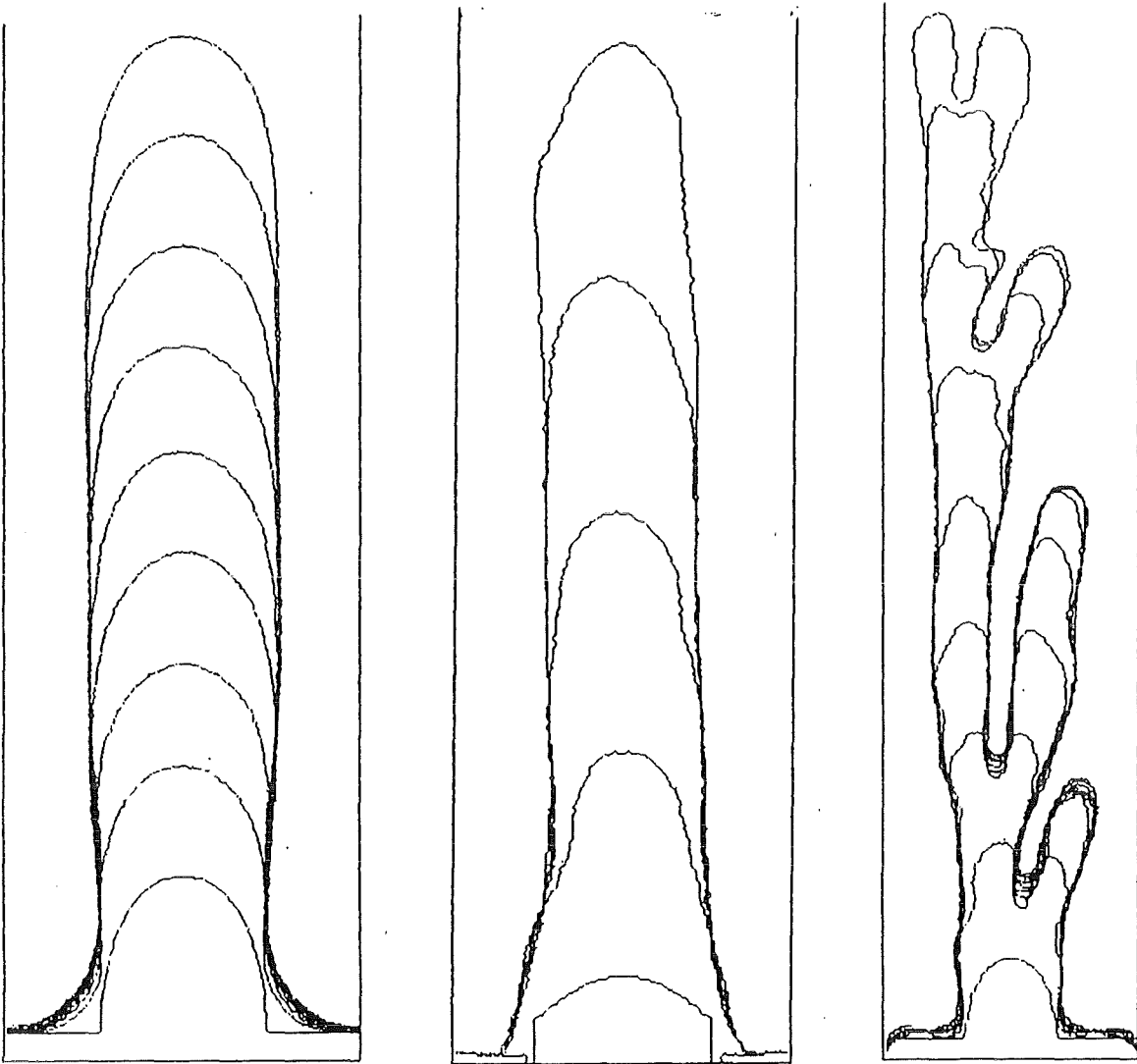


Fig. 2-4 Simulations for a Hele-Shaw-cell

(ramification of fingers for
decreasing surface tension)

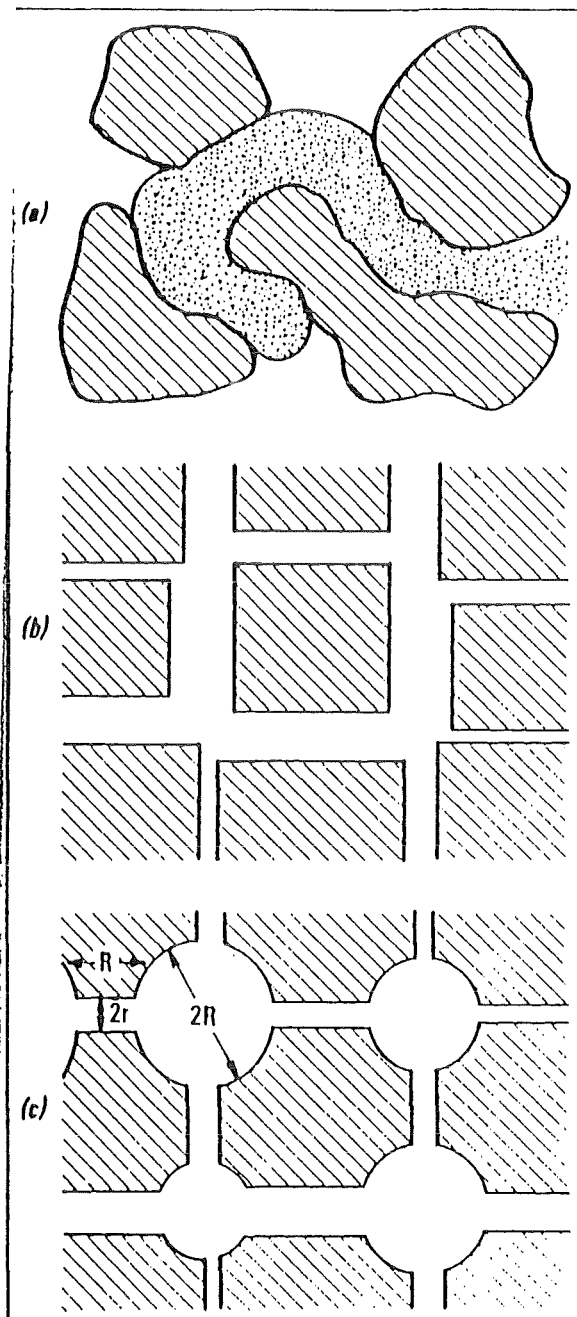


Fig. 2-5 Modelling of a 2D porous medium

3. Different types of transport

Now this is the place to ask for different mechanisms. These mechanisms will again be part of the considerations related to the representation of different types of displacement in section 4 (Differential equation).

3.1 Criteria for different mechanisms

It is frequently useful to obtain for 2-phase systems (e.g. of water and oil in porous media) a classification which relates to

- viscous forces and to
- surface tension.

We obtain this way the following types of systems:

- (1) Systems where usually viscous forces are LARGE compared to surface tensions. In those systems a viscous displacement occurs.
- (2) Systems where usually viscous forces are SMALL compared to surface tensions. Here different mechanism may occur. One of them is Invasion percolation [Weber].

It is also important to know, whether 2 phases are miscible or immiscible. (See for more details [Sahimi]).

Viscous displacement

For viscous displacement two types occur.

(1a) Displacement of fluid B by injection of the more viscous fluid A.

This displacement is stable. Here no strong deviations from a flat surface will occur. Clearly, deviations due to an inhomogeneous structure of pores still are possible.

(1b) Displacement of fluid B' by injection of the less viscous fluid A'.

Instabilities largely depend on

- viscous forces
- the type of the porous medium
- the question, how far the liquids are miscible or not.

Here mechanisms, similar to DLA, but also certain mechanisms of fingering and the occurrence of strongly splitted fingers are possible.

It has to be noted, that here we are in a situation with an clear analogy to the Hele-Shaw cell (sect. 2).

Displacement mainly due to capillary forces

We assume that fluids can be characterized as

- NON WETTING (NW)
- WETTING (W).

Note: Each fluid has a contact angle with the wall.

A fluid for which the contact angle is smaller than 90 degr., is called NON WETTING (NW, eg. oil is non-wetting).

A fluid for which the contact angle is larger than 90 degr., is called WETTING. (W, eg. water is wetting).

Several types of Displacement

In this relation we consider several types of displacement: Drainage, Imbibition.

DRAINAGE:

A displacement where a Non Wetting fluid is pushing the wetting fluid, is called DRAINAGE. NW —> W

IMBIBITION:

A displacement where a Wetting fluid is pushing the Non Wetting fluid, is called IMBIBITION. W —> NW

A table of essential flow mechanisms

Now a table of flow mechanisms is shown. We follow [Lenormand]. [Lenormand]. This table also refers to different types of porous media, but also types of pores (which allow flow by film etc.) Some of these types are characterized in figures.

	Type of flow	Large pores	Small pores
DRAINAGE	flow in ducts	invasion percolation	
IMBIBITION	no flow by film	invasion percolation	compact growth
	flow by film	bond percolation	compact cluster growth
VISCOUS FLOW	stable	flat interface between fluids	
	unstable	gradient governed growth (DLA, fingering)	

Table 3-1 Basic mechanisms

 Note on equivalence of gradient governed growth and DLA

Recently, it has been shown by Koza, that modelling of a diffusion limited aggregation (DLA) by an algorithm and modelling of the process of pushing an incompressible Newtonian fluid by an inviscid fluid through a porous medium by an algorithm leads to two equivalent models [Koza]. Here quantitative relations could be shown between

- hydrodynamics in random porous media and
- fractal theory of stochastic DLA-aggregates.

Thus in a field which is close to our considerations of invasion percolation an equivalence has been established. This makes it easier to relate the considerations for DLA, and for Invasion Percolation.

Next we consider in more detail the conditions how for viscous flow fingering arises.

3.2 Formation of viscous fingers

Now, a model for the formation of viscous fingers is described, which is useful for our consideration of mechanisms. It shows, under which conditions a viscous finger is likely to grow.

We assume that in a linear Hele-Shaw-cell the Darcy-law holds, see also [Lamb] and [Kessler].

$$v = - \frac{K}{\mu} * \text{grad}(p + \rho * g * x) = \text{grad } \phi \quad (3-1)$$

Note that

$$\phi = p + \rho * g * x$$

is called velocity potential.

For the Hele-Shaw-cell we have for permeability

$$K = \frac{b^2}{12 * \mu} \quad (3-2)$$

which will also be written as KH (referring to Hele-Shaw-cell). Now we assume that a small perturbation exists giving a wavelike form to the plane interface between the two liquids (eg. for the oil-water interface). This can in our cell be represented as

$$x = a * \exp(i * n * y + \delta * t) \quad (3-3)$$

with

- a = amplitude
- i = imaginary unity
- n = wave number
- δ = constant.

Note, that the wavelength for this wavelike interface is

$$\lambda = \frac{2 * \pi}{n} \quad (3-4)$$

Now we assume to have two

- immiscible and
- incompressible liquids.

Thus the following equation (Laplace-equation) holds for velocity V and velocity-potential respectively.

$$\text{div } v = \nabla^2 \phi = 0 \quad (3-5)$$

For two liquids (1), (2) we obtain, due to continuity of pressure

$$\frac{\partial \phi_1}{\partial x} = \frac{\partial \phi_2}{\partial x} \quad (3-6)$$

or, explicitly introducing the periodic perturbation of the interface

$$\frac{\partial \phi_1}{\partial x} = v + a \delta \exp(i n y + \delta t) \quad (3-7)$$

where

the first term of the r.h.s. refers to velocity of the interface, and the second term of the r.h.s. refers to the perturbation.

Due to the fact that one liquid is on one side of the perturbed interface while the other liquid is on the other side of the interface, we can write as follows:

$$\phi_1 = v x - (a \delta / n) \exp(i n y - n x + \delta t) \quad (3-8a)$$

$$\phi_2 = v x + (a \delta / n) \exp(i n y + n x + \delta t) \quad (3-8b)$$

These are solutions of (3-6) for ϕ_1 , ϕ_2 .

Now we note, that the pressure in liquid 1 is

$$p_1 = - (\mu_1 / KH) \phi_1 - \rho_1 g x \quad (3-9a)$$

This formula also holds for liquid 2:

$$p_2 = - (\mu_2 / KH) \phi_2 - \rho_2 g x \quad (3-9b)$$

Now we assume for the moment to be in a region where surface tension can be neglected. Thus we can relate the parameters (from (3-8), as follows:

$$\frac{\delta}{n} \left(\frac{\mu_1 + \mu_2}{KH} \right) = (\rho_1 - \rho_2) g + \left(\frac{\mu_1 - \mu_2}{KH} \right) v \quad (3-10)$$

It can be seen, that if the r.h.s. of (3-10) is positive, then also the l.h.s. is positive. From (3-3) we know, that only for $\delta > 0$ a small perturbation can increase, but for $\delta < 0$ it will vanish. This leads to some conditions for increasing perturbations, that is for growing fingers.

First we note this:

(a) We regard, for simplicity, to have a Hele-Shaw-cell which allows only horizontal movements, i.e. the $(\rho_1 - \rho_2)*g$ term vanishes.

(b) We assume, that for a horizontal movement viscous growth always appears when the less viscous fluid (2) is injected to displace the more viscous fluid (1, defender), i.e. when $\mu_1 > \mu_2$.

(c) In addition to the pressure (3-9) we also add a term for capillary pressure p_c .

Capillary pressure

We obtain the total pressure p_t with

$$p_t = p + \gamma^* K \quad (3-11)$$

with

γ^* = surface tension at interface,
 K = curvature of interface

From (3-3) we obtain an upper limit for the curvature as follows:

$$x'' > \frac{x''}{(1 + (x')^2)^{3/2}} = K \quad (3-12)$$

For x'' we can write

$$x'' = n^2 = \frac{(2*\pi)^2}{\lambda^2} \quad (3-13)$$

With (3-10) and (3-13) we obtain

$$\frac{\delta * \lambda}{2*\pi} \left(\frac{\mu_1 + \mu_2}{KH} \right) = \left(\frac{\mu_1 - \mu_2}{KH} \right) * V - \frac{4*\pi^2}{\lambda^2} * \gamma^* \quad (3-14)$$

Now we can state that $\delta > 0$ only if

$$0 < \left(\frac{\mu_1 - \mu_2}{KH} \right) * V + \frac{4*\pi^2}{\lambda^2} * \gamma^* \quad (3-15)$$

Solving for λ , we obtain a critical value of λ , which is useful as a criterion. We recall, that $KH = 12/b^2$.

$$\lambda_c = 2*\pi*b*\left(\frac{\gamma^*}{12*(\mu_1 - \mu_2)*V} \right)^{1/2} \quad (3-16)$$

The inequality $\lambda > \lambda_c$ (3-17)

is a necessary condition for instability within the horizontal Hele-Shaw-cell. For $\lambda < \lambda_c$, no instability will occur. It can be seen, that the following quantities can contribute to an instability (i.e. growth of fingers):

- (a) decreasing of b (thickness of cell),
- (b) decreasing of γ (surface tension) at interface between liquids,
- (c) increasing of $(\mu_1 - \mu_2) > 0$, (difference of viscosities μ_1, μ_2)
- (d) increasing of velocity V.

Note also this:

If we have a cell which is not horizontal, a more complicated version of (3-16) would apply. These considerations referring to instability can only represent a limited range of phenomena, see for more details, [Kessler] and for the distinction between miscible and immiscible liquids [Sahimi].

General formulation of criteria for growth

From the definition of $\tilde{\gamma}$ (which had been used for dimensionless variables for Hele-Shaw-cells, in sect. 2.1) we recall that

$$\tilde{\gamma} = \frac{\gamma}{12 * \mu * v_{\infty}^2} * (b/a) \quad (3-18)$$

Moreover, also the relation

$$\tilde{\gamma} = 1/C$$

holds, where C is the capillary number.

Thus with (3-16) it can be said, that λ_c is a monotonous function of $\tilde{\gamma}$ and of $1/C$.

This gives the following rules [R1], [R2] :

[R1]

For DECREASING $\tilde{\gamma}$, we have DECREASING λ_c , thus an INCREASING INSTABILITY, an increasing tendency for fingers to grow.

And also,

[R2]

For INCREASING C (CAPILLARY NUMBER) we have DECREASING λ_c , thus an INCREASING INSTABILITY, an increasing tendency for fingers to grow.

It will be seen in sect. 3.2 that these rules are equivalent to a part of the considerations for 2D-porous media, and that they are also useful for interpretation of the parameters of the ODE in section 4.

3.3 A phase diagram showing different mechanisms

As can be seen in Table 3-1, we have for 2 phase flow basically 3 mechanisms (sect. 3.1):

- stable flow (also called anti-DLA)
- DLA (also related to fingering)
- Invasion Percolation

There are usually some considerations for different mechanisms:

- (1) Experimental techniques, especially in 2 dimensions (Hele-Shaw-Cell, sect. 2, see [Lenormand]).
- (2) Results from simulation or statistics (see [Lenormand]).
- (3) Results related to statistical mechanics or renormalization, with critical states, percolation, invasion percolation, fractals, fractal dimensions ([Lenormand], [Pietronero], [Weber]). Some conditions related to invasion percolation in 2- and 3-dimensions have been discussed applying fractal dimensions [Weber].
- (4) Some considerations closely related to physical properties, such as viscosities and capillary numbers (see sect. 3.2).
- (5) Finally also the analytic evaluation of two phase flow in a porous medium are shown in sects. 4 and 5 of this report. This gives rather interesting relations of flow to certain mechanisms.

Now in Fig. 3-1 (Phase Diagram) conditions for the different mechanisms of flow are shown. Thus we obtain criteria, under which conditions for

- capillary number C (given as $\ln C$) and
- relation of viscosity (μ_2) of injected fluid and viscosity (μ_1) if displaced fluid

$$M = \frac{\mu_2}{\mu_1}$$

one of the three mechanisms occurs, and also where transition from one of the mechanisms to an other mechanisms is to be expected.

It can also be seen more exactly, where the transitions are to be expected (see [Lenormand]). Also the discussion from sect. 3.2 gives some details for transitions, i.e. for stable ---> unstable.

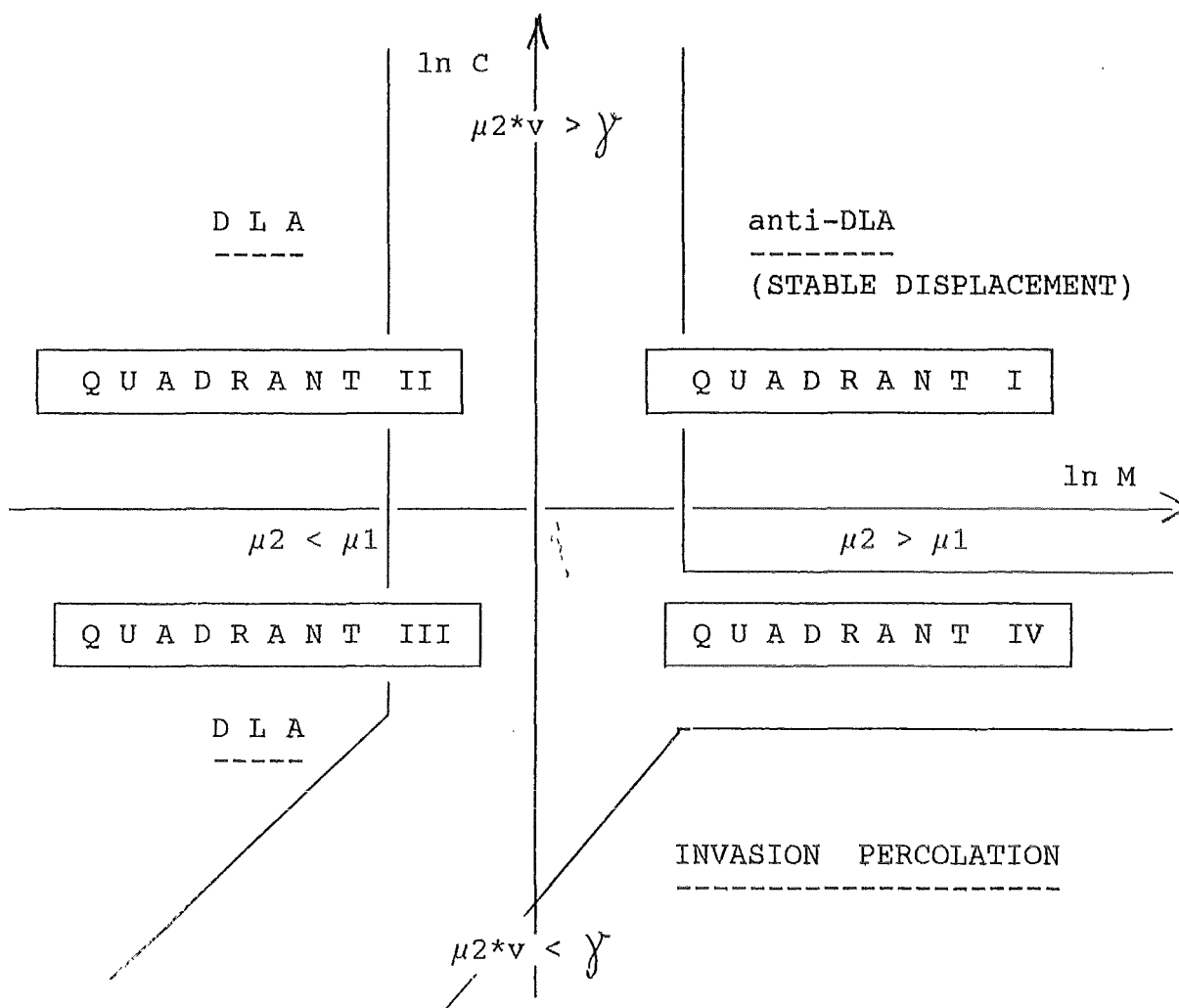


Fig.3-1 Phase-Diagram, showing 3 different mechanisms

For Fig. 3-1 the following notations are used:

$$C = \frac{\mu_2 * v}{\gamma} \quad \text{capillary number}$$

$$M = \frac{\mu_2}{\mu_1} \quad \mu_i \text{ viscosity with } \begin{array}{l} i = 2 \text{ injected fluid} \\ i = 1 \text{ displaced fluid} \end{array}$$

Note: It can be seen that the following MECHANISMS are in QUADRANTS I, II, III, and IV:

- DLA is in QUADRANT II and III
- anti-DLA is in QUADRANT I and partly in QUADRANT IV
- INVASION PERCOLATION is in QUADRANT III and IV

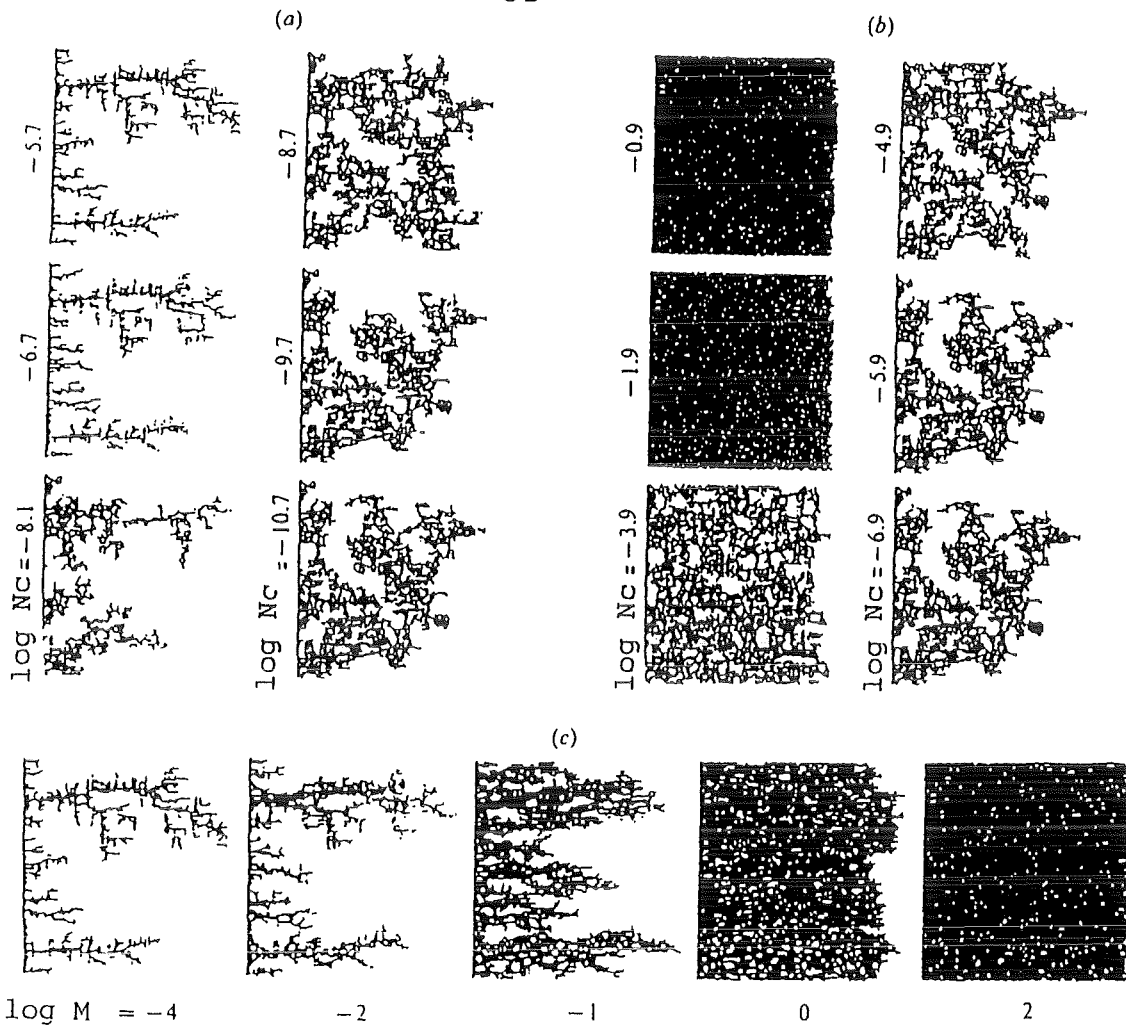


Fig. 3-2 Some transitions (see [Sahimi2])

(a) From viscous to capillary fingering (invasion percolation)				
$\log M = -4.7$				
$\log N_c = -8.1$	-6.7	-5.7	(viscous fingering)	
$\log N_c = -10.7$	-9.7	-8.7	(capillary fingering)	
(b) From stable displacement to capillary fingering				
$\log M = 1.9$				
$\log N_c = -3.9$	-1.9	-0.9	(stable displacement)	
$\log N_c = -6.9$	-5.9	-4.9	(capillary fingering)	
(c) From viscous fingering to stable displacement				
$\log N_c = 0$				
transition				
$\log M = -4$	-2	-1	0	2

(viscosity ratio $M = \mu_2/\mu_1$, capillary number N_c)

4. Evaluation of two phase flow in a porous medium

4.1 Basic Equations

Introduction

Following some considerations mainly referring to multiphase flow phenomena, we now come to an analytical description of multiphase flow phenomena in a porous medium. We frequently will also make comparisons with the concepts of sections 2 and 3, which will be most helpful for an understanding of the mechanisms, eg. to decide where are

- stable flows (comparable to anti-DLA)
 - fingering instabilities due to prevalent viscous forces (related to DLA)
 - instabilities due to capillary forces (related to invasion percolation)
- to be expected.

It is to be noted, that the following analytical solution bases on the similarity transformations of independent and dependent variables of a partial differential equation, which is discussed in Appendix A1. In this section, we are closely following the line of [Pistiner].

Darcy Equations

We first note the generalized Darcy-Equations, relating the flows of two phases, such as water (w) and a fuel (f), eg. oil, which are nonmiscible, q_w , q_f and the respective pressures, P_w , P_f :

$$q_w = - \frac{k \cdot K_{rw}(S_w)}{\mu_w} * \frac{\partial P_w}{\partial x} \tag{4-1}$$

$$q_f = - \frac{k \cdot K_{rf}(S_f)}{\mu_f} * \frac{\partial P_f}{\partial x} \tag{4-2}$$

where

- k permeability of porous medium
- $K_{rw}(S_w)$, $K_{rf}(S_f)$ relative permeabilities
- S_w , S_f are the degrees of saturation of fluids, water and fuel (which can vary between 0 and 1),
- μ_w , μ_f is the viscosity of water (w) and a different fuel (f), eg. oil,
- P_w , P_f is the pressure, for the water and the fuel.

It has to be noted, that permeabilities $K_{rw}(S_w)$ and $K_{rf}(S_f)$ in the simplest cases are power-law dependent on S_w , S_f . This will be discussed in more detail in Appendix A4. Here we only note, that for this section, the power law can be approximated by some integer exponents.

Saturation

We note, that when water and liquid completely saturate the porous medium, the fluid saturations satisfy the following relations:

$$S_w + S_f = 1. \quad (4-3)$$

Capillary pressure

For surfaces between water and fuel the following pressure arises, due to the difference of P_w , P_f :

$$P_c(S_f) = P_f - P_w \quad (4-4)$$

For P_c the following relation exists:

$$\frac{d P_c}{d S_f} > 0 \quad (4-5)$$

This means, that P_c is always a nondecreasing function of S_f .

4.2 Continuity equations

We can write conservation laws for each phase (having no chemical reaction or adsorption and any other mechanism which would require a different form of conservation laws).

We note, that the quantities q_w , q_f and the quantities S_w , S_f enter these conservation equations (conservation of q_w and S_w):

$$\frac{\partial q_w}{\partial x} + \theta * \frac{\partial S_w}{\partial t} + q_{wL} = 0 \quad (4-6)$$

$$\frac{\partial q_f}{\partial x} + \theta * \frac{\partial S_f}{\partial t} + q_{fL} = 0 \quad (4-7)$$

where

- θ is the porosity of the porous medium
- q_{wL} , q_{fL} are contributions from a level of the soil, which is clearly a "less permeable part", having significantly lower permeability than the main section. These contributions can be neglected here.

This way, we have for the simplified consideration of the water-phase.

$$\frac{\partial q_w}{\partial x} + \theta * \frac{\partial S_w}{\partial t} = 0 \quad (4-8)$$

And similarly also for q_f , the fuel-phase.

4.3 Continuity and Darcy-Law

On the basis of saturation and fractional flow we can now relate continuity and Darcy-Law in an a way quite analogous to the convection equation for single phase problems.

We first introduce the fractional flow $F(S_f)$, which is the relation of

$$\frac{\text{flow of fuel}}{\text{flow of fuel} + \text{flow of water}} = \frac{\text{flow of fuel}}{\text{total flow}} \quad (4-9)$$

With the generalized Darcy-law (4-1), (4-2) we obtain

$$F(S_f) = \frac{\frac{k * K_{rf}}{\mu_f} * \frac{\partial P}{\partial x}}{\frac{k * K_{rf}}{\mu_f} * \frac{\partial P}{\partial x} + \frac{k * K_{rw}}{\mu_w} * \frac{\partial P}{\partial x}} \quad (4-10)$$

which is equivalent to

$$F(S_f) = \frac{1}{1 + (\mu_w * K_{rf}) / (\mu_f * K_{rw})} \quad (4-11)$$

In Appendix A4, equ. (A4-15) it is shown how K_{rf} and K_{rw} depend on the saturation S_f by a power law. This power law is related to the normal percolation, as is discussed in the Appendix A3 and A4.

A quantity similar to the fractional flow $F(S_f)$ is related to the capillary forces, it is denoted by $G(S_f)$. We have for the capillary pressure, P_c , and its derivative P_c' :

$$P_c'(S_f) = \frac{d P_c(S_f)}{d S_f} \quad (4-12)$$

(See also equ. (4-5), stating that P_c' is positive). $G(S_f)$ is defined

$$G(S_f) = \frac{k * (K_{rw} / \mu_w) * P_c'(S_f)}{1 + (K_{rw} * \mu_f) / (K_{rf} * \mu_w)} \quad (4-13)$$

as can be seen in Appendix A2.

This quantity is required to complete the convection equation for two phases.

Convection equation

 If we introduce a further quantity, the total flow

$$q(t) = q_w + q_f, \quad (4-14)$$

we can write the following convection equation:

$$\theta * \frac{\partial S_f}{\partial t} = \frac{\partial}{\partial x} * (G * \frac{\partial S_f}{\partial x}) - q(t) * \frac{\partial F}{\partial x} \quad (4-15)$$

Here we have

- θ Porosity
- S_f Saturation
- F fractional flow (see equ. (4-11))
- G a quantity related to capillary forces, and fractional flow (see (A2-5) and (4-13)),
- $q(t)$ specific flow.

The specific flow can also be written as a product:

$$q(t) = q_0 * q_e(t) \quad (4-15)$$

Note: The factor q_0 will be used for our dimensionless approach.

Assumptions for Saturation

 The fuel saturation consists of two contributions:

- continuous (or flowing) part S_{fc}
- discontinuous (or stagnant) part S_{fd}
 (due to pores or paths where no output is possible)

$$S_f = S_{fc} + S_{fd} \quad (4-16)$$

We assume that saturations S_{fc} and S_{fd} are in equilibrium, thus it is possible to say that S_{fd} and S_{fc} are related by a time-independent factor:

$$S_{fd} = c_k * S_{fc} \quad (4-17)$$

As a further simplification we assume here that the factor ck is of the order of 1.

Representation of fractional flow F

We already noted, that K_{rw} , K_{rf} depend on power laws (see Appendix A4). This way it will also be possible to approximate $F(S_f)$ by a power law, writing

$$F(S_{fc}) = F_0 * S_{fc}^n \quad (4-18)$$

where

- n is an exponent
- F_0 is a factor which depends on the ration (μ_f/μ_w) but is independent of S_f (see also section 2 and [Lenormand]).

Representation for Derivative of $P_c(S_{fc})$

Also the derivative of $P_c(S_{fc})$ (capillary pressure, eq. (4-12), can be represented by a power law, if we multiply this quantity by the factor $K_{rw}(S_{fc})$:

$$P_c'(S) * K_{rw}(S_{fc}) = \gamma_{fw} * P_{co} * K_{ro} * S_{fc}^{-m} \quad (4-19)$$

where

- γ_{fw} fuel-water surface tension
- P_{co} , K_{ro} are constants (>0), related to the geometry of the porous medium,
- m is an exponent.

Representation of G-function

With (4-11), (4-12) as well as (4-18), (4-19) we also obtain

$$G(S_{fc}) = \frac{k * K_{ro}}{\mu_w} * F_0 * P_{co} * \gamma_{fw} * S_{fc}^{n-m} \quad (4-20)$$

We note, that all the terms used here, are already defined in equations (4-18), (4-19).

Note: Now the subscript fc will be dropped for the respective quantities, we will write S instead of S_{fc} , since no confusion is possible.

4.4 Dimensionless considerations

For some considerations, e.g. for statistical physics of sedimentary rocks (see [Po-zen Wong]), it is convenient to use quantities as "characteristic throat size" and "characteristic length". This is not to obtain precision; but note, that some

approaches considerably simplify, if it can be assumed that one is in a region, where all lengths are large compared to the characteristic length. Similarly, we also introduce two characteristic quantities here, to see that we are in an asymptotic region.

Characteristic length

$$L = k \cdot K_{ro} \cdot P_{co} \quad (4-21)$$

where

- k permeability
- K_{ro} , P_{co} factors which have been used for (4-19)

Characteristic time

$$T = \frac{L \cdot \theta \cdot (1 + ck)}{q_o \cdot F_o} \quad (4-22)$$

where

- L (see (4-21), characteristic length)
- θ porosity
- ck proportionality factor between S_{fd} , S_{fc}
- q_o proportionality factor (see (4-15a))
- F_o factor dependent on (μ_f/μ_w) (see (4-18)).

Using (4-21), (4-22) we introduce the following dimensionless quantities.

Dimensionless length

$$\hat{x} = x/L \quad (4-23a)$$

Dimensionless time

$$\hat{t} = t/T \quad (4-23b)$$

Dimensionless continuity equation

Now we can write a dimensionless continuity equation. But first note the following: We assume that the less permeable part (above and below the considered porous medium) is now of a permeability which may be neglected. Thus we can write

$$\frac{\partial S}{\partial \hat{t}} + \frac{\partial I_s}{\partial \hat{x}} = 0 \quad (4-24)$$

with

$$I_s = q_e(\hat{t}) \cdot S^n - (1/N_c) \cdot S^{n-m} \cdot \frac{\partial S}{\partial \hat{x}} \quad (4-25)$$

Here, I_s has been called fuel flux. It is a function of q_e (flow) and of S (saturation), as well as of N_c (capillary number). In sect. 6, a thorough discussion of the concept of fuel flux is given.

Capillary number N_c

Note that N_c is the capillary number N_c :

$$N_c = \frac{\mu_w * q_0}{\gamma_{fw}} \quad (4-26)$$

where

- μ_w viscosity of water
- γ_{fw} surface tension
- q_0 a factor related to q

Note: For more details on the capillary number see sect. 2, 3.

With this continuity equation a relation between transport of fuel and water in a porous medium and limits of fractal patterns ([Lenormand], [Kessler]) can be established.

Relations of properties to boundary conditions

Solution of (4-24), (4-25) (in the region $-\infty < \hat{x} < +\infty$) gives I_s (fuel flux in a porous medium). We note here that

$$I_s(\hat{x}, \hat{t}) \rightarrow 0 \quad \text{for } |\hat{x}| \rightarrow \infty \quad (4-27)$$

For $S(\hat{x}, \hat{t})$ we obtain a dimensionless fuel mass for the porous medium as follows:

$$M(\hat{t}) = \int_{-\infty}^{+\infty} S(\hat{x}, \hat{t}) d\hat{x} \quad (4-28)$$

We note, that with some changes of the equations (4-27)-(4-28) used here, also finite but small permeability of the lower medium can be included in the calculation. We consider only one level without interaction with upper or lower medium.

4.5 Similarity variables -----

Now we come to a representation, with transformed variables and functions. It is possible, by this type of transform to obtain from a partial differential equation an ordinary differential equation. This is called "similarity method" and is discussed in Appendix A1. We note here, that equivalent to equations (A1-1a) and (A1-7b) we obtain the following transformations;

$$\xi = \hat{x} \hat{t}^{-1/2} \quad (4-29)$$

$$S_e = f(\xi) \hat{t}^{-1/2} \quad (4-30)$$

As can be seen in Appendix A1 and in the literature (see e.g. [Bluman], [Dresner]) this transformation for the independent variables (x, t) , and the dependent variable (Se) , which come from the continuity equation (4-24) and (A2-8). We obtain this way f and the following intermediate quantity, g , which are closely related to the continuity equation, but now on the "level" of ordinary differential equations.

The corresponding ordinary differential equation

 Now, due to a transformation of the continuity equation the following intermediate quantity $g(\xi)$ (related to fuel flux) is obtained:

$$g(\xi) = f^n - \frac{1}{Nc} * f' \quad (4-31)$$

Thus we come to the ordinary differential equation which corresponds to our continuity equation (24).

$$[g - b * \xi * f]' = 0 \quad (4-32)$$

To this differential equation we introduce boundary conditions which are clearly related to an asymptotic behavior of g and flux I_s . We have

$$g \rightarrow 0 \quad \text{for} \quad |\xi| \rightarrow \infty \quad (4-33a)$$

and also with (27)

$$f \rightarrow 0 \quad \text{for} \quad |\xi| \rightarrow \infty \quad (4-33b)$$

With these conditions the fuel flux I_s can be rewritten as in relation to g

$$I_s = g(\xi) * t^{-1} \quad (4-34)$$

An integration of (4-32) gives this:

$$g - b * \xi * f = C1 \quad (4-35)$$

Note that $C1$ is an integration constant. Due to the boundary conditions (4-33), (4-34) this will be

$$C1 = 0 \quad (4-36)$$

With (4-31) and (4-32) we will have the following ordinary differential equation for the transformed variable f , related to saturation.

$$f' = Nc * (f^n - (1/2) * f * \xi) \quad (4-37)$$

It may be noted, that for

$n = 2$ this is the Riccati-equation (see e.g. [Davis]).

But also for other values of n , some analytical solutions have been obtained (see e.g. [Pistiner]).

We see that in (4-37)

- the function f is defined, the transformed and nondimensional saturation of the fuel
- and that its variable is ξ , the transformed nondimensional coordinate, related to location.

We also note that N_c , the capillary number enters (4-37) as a parameter.

4.6 Analytic solution

For the analytic solution we introduce first a dimensionless reduced mass of the fuel Me

$$Me = \int_{-\infty}^{+\infty} f(\xi) d\xi \quad (4-38)$$

We could have two ranges of parameter n

$$\begin{aligned} n &> 1 \\ n &< 1 \end{aligned} \quad (4-39)$$

We deal here mainly with $n > 1$, and obtain the following analytic solution:

$$f(\xi) = \frac{\exp(-\frac{1}{4}N_c \xi^2)}{[f^{-1}(0) - (\pi N_c (n-1))^{-1/2} - \operatorname{erf}(\frac{1}{2}(N_c)^{1/2} \xi)]} \quad (4-40)$$

Note that $f(0)$ depends on the reduced mass Me . Now, for $n = 2$, we have a Riccati-equation and the solution is

$$f(\xi) = \frac{\exp(-\frac{1}{4}N_c \xi^2)}{(\pi N_c)^{-1/2} * (1/(\tanh(\frac{1}{2}N_c) - \operatorname{erf}(\frac{1}{2}(N_c)^{1/2} \xi)))} \quad (4-41)$$

Note that the effective capillary number is

$$N_{ce} = Me * N_c \quad (4-42)$$

with the reduced fuel mass

$$Me = (1/N_c) * \ln\left(\frac{1 + \tanh(\frac{1}{2}N_{ce})}{1 - \tanh(\frac{1}{2}N_{ce})}\right) \quad (4-43)$$

Evaluation of (4-41)

 In the following calculations it is possible to work with $M_c = 1$. Now equation (4-41) has been used for a GAUSS-computer program [GAUSS]. It is shown in Appendix A5. All results available from this similarity solution are given in sect. 5.

4.7 Further results related to similarity transform

 Until now, we discussed the following ODE, due to the similarity transform:

$$f' = Nc * (f^n - (1/2 * f * \xi)) \quad (4-37)$$

In the previous sections (4.5) and (4.6) we specialized on the case $n = 2$, thus obtaining a Riccati-equation. In can be seen, that this equation was obtained by using for (4-25)

$$I_s = qe(t) * S^n - (1/Nc) * S^{n-m} * \frac{\partial S}{\partial \hat{x}} \quad (4-25)$$

the following assumptions:

$$\begin{aligned} n - m &= 0 \\ n &= 2 \end{aligned} \quad (4-44)$$

By a suitable generalization, now assuming

$$n - m < 0 \quad (4-45)$$

or

$$m + m > 0 ,$$

we obtain the following differential equation:

$$f' = Nc (f^n - b * \xi^{(1-m+n)} * f) \quad (4-46)$$

Equation (4-46) gives, due to different values for the exponents m, n , further similarity solutions. The most interesting of these solutions are discussed in sect. 8.

5. A first characteristic for transport

5.1 Introduction

It is now possible, following sect. 4, to show characteristics for the transport in porous media, based on equation (4-41):

$$f(\xi) = \frac{\exp(-\frac{1}{4}Nc\xi^2)}{(\pi Nc)^{1/2} * (1/\tanh((1/2)Nc) - \operatorname{erf}((1/2)(Nc)^{1/2}\xi))} \quad (4-41)$$

Here $f(\xi; Nc, Me)$ is the reduced saturation (see (4-30), it is a function of the similarity variable,

$$\xi = \frac{x}{\sqrt{t}}^{-1/2} \quad (4-29)$$

and of the two parameters

Nc capillary number (see (4-28)),
 Me the dimensionless reduced mass (see (4-42)).

We set in this section again $Me = 1$, thus we have only Nc as a parameter. If some other values of Me are of interest, this will be explicitly mentioned.

For the maximum of $f(\xi)$ we can state with (4-37) the following relation

$$f'(\xi) = Nc * (f^n - (1/2)) * f * \xi = 0 \quad (5-1)$$

Thus, this maximum is clearly related with Nc . We have only the parameter Nc left, and get a family of f -curves (similarity solutions).

5.2 Figures and Tables

Figures

The similarity solution (reduced saturation) f is shown as a function of the similarity variable (see Fig. 5-1, to 5-6).

Tables

All maxima of the f -curves could be identified by a procedure, giving the coordinates for f_{max} : $(\xi, f)_{max}$. These are listed in tables: Table 5-1 to 5-4.

LIST OF RESULTS

ranges for Nc	Figures	Tables
0.1 to 1.0	5-1 5-2	Table 5-1
1.0 to 10.0	5-3	
11.0 to 20.0	5-4	Table 5-2
20.0 to 30.5	5-5 5-6	
22.2 to 24.0	-	Table 5-3
23.4 to 23.58	-	
10.0 to 100.0	-	Table 5-4
100.0 to 1000.0	-	

5.3 Interpretation of results

The results given in evaluations of $f(x_i; N_c)$ are shown in the LIST OF RESULTS. We have here regions showing a different behavior related to the N_c -value used for the reduced saturation.

Region A:

We have for capillary numbers N_c , where

$$0 < N_c < 23.44$$

the following behavior:

The maximum of $f(x_i; N_c)$ (similarity solution, red. saturation) is INCREASING WITH N_c , and the x_{im} -coordinate for the maximum is slightly shifting to the right with increasing N_c . (See Figs. 5-1 to 5-6, Tables 5-1 and 5-2).

Region B:

We have for capillary numbers N_c , where

$$N_c > 23.44$$

the following behavior:

The maximum of $f(x_i; N_c)$ (similarity solution, red. saturation) is DECREASING WITH N_c , and the x_i -coordinate for the maximum is shifting to the left with increasing N_c . (See Fig. 5-6, Table 5-3 and 5-4).

Location of the highest value for $f(x_i; N_c)$:

In Table 5-3 it can be seen, that for $N_c = 23.44 + 0.02$ the location for the highest value for $f(x_i; N_c)$ occurs. This is important to note for the interpretation of the similarity solution (red. saturation) in relation to possible mechanisms.

5.4 Some 3-dimensional representations for $f(x_i; N_c)$ -----

In Figs. 5-6, 5-7, 5-8, 5-9 the following behavior of $f(x_i, N_c)$ is shown with 3-dimensional representations.

Values for $f(x_i, N_c)$:

In Fig. 5-6, 5-7 the evaluation of $f(x_i, N_c)$ is shown: Fig. 5-6, 5-7a with 3-dimensional representation of $f(x_i, N_c)$, Fig. 5-7b Lines of constant $f(x_i, N_c)$, projected on x_i, N_c -plane.

Partial derivative of $f(x_i, N_c)$ with regard to x_i

In Fig. 5-8 the partial derivative $\partial f(x_i, N_c) / \partial x_i$ is shown, giving the slope of $f(x_i, N_c)$. Note that the partial derivative of $f(x_i, N_c)$ with regard to x_i has been evaluated by symbolic calculation using the MAPLE-system, as is given in Appendix A6.

Partial derivative of $f(x_i, N_c)$ with regard to N_c

In Fig. 5-9 the partial derivative $\partial f(x_i, N_c) / \partial N_c$ is shown. It is interesting to note these results to obtain further insights for the interpretation of the behavior of the reduced saturation in relation to N_c -values. This partial derivative is also obtained using the MAPLE-system (see also Appendix A6).

Also note the following: For the curves of section 5, a GAUSS computer program has been used, which is given in Appendix A5. For information on the program see [GAUSS].

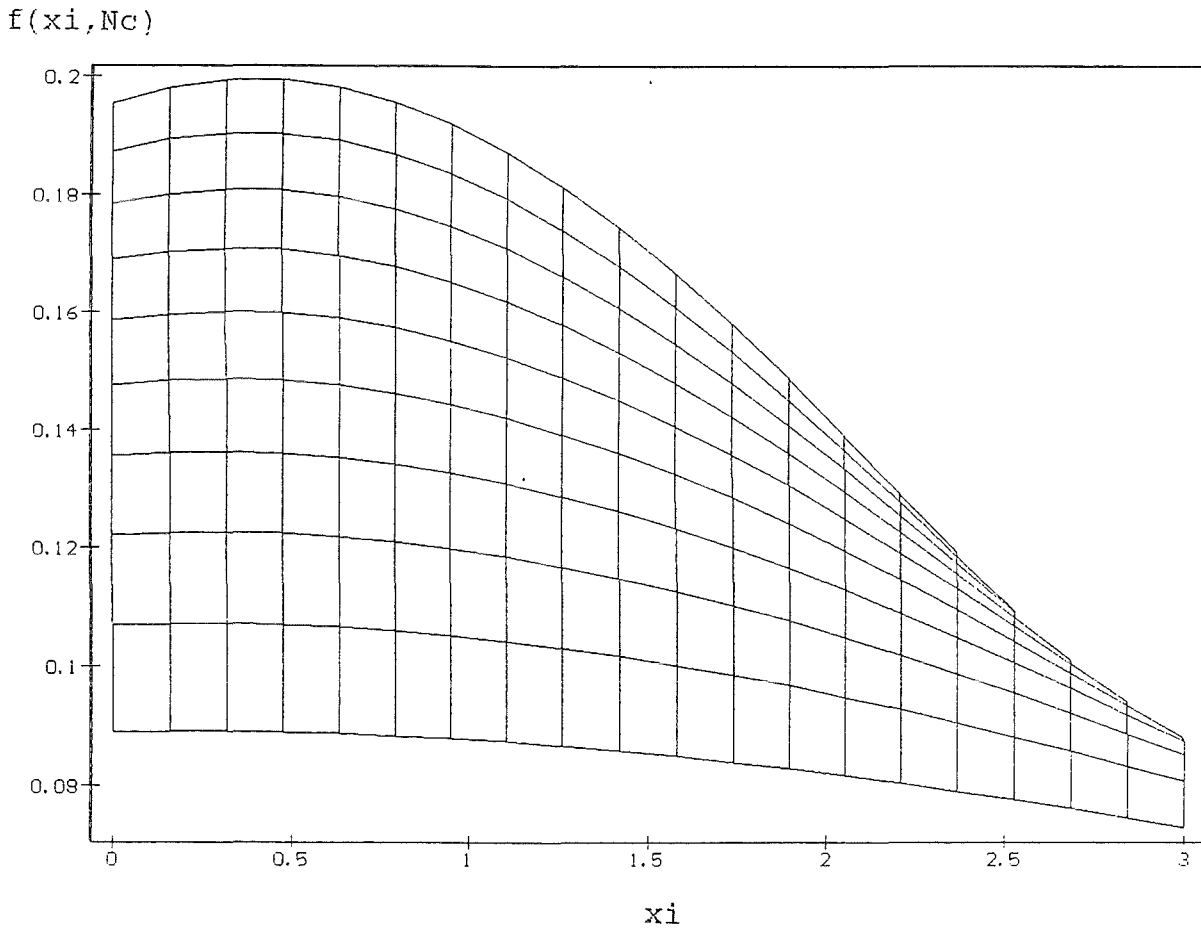


Fig. 5-1 Representation of $f(\xi, N_c)$, $N_c = 0.1..0.5$

$f(x_i, N_c)$

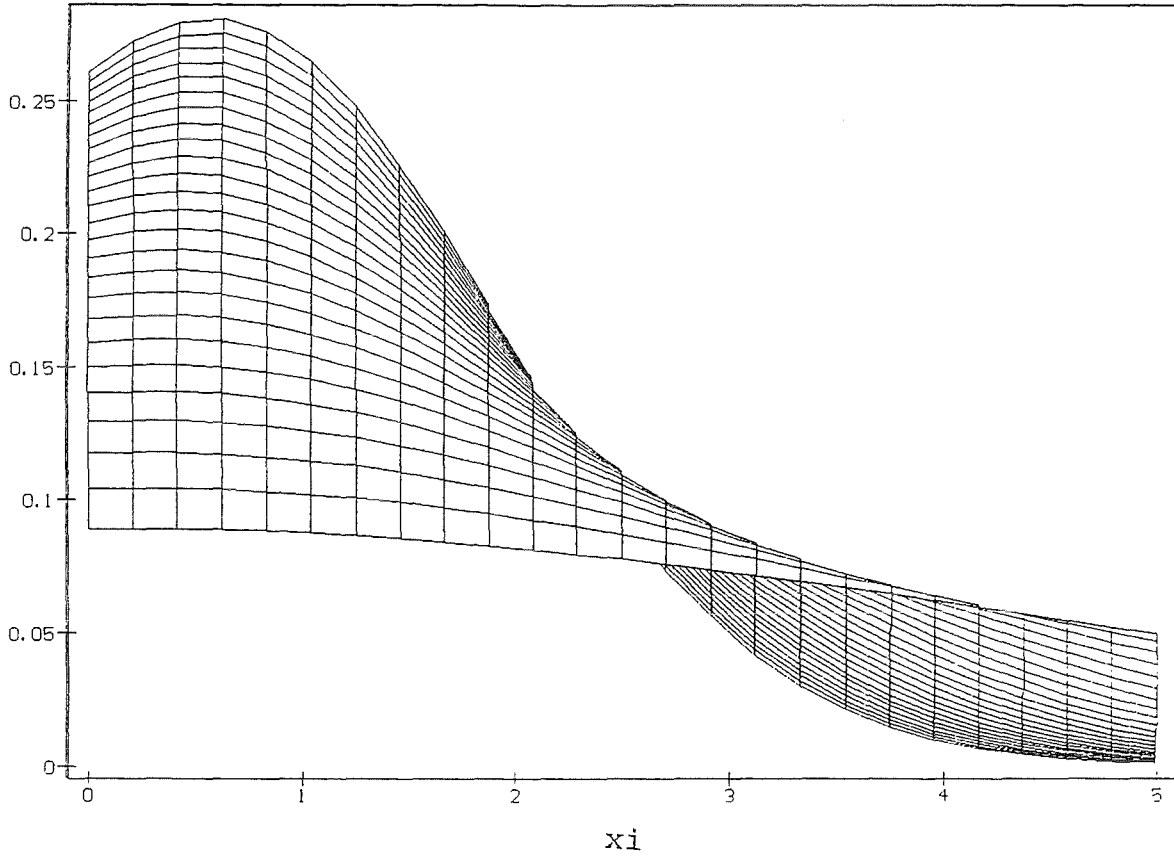


Fig. 5-2 Representation of $f(x_i, N_c)$, $N_c = 0.5..1.0$

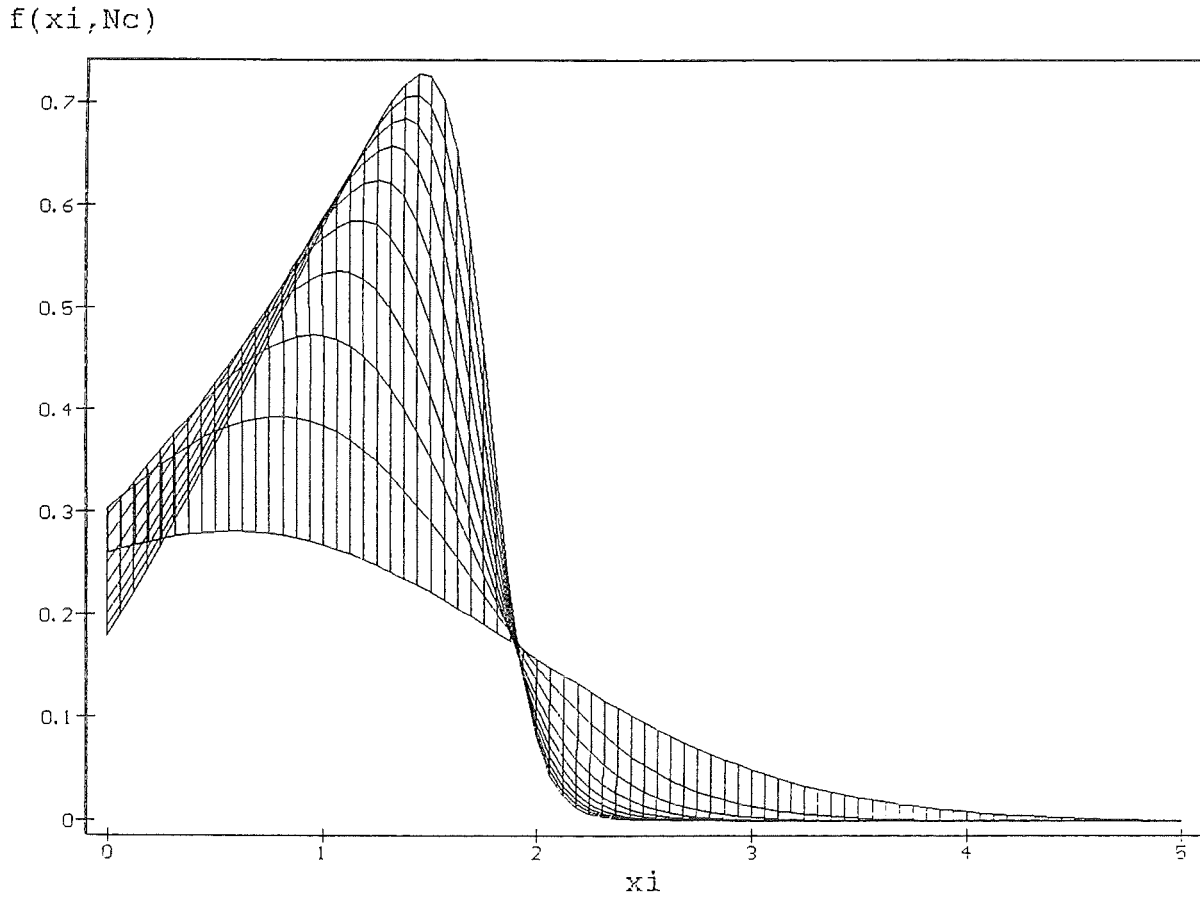


Fig. 5-3 Representation of $f(\xi, N_c)$, $N_c = 1.0..10.0$

$f(x_i, N_c)$

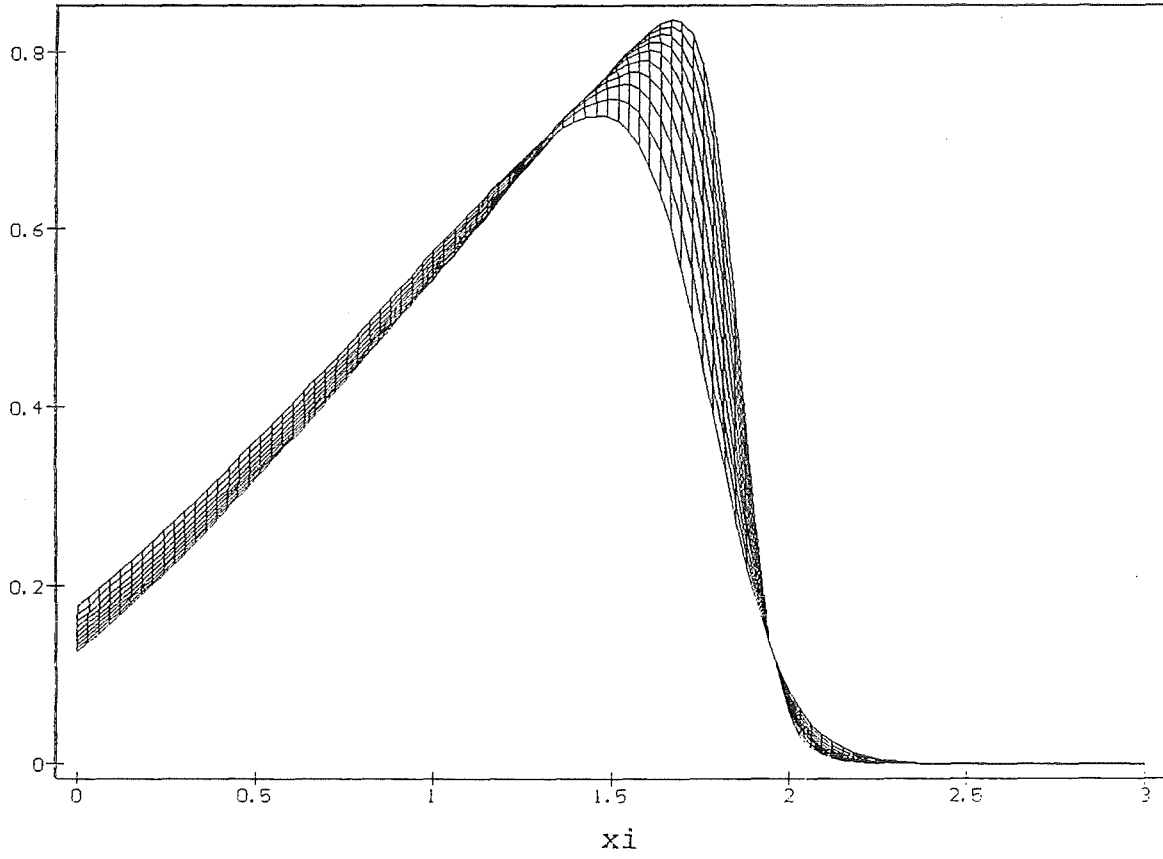


Fig. 5-4 Representation of $f(x_i, N_c)$, $N_c = 10.0..20.0$

$f(x_i, N_c)$

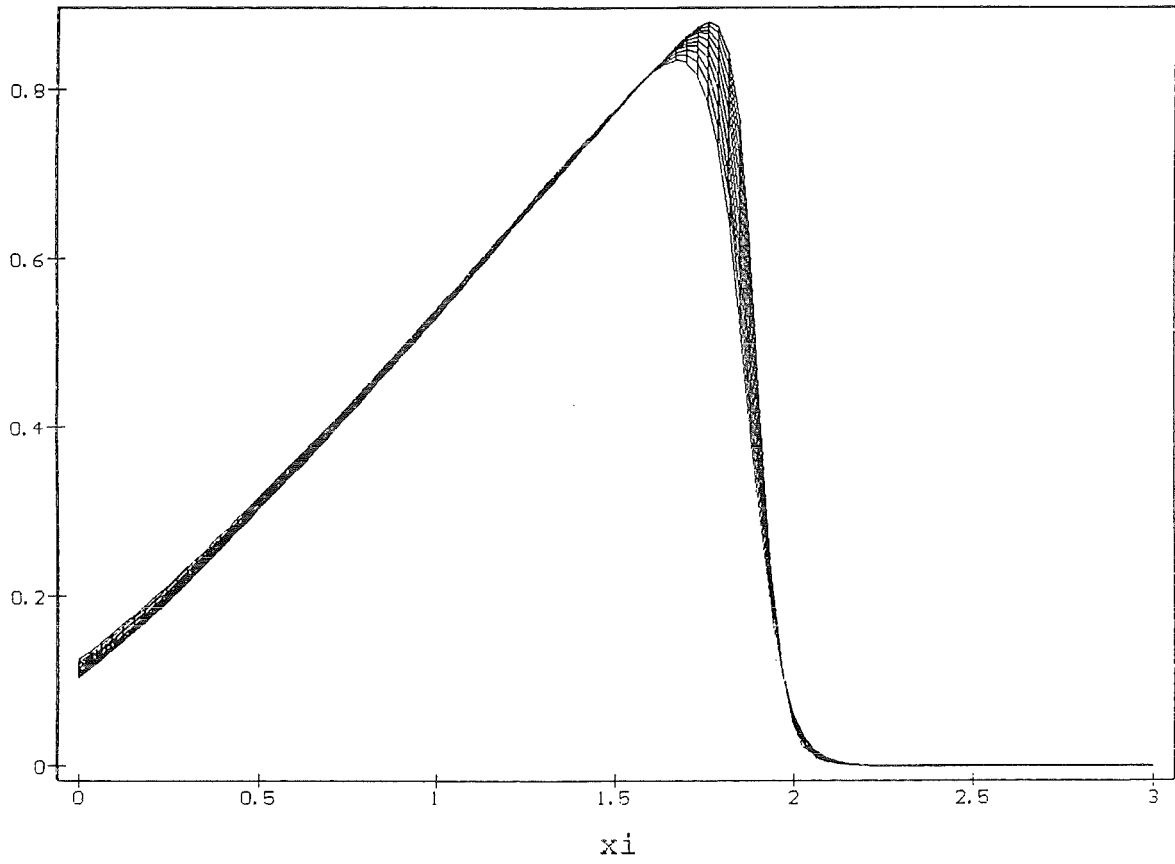


Fig. 5-5 Representation of $f(x_i, N_c)$, $N_c = 20.0..30.0$

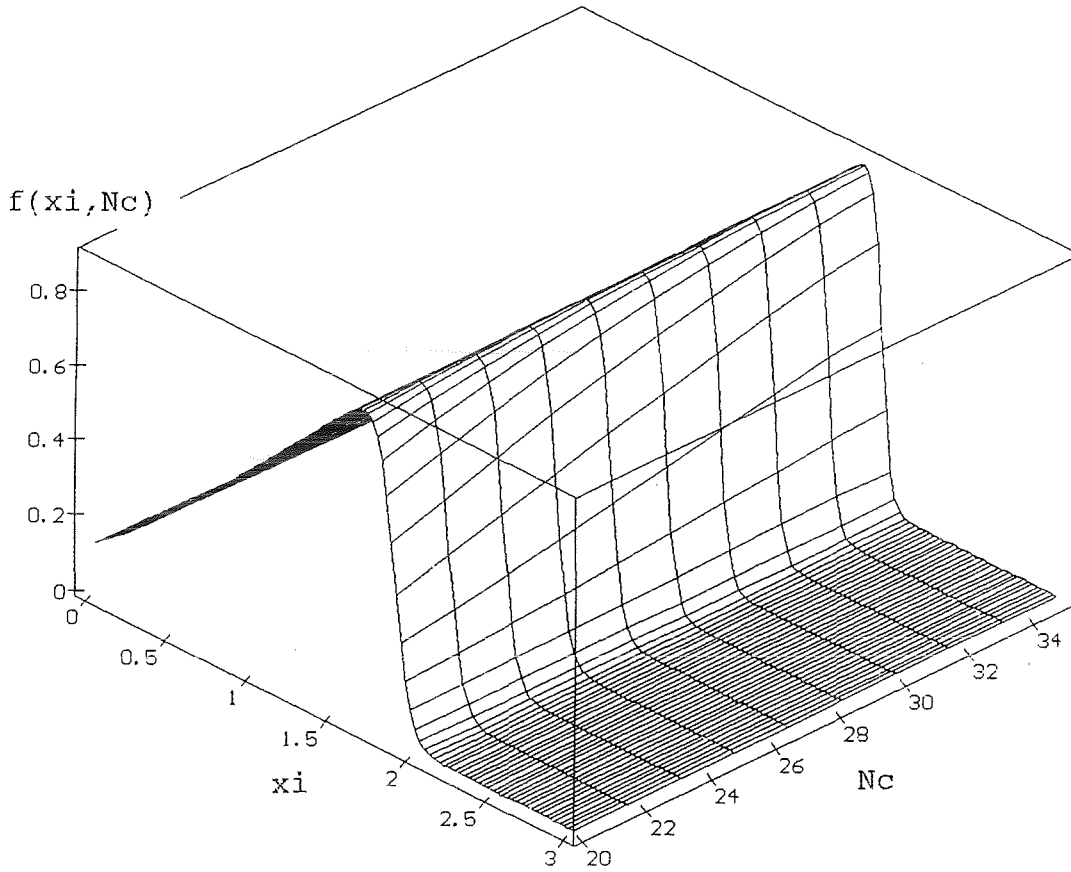


Fig. 5-6 Representation of $f(\xi, N_c)$, $N_c = 20.0..35.0$

(3-D-representation)

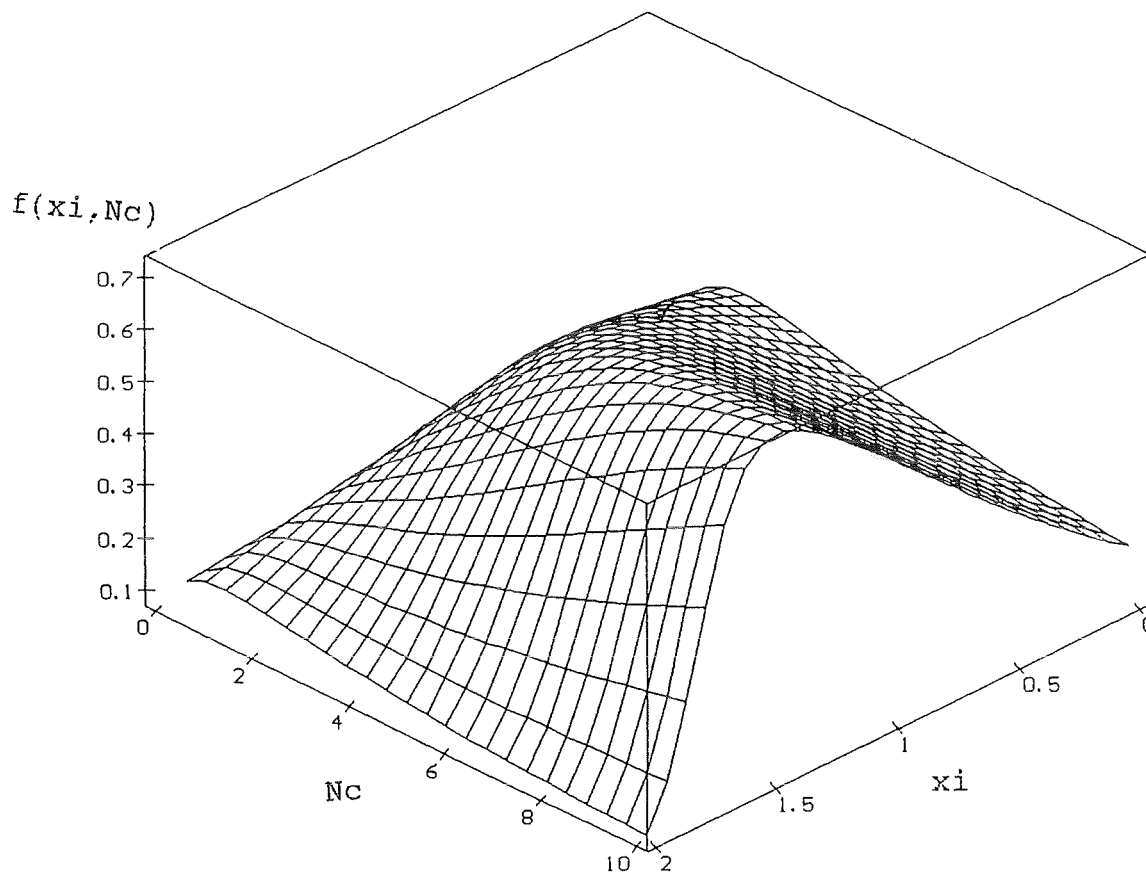


Fig. 5-7a Representation of $f(\xi, N_c)$ (3-Dim)

)

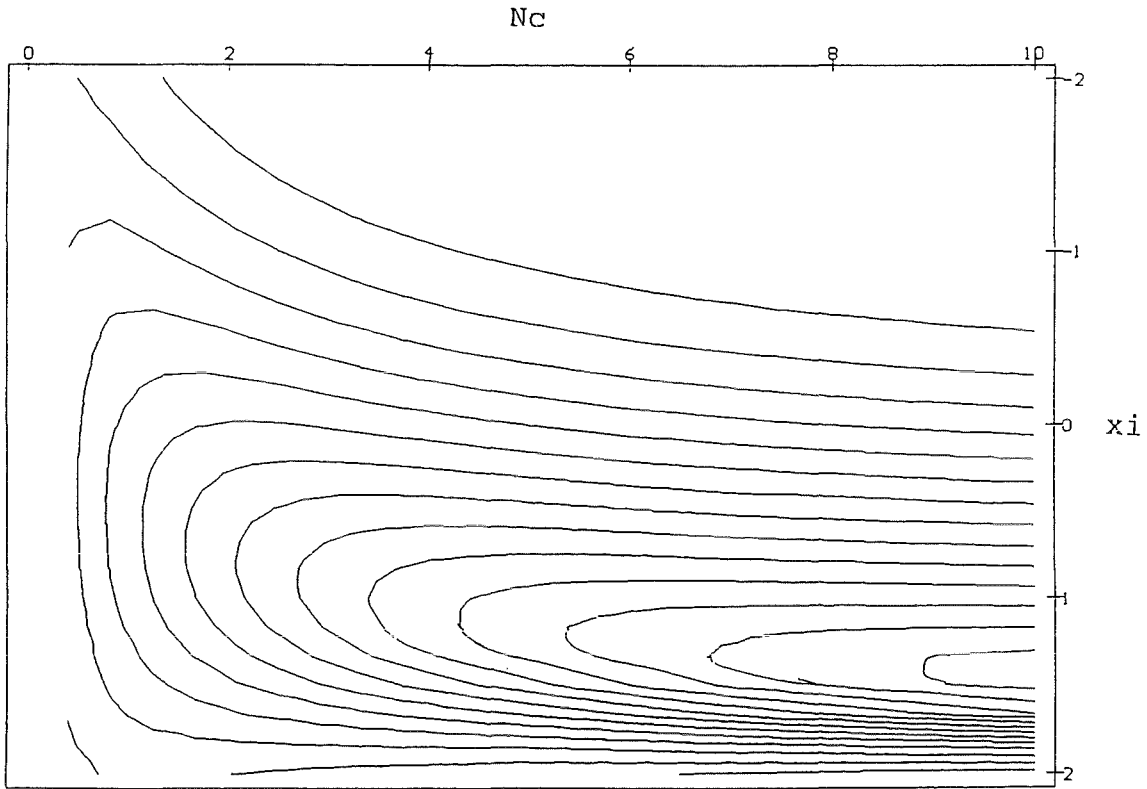


Fig. 5-7b Lines of constant $f(\xi, N_c)$ (projection)

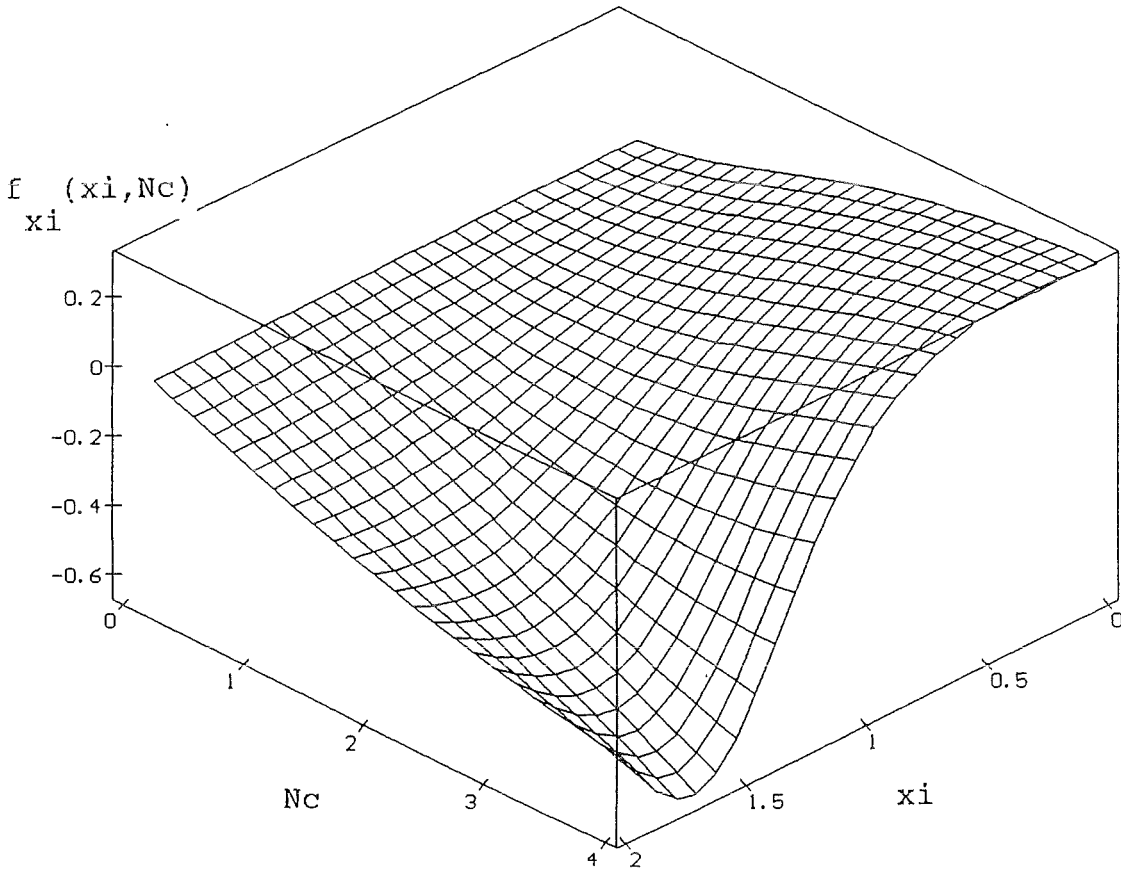


Fig. 5-8 Partial derivative $f_{xi}(xi, Nc) = \frac{\partial f(xi, Nc)}{\partial xi}$

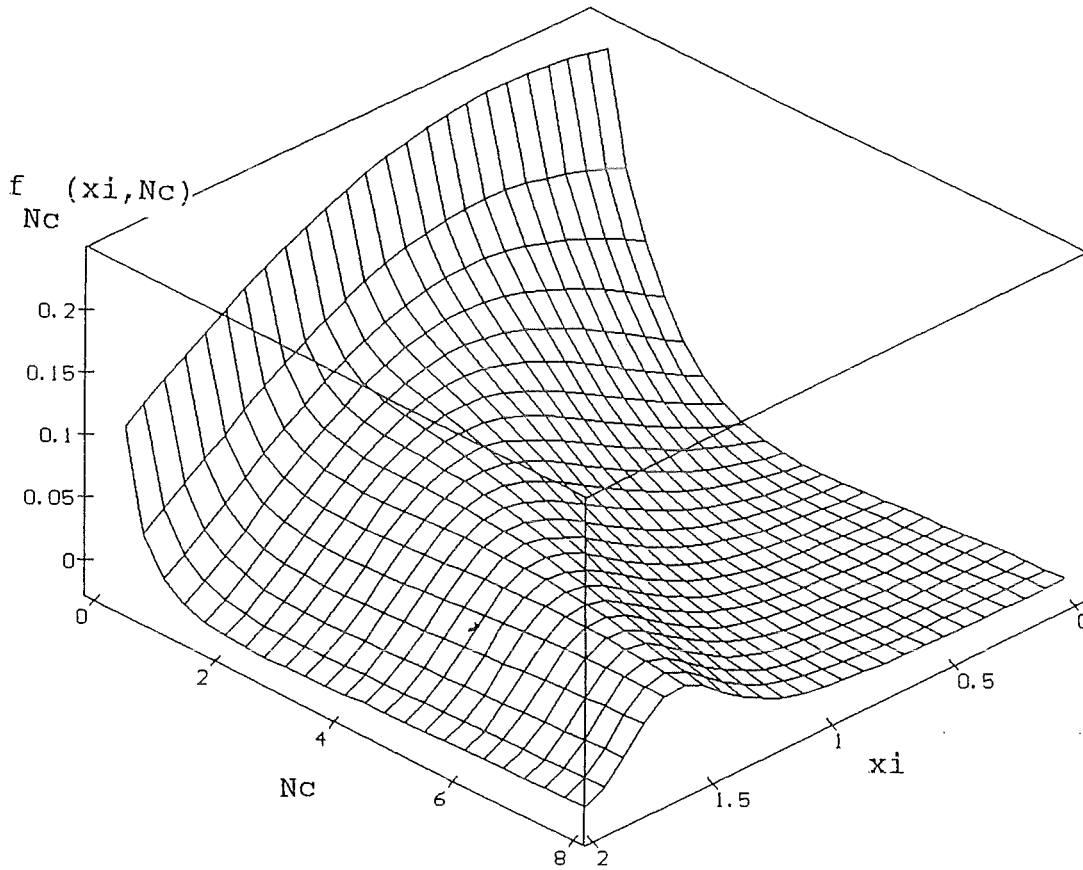


Fig. 5-9 Partial derivative $f_{Nc}(xi, Nc) = \frac{\partial f(xi, Nc)}{\partial Nc}$

RESULTS (range $N_c = 0.10$ to 1.00)

COORDINATES OF MAXIMUM (x_{im} , $f(x_{im})$)

N_c	x_{im}	f_m
0.10	0.20000000	0.08920210
0.20	0.30000000	0.12613731
0.30	0.35000000	0.15445750
0.40	0.40000000	0.17830521
0.50	0.45000000	0.19928119
0.60	0.50000000	0.21819741
0.70	0.50000000	0.23558067
0.80	0.55000000	0.25170955
0.90	0.55000000	0.26677945
1.00	0.60000000	0.28104848

=====

RESULTS (range $N_c = 1.00$ to 10.00)

COORDINATES OF MAXIMUM (x_{im} , $f(x_{im})$)

N_c	x_{im}	f_m
1.00	0.60000000	0.28104848
2.00	0.85000000	0.39313070
3.00	1.00000000	0.47370813
4.00	1.10000000	0.53578587
5.00	1.20000000	0.58514608
6.00	1.30000000	0.62515881
7.00	1.35000000	0.65815782
8.00	1.40000000	0.68555944
9.00	1.45000000	0.70892873
10.00	1.50000000	0.72896388

=====

Table 5-1 Maxima of $f(x_i; N_c)$

RESULTS (range Nc = 11 to 20)

COORDINATES OF MAXIMUM (xim, f(xim))

Nc	xim	fm
11.00	1.5500000	0.74555946
12.00	1.5500000	0.76094193
13.00	1.6000000	0.77425242
14.00	1.6000000	0.78591824
15.00	1.6500000	0.79602475
16.00	1.6500000	0.80631099
17.00	1.6500000	0.81364963
18.00	1.7000000	0.82180120
19.00	1.7000000	0.82970929
20.00	1.7000000	0.83545798

=====

RESULTS (range Nc = 20 to 29)

COORDINATES OF MAXIMUM (xim, f(xim))

Nc	xim	fm
20.00	1.7000000	0.83545798
21.00	1.7000000	0.83977318
22.00	1.7500000	0.84572892
23.00	1.7500000	0.84957135
24.00	1.7500000	0.84756914
25.00	1.7000000	0.84366005
26.00	1.7000000	0.83791725
27.00	1.6500000	0.81735071
28.00	1.6500000	0.80594792
29.00	1.6000000	0.78805031

=====

Table 5-2 Maxima of $f(x_i; N_c)$

RESULTS (range $N_c = 22$ to 24)

COORDINATES OF MAXIMUM (x_{im} , $f(x_{im})$)

N_c	x_{im}	f_m
22.20	1.7500000	0.84646251
22.40	1.7500000	0.84678552
22.60	1.7500000	0.84651433
22.80	1.7500000	0.84967250
23.00	1.7500000	0.84957135
23.20	1.7500000	0.84875620
23.40	1.7500000	0.84688471
23.60	1.7500000	0.85169245
23.80	1.7500000	0.85027077
24.00	1.7500000	0.84756914

=====

RESULTS (range $N_c = 23.4$ to 23.6)

COORDINATES OF MAXIMUM (x_{im} , $f(x_{im})$)

N_c	x_{im}	f_m
23.40	1.7500000	0.84688471
23.42	1.7500000	0.84662161
23.44	1.7500000	0.85219411 (*)
23.46	1.7500000	0.85215596
23.48	1.7500000	0.85211132
23.50	1.7500000	0.85205996
23.52	1.7500000	0.85200160
23.54	1.7500000	0.85193597
23.56	1.7500000	0.85186279
23.58	1.7500000	0.85178176

=====

Table 5-3 Maxima of $f(x_i; N_c)$

(*) Note that $N_c = 23.44 + 0.02$ is the location which gives the highest value for $f(x_{im}, N_c)$.

RESULTS (range Nc = 10 to 100)

COORDINATES OF MAXIMUM (xim, f(xim))

Nc	xim	fm
10.00	1.5000000	0.72896388
20.00	1.7000000	0.83545798
30.00	1.6000000	0.77455142
40.00	1.3500000	0.67056218
50.00	1.2000000	0.59391256
60.00	1.1000000	0.54244269
70.00	1.0500000	0.51324423
80.00	0.9500000	0.46536509
90.00	0.9000000	0.44119881
100.00	0.8500000	0.41523894

=====

RESULTS (range Nc = 100 to 1000)

COORDINATES OF MAXIMUM (xim, f(xim))

Nc	xim	fm
100.00	0.85000000	0.41523894
200.00	0.60000000	0.28810317
300.00	0.50000000	0.23635741
400.00	0.45000000	0.20994640
500.00	0.40000000	0.18491138
600.00	0.35000000	0.16002300
700.00	0.35000000	0.15872356
800.00	0.30000000	0.13448896
900.00	0.30000000	0.13392032
1000.00	0.30000000	0.13295212

=====

Table 5-4 Maxima of f(xi;Nc)

6. A further characteristic for transport

6.1 Continuity equations and flux

Now, a further characteristic for the transport in porous media will be shown. We start from

- continuity equations and
- the reduced flow.

We recall, that in

- sect. 4.3 (Continuity and Darcy law) and
- sect. 4.4 (Dimensionless considerations)

the following dimensionless continuity equation was used:

$$\frac{\partial s}{\partial t} + \frac{\partial J_s}{\partial x} = 0 \quad (4-24)$$

with

$$J_s = qe(\hat{t}) * S^n - (1/Nc) * S^{n-m} * \frac{\partial S}{\partial \hat{x}} \quad (4-25)$$

where J_s has been called fuel flux. It has been noted that (4-24) is a simplified and dimensionless version of the continuity equations (4-6), (4-7) for flow and saturation S (of water and fluid). Using the concept of fractional flow (4-9)-(4-11) the two equations (4-6) and (4-7) for flow and saturation (of water and fluid) have been reduced to one equation.

Relations of fractional flow to a power law (see (4-18) to (4-20)), contribute to the explicit version of (4-25), as discussed in further detail in Appendix A4. However

$$\frac{\partial S}{\partial \hat{x}}$$

can be calculated with the analytic solution for saturation by means of similarity variables (sect. 4.6), see especially eqs. (4-37)-(4-45) and Appendix A1.

Note that solution (4-43) applies only to a transport which is horizontal.

Non-horizontal flow

If we have to consider also gravity and some other influences, some further analytic solutions are available ([Pistiner1]). This leads to the following formula for Saturation flux (6-1) which is given here:

$$J = q (\hat{t}) * S^n - (1/Nc) * S^{n-m} * \frac{\partial S}{\partial \hat{x}} - (NB/Nc) * S^l \quad (6-1)$$

where

- J fuel saturation flow
- S Saturation
- \hat{x}, \hat{t} reduced coordinates
- n, m exponents related to fractional flow (cf. (4-18)-(4-20))
- l a further exponent
- Nc capillary number
- $q_*(\hat{t})$ a time dependent function

We note that

$$NB = \text{sign}(q) \frac{*Kro(\rho_w - \rho_f)*g}{f_w} \quad (6-2a)$$

with

a factor related to ρ_w (density of water), ρ_f (density of fluid), and gravity force g.

Considering a horizontal flow only, we evidently set

$$NB = 0 \quad (6-2b)$$

Assumptions

Assuming a horizontal flow and a relation to analytic solution of sect. 4.6 we obtain:

$$NB = 0,$$

$$m = n = 1$$

Moreover, we have for

$$u = \frac{2 - m}{2 + n - m} = 1/2 \quad (6-3)$$

and for $q(t)$ we obtain

$$q_*(\hat{t}) = \hat{t}^{-1/2} \quad (6-4)$$

With these assumptions, the saturation flux J introduced in (6-1) can be rewritten

$$J = \hat{t}^{-1/2} *S - (1/Nc)* \frac{\partial S}{\partial \hat{x}} \quad (6-5)$$

6.2 Interpretation of flux curve $J(S;t,Nc)$

For a detailed evaluation and interpretation of the J-curves some considerations for the dimensionless continuity equation (4-24) are useful. We recall the continuity equation:

$$\frac{\partial S}{\partial \hat{t}} + \frac{\partial J}{\partial \hat{x}} = 0 \quad (4-24)$$

Substitution in the continuity equation

For this equation we make the following substitution:

$$\frac{\partial S}{\partial \hat{t}} + \frac{\partial J}{\partial S} * \frac{\partial S}{\partial \hat{x}} = 0 \quad (6-6)$$

The term $\partial J / \partial S$ is of special interest for the interpretation of the J-curve given in sect 6.3:

$$W = \frac{\partial J}{\partial S} \quad (6-7)$$

With (6-7) equ. (6-6) can be written:

$$\frac{\partial S}{\partial \hat{t}} + W * \frac{\partial S}{\partial x} = 0 \quad (6-8)$$

Interpretation of W

- (a) It is to be noted that W is also called "group velocity". [Pistiner2]. The concept of group velocity can evidently be related to electromagnetic waves.
- (b) Note that W especially describes the propagation of "iso-saturation lines" (lines in space where saturation remains constant). An example for iso-saturation lined is shown in Fig. 6-1: Lines for constant S on x,t-plane.
- (c) There is also a relation to the dimensionless quantities used for the Hele-Shaw cell (sect.2.2). In (2-8a) we introduced the reduced pressure, ϕ . Here (e.g. in case of an air/water interface) in the Hele-Shaw cell the condition for constant ϕ on the interface can be written:

$$\frac{\partial \phi}{\partial t} + v^* \nabla \phi = 0 \quad (6-9)$$

These are three relations useful for the discussion of W. This way it can be said that iso-saturation lines

Different behavior of flow of two phases

It can be stated that, in this model the following types of movements of two phases occur. We say that fuel has

- (1) a movement against the water flow, if $W > 0$,
- (2) a movement along the water flow, if $W < 0$.

Now from (6-8) we have

$$W = \frac{\partial J}{\partial s} \Big|_{\hat{t}} = - \frac{\frac{\partial s}{\partial \hat{t}} \Big|_{\hat{x}}}{\frac{\partial s}{\partial \hat{x}} \Big|_{\hat{t}}} \quad (6-10)$$

Note that the partial derivatives are for fixed values of \hat{t}, \hat{x} respectively. As will be seen in sect, 6.3, this relation gives interesting information on the J-curves.

Relation of J to functions f, g (4-35), (4-37)

The relation

$$J = \frac{s^* \hat{x}}{2^* \hat{t}} \quad (6-11)$$

can be shown using eqs(4-29), (4-39) (see also Appendix A1):

$$\hat{x} = \hat{t}^{1/2} \quad (4-29)$$

$$s = f^* \hat{t}^{-1/2} \quad (4-30)$$

Multiplying we obtain

$$s^* \hat{x} = \xi^* f \quad (6-12)$$

or evidently (6-11).

With (4-25) we also have

$$g = b^* \xi^* f \quad (4-35)$$

and with $b = 1/2$, we are at (4-34):

$$J = \frac{g}{\hat{t}} \quad (4-34)$$

These are important relations used for the GAUSS-program (see Appendix A5) for evaluation of the $J(S;\hat{t},Nc)$ -curve.

Additional relations for W (group velocity)

A second expression for W can be obtained, differentiating formula (6-11), which gives

$$W = U_s + S * \left. \frac{\partial U_s}{\partial S} \right|_{\hat{t}} \quad (6-13)$$

Here we introduce

$$U_s = \frac{\hat{x}}{2 * \hat{t}} \quad (6-14)$$

Note that the partial derivative is for a fixed value of \hat{t} , and that U_s is called "phase velocity" (or wave velocity ([Pistiner1])).

It is also to be noted that (6-13) has interesting connections to electromagnetic waves. Eq. (6-13) is formally the same expression als the equation showing the "group velocity" as a function of "phase velocity".

6.3 Some details of Js-flux curve

A few details of interpretation of flux curves are given here. It is to be noted, that some of statements, such as properties of group velocity W are based on sects. 6.1 and 6.2.

Description of curve

In Fig. 6-2 we can see that this curve can be divided in the following sections:

We start with A, then divide the curve in 4 sections:

A-B, B-C, D-C, A-C.

It can also be seen that for the points

B, C and D there is a horizontal and vertical tangent.

This will be related to the derivative $\partial J / \partial S$ which is equivalent to W.

Group velocity W

Recall the definition of W (6-10):

$$W = \frac{\partial J}{\partial S} \Big|_{\hat{t}} = \frac{\frac{\partial S}{\partial \hat{t}} \Big|_{\hat{x}}}{\frac{\partial S}{\partial \hat{x}} \Big|_{\hat{t}}} \quad (6-10)$$

With the r.h.s. of (6-10) the following statements can be made:

(a) The J-curve has a horizontal tangent ($W = 0$) if

$$\frac{\partial S}{\partial \hat{t}} \Big|_{\hat{x}} = 0 \quad (6-15a)$$

(b) The J-curve has a vertical tangent (W very large) if

$$\frac{\partial S}{\partial \hat{x}} \Big|_{\hat{t}} = 0 \quad (6-15b)$$

(c) Sign of W

it can be seen from the definition of W (6-10) that we have $W > 0$ if the conditions

$$\frac{\partial S}{\partial \hat{t}} > 0 \quad \text{and} \quad \frac{\partial S}{\partial \hat{x}} < 0 \quad (6-16a)$$

or if the conditions

$$-\frac{\partial S}{\partial \hat{t}} < 0 \quad \text{and} \quad \frac{\partial S}{\partial \hat{x}} > 0 \quad (6-16b)$$

hold. Similarly, we have $W < 0$ if the conditions (6-16c)

$$\frac{\partial S}{\partial \hat{t}} > 0 \quad \text{and} \quad \frac{\partial S}{\partial \hat{x}} > 0 \quad (6-16c)$$

or if the conditions (6-16d)

$$\frac{\partial S}{\partial \hat{t}} < 0 \quad \text{and} \quad \frac{\partial S}{\partial \hat{x}} < 0 \quad (6-16d)$$

hold. As will be confirmed in sect. 7, by some 3-dimensional representations, there exist pairs of $(\partial S / \partial \hat{t}$ and $\partial S / \partial \hat{x})$, which cause in various ways $W > 0$ or $W < 0$.

6.4 Interpretation of various conditions of flow

Flow direction

In (6-10) to (6-16) we see that W (group velocity) depends on the quantities

$$\frac{\partial S}{\partial \hat{x}} \quad \text{and} \quad \frac{\partial S}{\partial \hat{t}}$$

Assume now a saturation curve S which presents the injection of a fuel at a permanent point source at x_0 with a water flow in the porous medium in the x -direction only (from left to right, at a fixed time \hat{t}_1).

Then we have, under the condition $\partial S / \partial \hat{t} < 0$, as is shown in Fig. 6-3, the following two cases:

- (a) For the fuel which is flowing against the water flow, i.e. on the left of the point-source, x_0 , we have

$$\left. \frac{\partial S}{\partial \hat{x}} \right|_{\hat{t}_1} > 0 \quad (6-17a)$$

- (b) For the fuel which is flowing in the same direction as the water flow, i.e. on the right of the point source, x_0 , we have

$$\left. \frac{\partial S}{\partial \hat{x}} \right|_{\hat{t}_1} < 0 \quad (6-17b)$$

This evidently leads to a increasing and decreasing W-curve.

Note:

Similar considerations can also be made for other conditions, leading to various pairs of $(\partial S / \partial \hat{t}, \partial S / \partial \hat{x})$, with the 3-dimensional representation of $S(\hat{x}, \hat{t})$ in sect. 7.

Relations to drainage and to imbibition

As can be seen from the literature [Pristiner1], the sections of of the J - curve are related with

- drainage (oil pushes water)
- imbibition (water pushes oil),

see sect. 3.1. It is also interesting to make the following consideration. It has to be noted, that the following is only an illustration, but not a derivation of this type of an interpretation.

As can be seen in Fig. 6-4, there is a relation between saturation S and capillary pressure, also based on experiments [Sahimi]. Similar considerations apply to relations of the saturation and relative permeability K_r (see Appendix A4). It can be seen, that for different values of saturation S various mechanisms occur, such as drainage and imbibition. In Fig. 6-4 we also note, that different mechanisms, such as

- drainage
- spontaneous imbibition
- forced imbibition

occur in sequence.

Since also flux J is again related to the relative permeability K_r , this gives us a plausible interpretation of the mechanism related to various parts of our J-curve.

Different entries of Table 6-1

Now the collums of Table 6-1 will be listed, to be considered with the curve in Fig.6-2. All this is required for the interpretation of the results given in Figs. 6-5.

- (1) collumn 1: parts of J-scurve are indicated (see Fig. 6-2)
- (2) collumn 2: describes curve (increasing, decreasing, tangents)
- (3) collumn 3: gives group velocity W, defined in (6-10)
- (4) collumn 4: describes iso-saturation lines (6-9a), (6-9b)
- (5) collumn 5: gives $\partial S / \partial \hat{t}$ (6-10); (6-15), (6-16)
- (6) collumn 6: gives $\partial S / \partial \hat{x}$ (6-10); (6-15), (6-16)
- (7) collumn 7: states if water/oil is in same direction or not
- (8) collumn 8: states if oil pushes water (drainage) or if water pushes oil (imbibition).

Table 6.1 referring to Js-flux curve

(1)	(2)	(3)	(4)	(5)	(6)	(7)	(8)
parts of Js curve	Js flux-curve	W group-vel.	move of iso-satur. lines	$\frac{\partial S}{\partial t}$	$\frac{\partial S}{\partial x}$	water/oil	imbib. or drain
A	incr. and decr.	> 0 and < 0	-	not 0	not 0	-	-
A-B	incr.	> 0	against water-flow	< 0 - - - or - - - > 0	> 0 - - - or - - - < 0	→ ←	oil pushes water (drain)
B	horiz.	= 0	-	= 0	not 0	-	-
B-C	decr.	< 0	along water-flow	< 0 - - - or - - - > 0	< 0 - - - or - - - > 0	→ →	water pushes oil (imbib)
C	vert.	= ∞ (*)	-	not 0	= 0	-	-
D-C	incr.	> 0	against water-flow	< 0 - - - or - - - > 0	> 0 - - - or - - - < 0	→ ←	water pushes oil (imbib)
D	horiz.	= 0	-	= 0	not 0	-	-
A-D	decr.	< 0	along water-flow	< 0 - - - or - - - > 0	< 0 - - - or - - - > 0	→ →	oil pushes water (drain)

(*) Note:
 $W = \infty$ just is due to the vanishing of the denominator in (6-10).

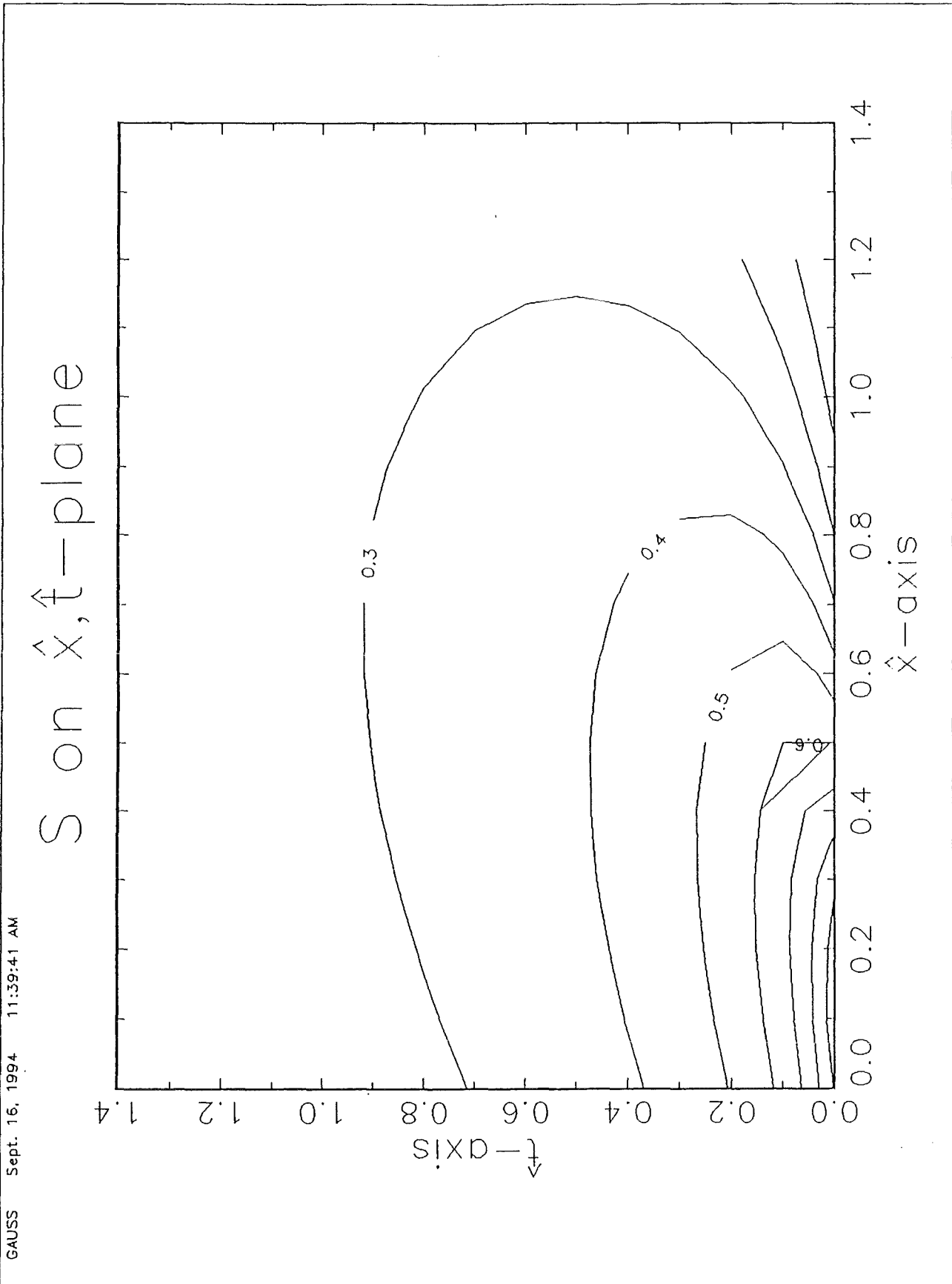
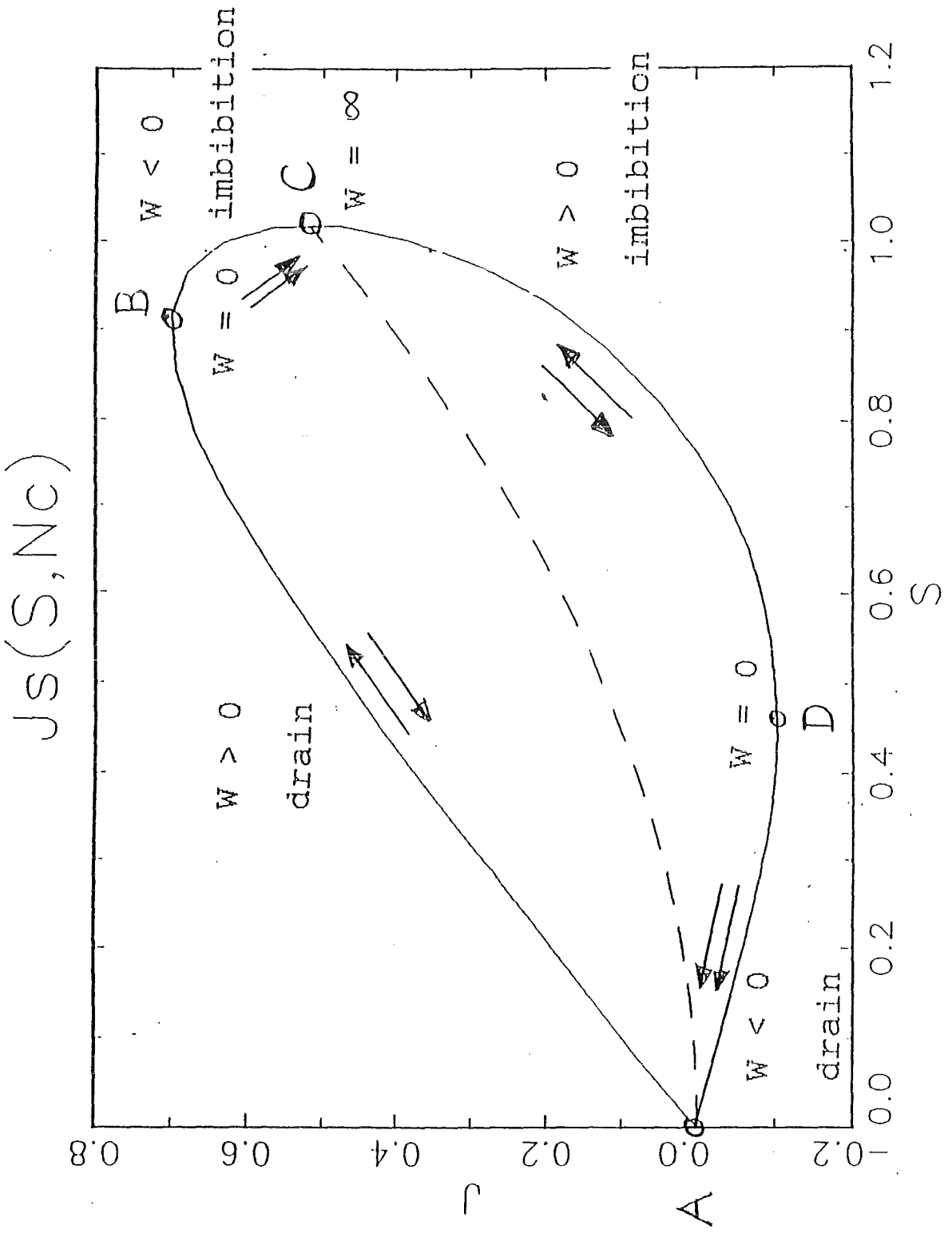


Fig. 6-1 Isosaturation lines (in \hat{x} - \hat{t} plane)



GAUSS July 15, 1994 10:40:48 AM

Fig. 6-2 Mechanisms related to parts of flux curve

Saturation S

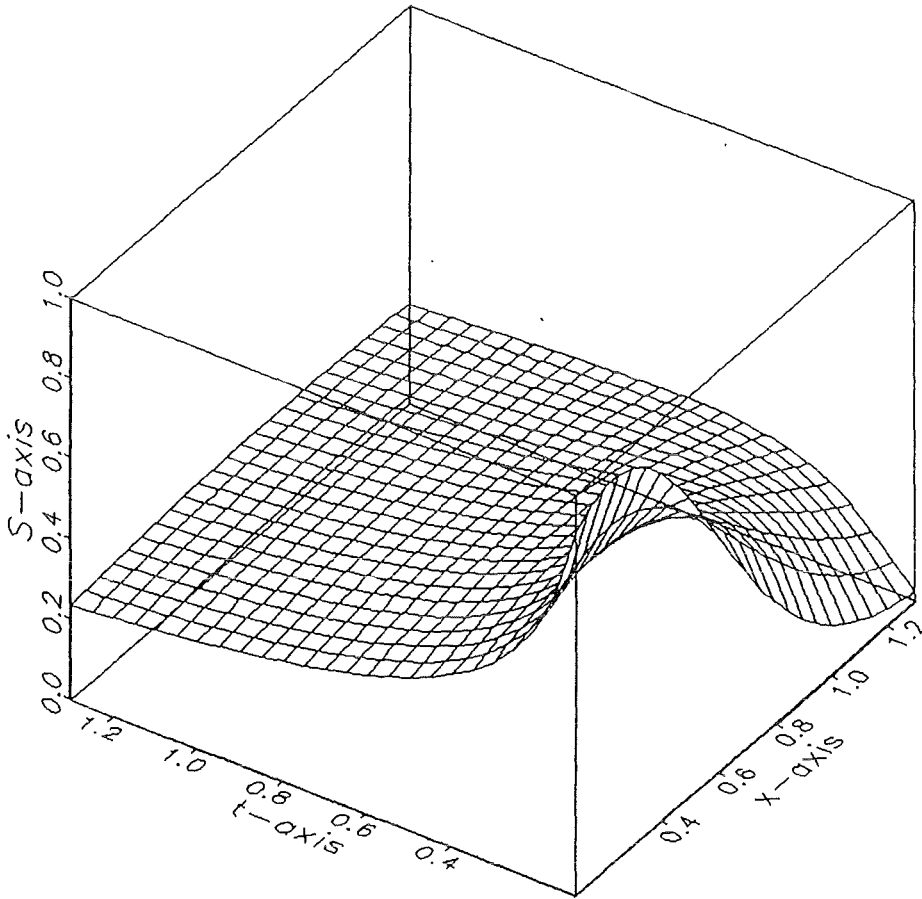


Fig. 6-3 Increase and decrease of Saturation $S(x, t)$

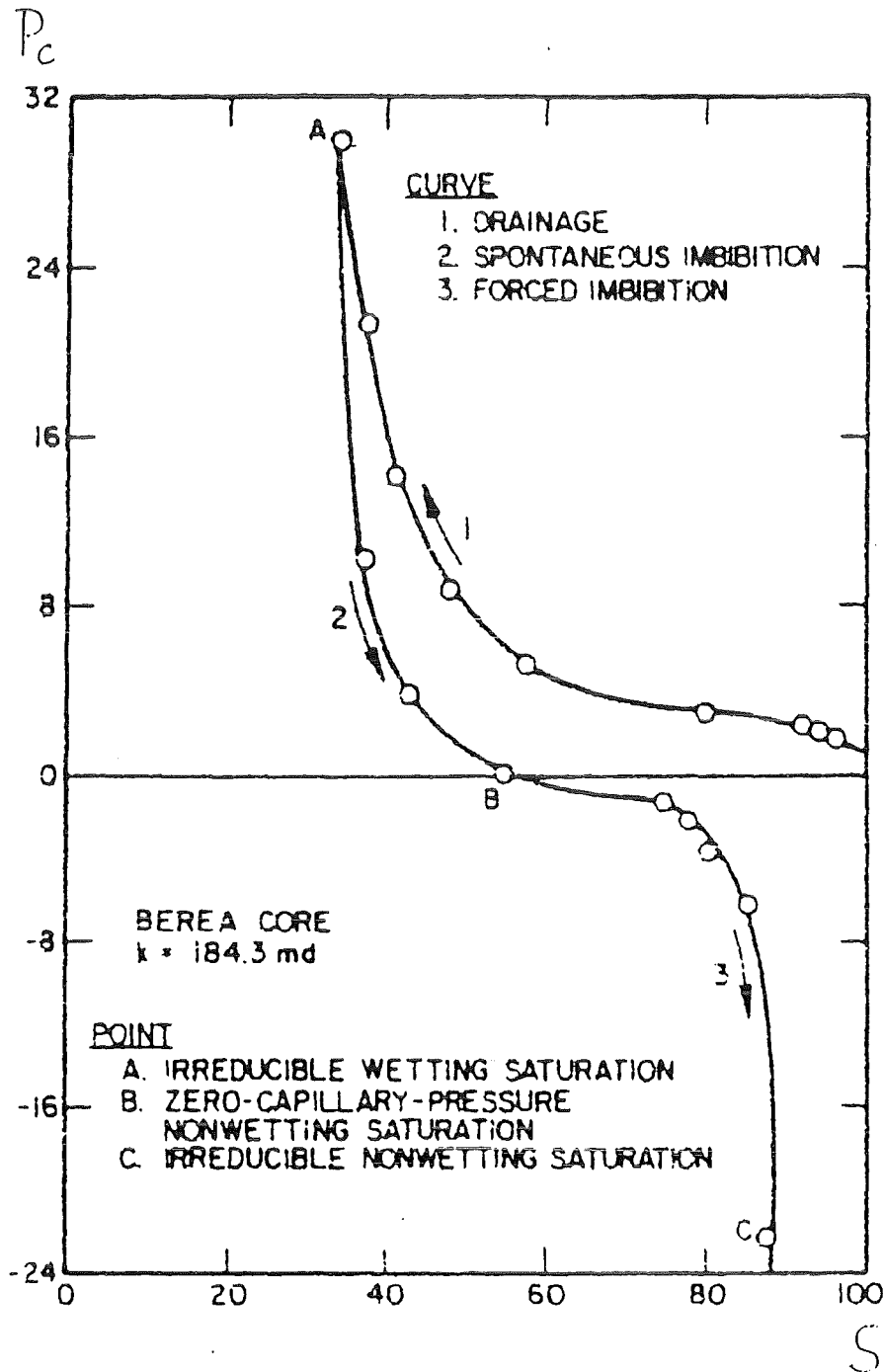


Fig. 6-4 An example for the following relations:

- (a) water saturation S (in percent) and
- (b) capillary pressure P_c

6.5 Figures and Tables

Here results for the fuel saturation flux J are shown. This gives some examples for the function (6-5):

$$J = \hat{t}^{-1/2} * S - (1/Nc) * \frac{\partial S}{\partial \hat{x}} \tag{6-5}$$

For a number of different values of Nc and t we show results in Figures and Tables. Note also that in Fig. 6-5 a series of f(ξ)-curves ist presented.

RESULTS

		$\hat{t} = 1, 2, 3, 4, 5, 6$
Nc = 0.5	Fig. 6-6	Table 6-2
1	Fig. 6-7	
2	Fig. 6-8	
4	Fig. 6-9	Table 6-3
6	Fig. 6-10	
8	Fig. 6-11	
10	Fig. 6-12	Table 6-4
20	Fig. 6-13	
30	Fig. 6-14	

6.6 Interpretation of the results

We note from the figures and tables the following:

- (1) If Nc is constant, and t increases, the dimensions of the curve decrease, including the maxima, see Figs. 6-6 to 6-14.
- (2) If t is constant, and Nc increases, the dimensions of the curve increase, including the maxima. This is closely related to the results of sect. 5, see Figs. 6-6 to 6-14.
- (3) At the same time also the shapes of the curve change (all Figures of sect. 6).

- (4) For horizontal/vertical tangents we have a change in the mechanisms
 - (a) from drain to imbibition (see Fig. 6-2 point B)
 - (b) from imbibition to drain (see Fig. 6-2 point D)
 - (c) there are also changes of the direction of the movement for iso-saturation lines (see Fig.6-2, and Table 6-1).

- (5) It can be seen (Figs. 6-6 to 6-14), that with increasing N_c , close, i.e. points B and D become increasingly close (i.e. the coordinates for change in the mechanisms).

Note: For the curves shown in sect. 6 and the coordinates given in Tables of sect. 6, a GAUSS computer program was used, which is given in Appendix A5. For information on the program see [GAUSS].

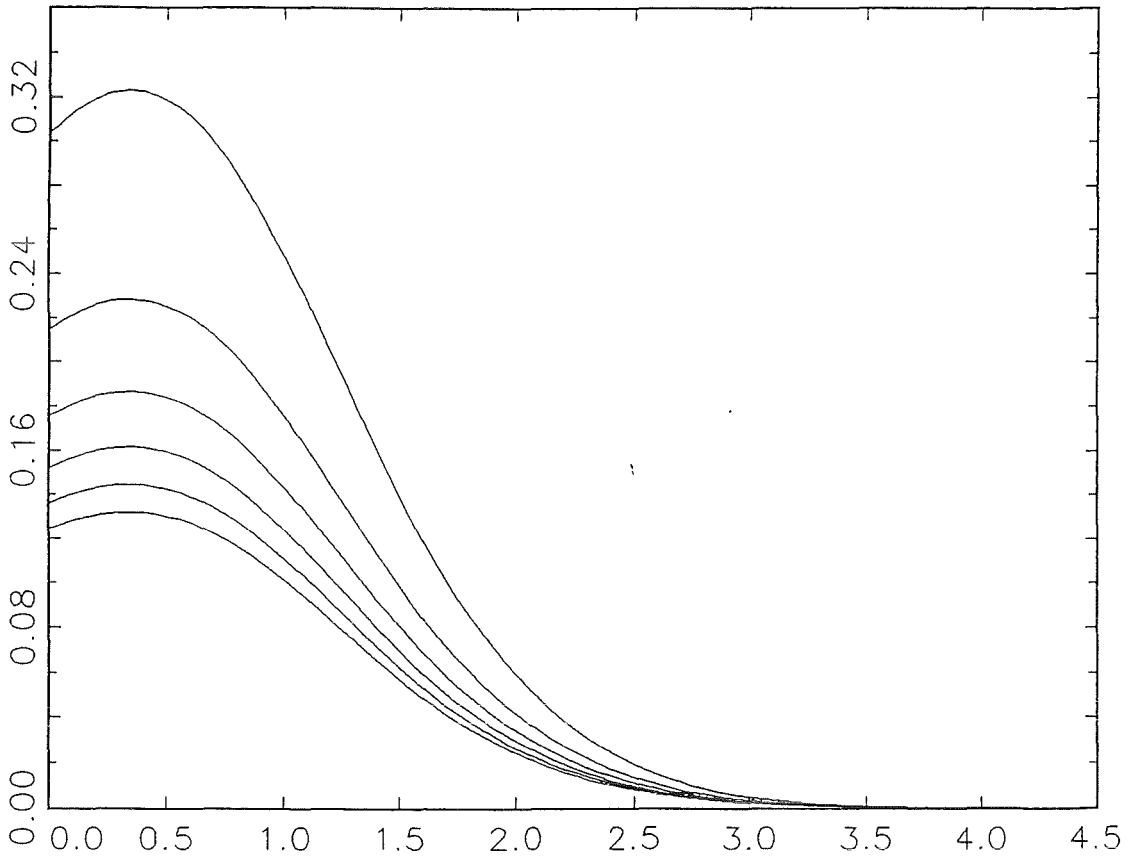


Fig. 6-5 Saturation $S(\hat{x}; Nc)$ dependent on Nc

$^{-76}\text{I}_s(\text{Se})$

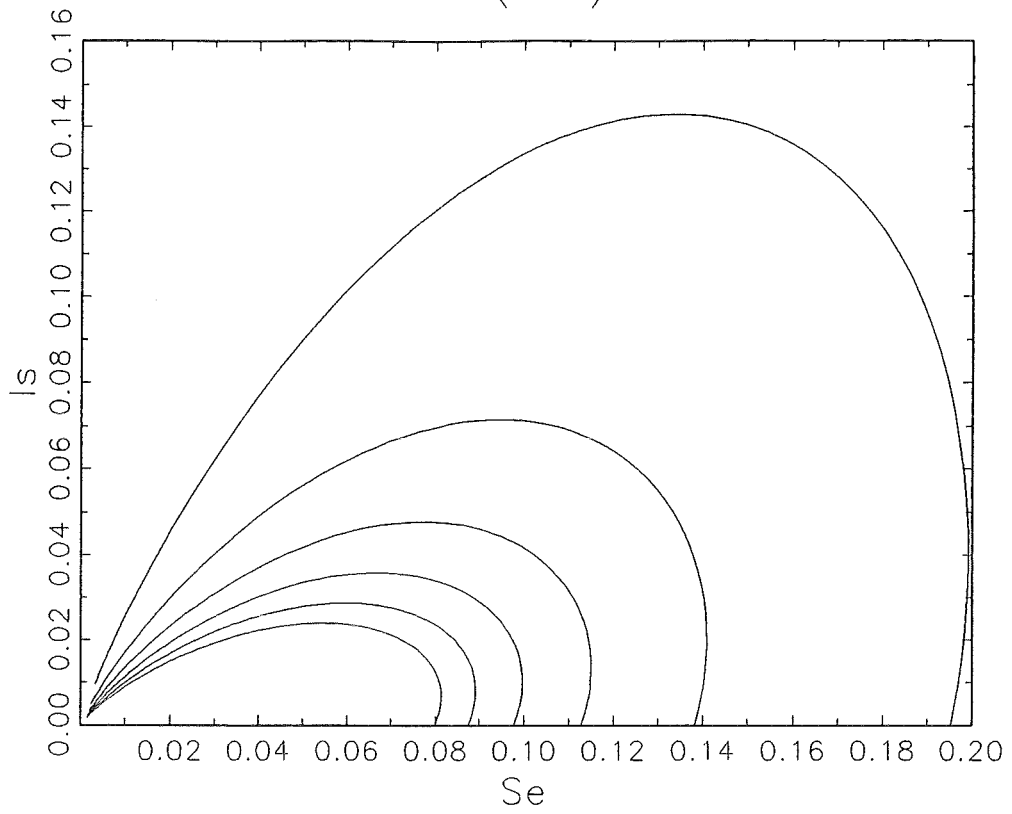


Fig. 6-6 Flux $I_s(\text{Se})$, $N_c = 0.5$, $t = 1, 2, \dots, 6$

-77-
 $I_s(\text{Se})$

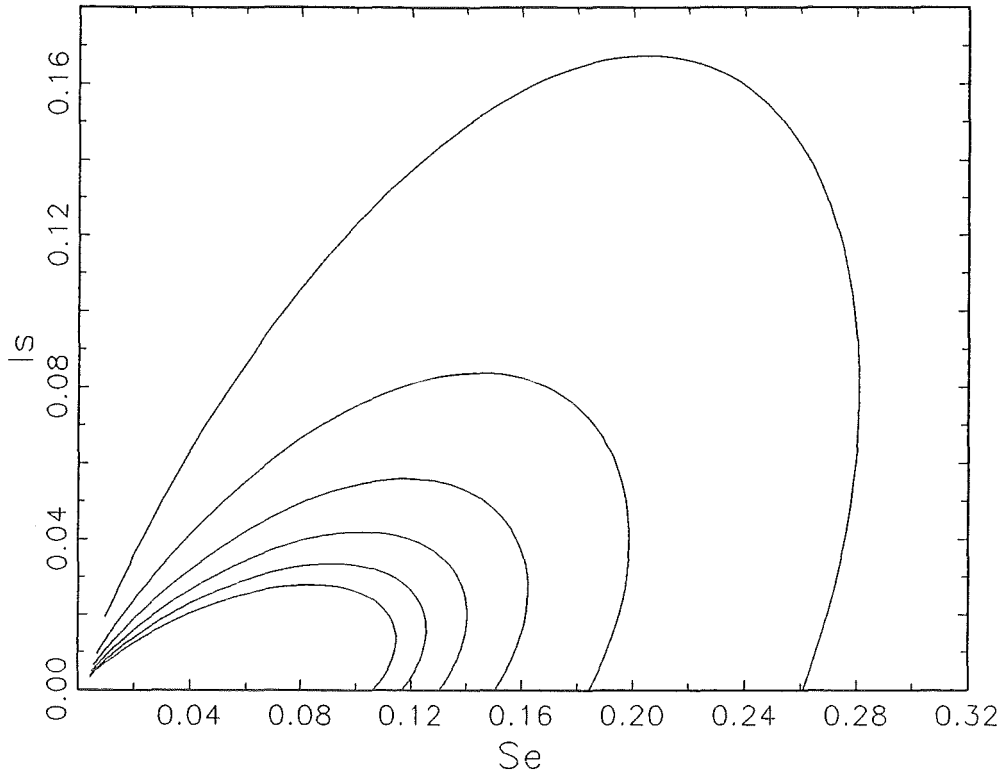


Fig. 6-7 Flux $I_s(\text{Se})$, $N_c = 1$, $t = 1, 2, \dots, 6$

-78-
 $I_s(\text{Se})$

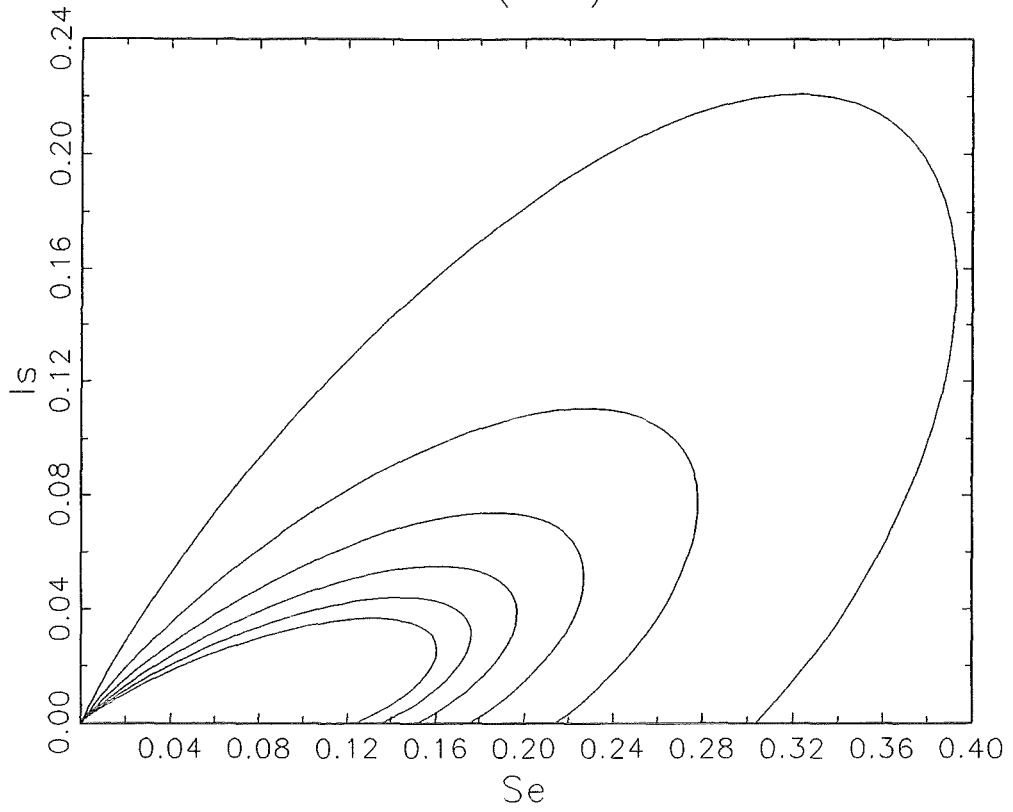


Fig. 6-8 Flux $I_s(\text{Se})$, $N_c = 2.0$, $t = 1, 2, \dots, 6$

$I_s(\text{Se})$

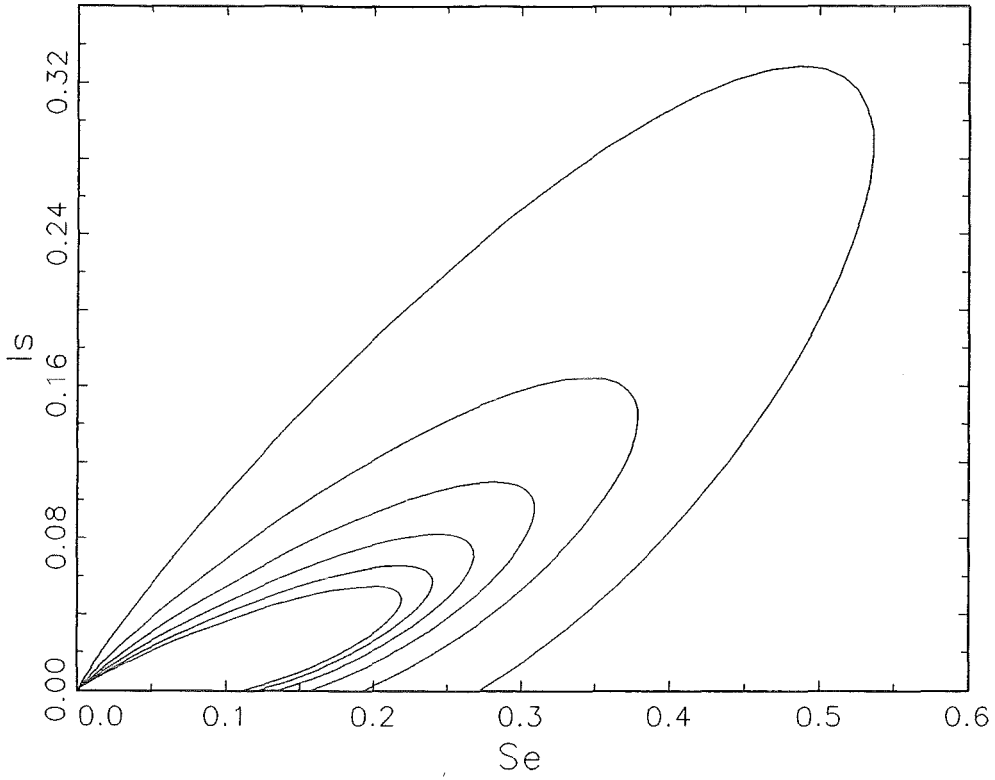


Fig. 6-9 Flux $I_s(\text{Se})$, $N_c = 4.0$, $t = 1, 2, \dots, 6$

-80- $I_s(\text{Se})$

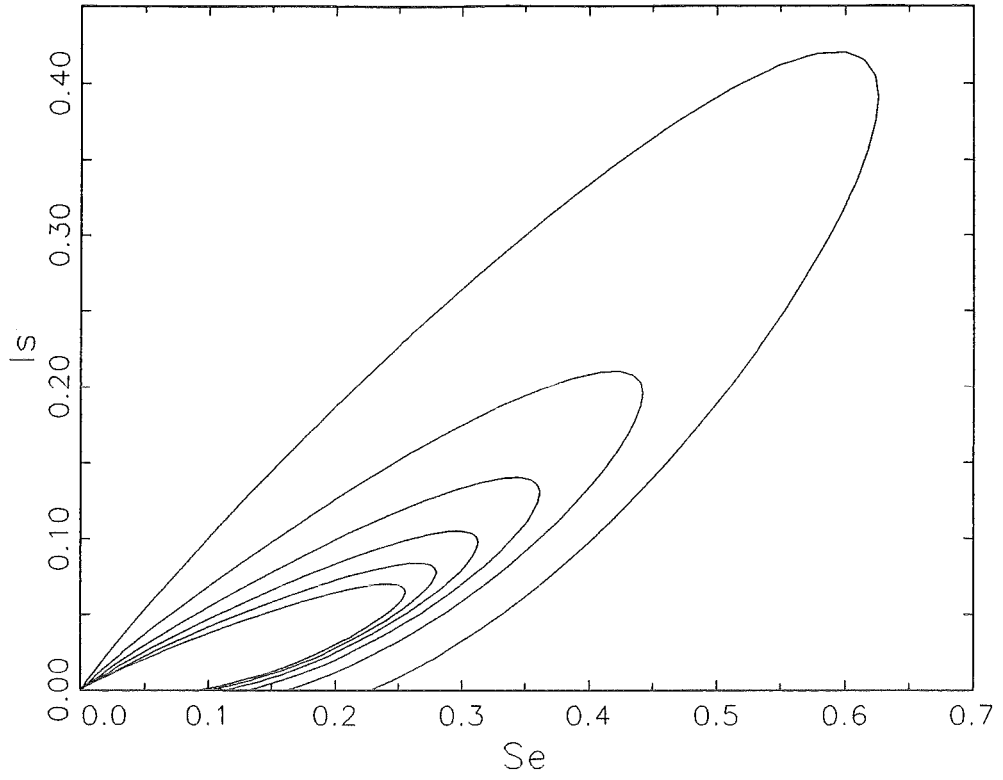


Fig. 6-10 Flux $I_s(\text{Se})$, $N_c = 6.0$, $t = 1, 2, \dots, 6$

$I_s(\text{Se})$

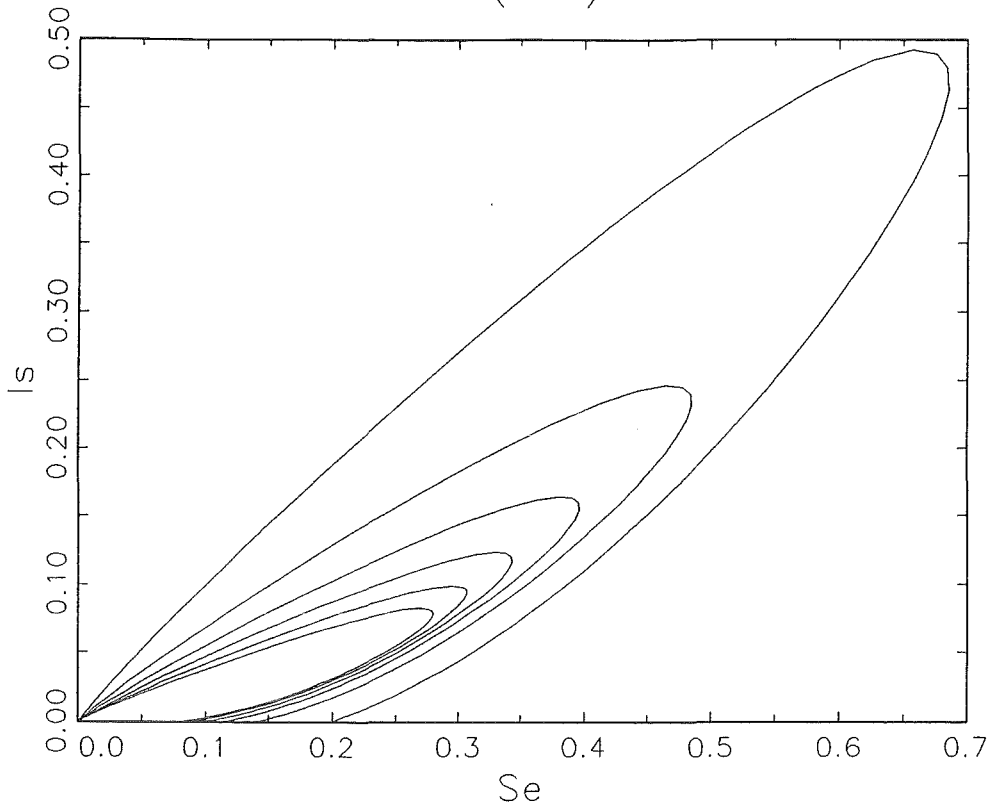


Fig. 6-11 Flux $I_s(\text{Se})$, $N_c = 8.0$, $t = 1, 2, \dots, 6$

Is(Se)

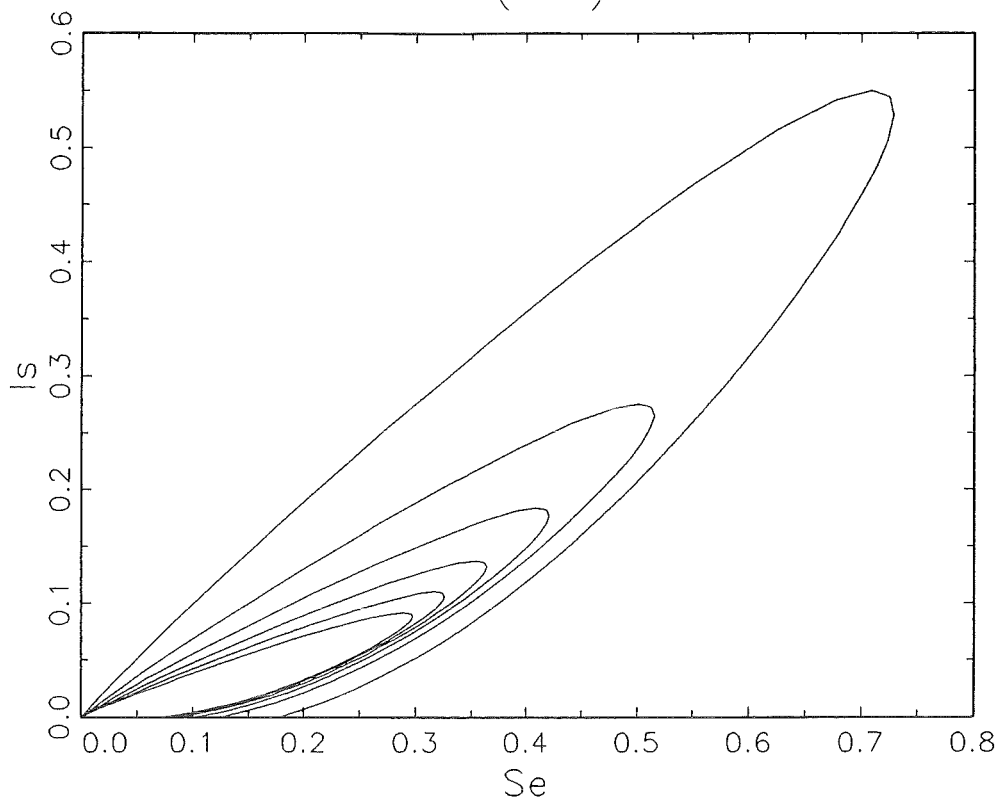


Fig. 6-12 Flux Is(Se), Nc = 10.0, t = 1,2,...,6

EXTREMA OF Is-CURVE

Nc = 0.500

time t	max(Se)	Is(Se)
1.00	0.199	0.0397
2.00	0.141	0.0199
3.00	0.115	0.0132
4.00	0.010	0.0099
5.00	0.089	0.0079
6.00	0.081	0.0066

EXTREMA OF Is-CURVE

Nc = 1.00

time t	max(Se)	Is(Se)
1.00	0.281	0.0790
2.00	0.199	0.0395
3.00	0.162	0.0263
4.00	0.141	0.0197
5.00	0.126	0.0158
6.00	0.115	0.0132

EXTREMA OF Is-CURVE

Nc = 2.00

time t	max(Se)	Is(Se)
1.00	0.393	0.155
2.00	0.278	0.0773
3.00	0.227	0.0515
4.00	0.197	0.0387
5.00	0.176	0.0309
6.00	0.161	0.0258

Table 6-2 Extrema of Is-curves

EXTREMA OF Is-CURVE
Nc = 4.00

time t	max(Se)	Is(Se)
1.00	0.536	0.287
2.00	0.379	0.143
3.00	0.309	0.0956
4.00	0.268	0.0717
5.00	0.240	0.0574
6.00	0.219	0.0478

EXTREMA OF Is-CURVE
Nc = 6.00

time t	max(Se)	Is(Se)
1.00	0.625	0.391
2.00	0.442	0.195
3.00	0.361	0.130
4.00	0.313	0.0977
5.00	0.280	0.0782
6.00	0.255	0.0652

EXTREMA OF Is-CURVE
Nc = 8.00

time t	max(Se)	Is(Se)
1.00	0.685	0.469
2.00	0.484	0.235
3.00	0.396	0.156
4.00	0.343	0.117
5.00	0.306	0.0939
6.00	0.280	0.0782

Table 6-3 Extrema of Is-curves

EXTREMA OF Is-CURVE

Nc = 10.0

time t	max(Se)	Is(Se)
1.00	0.729	0.531
2.00	0.515	0.266
3.00	0.421	0.177
4.00	0.364	0.133
5.00	0.326	0.106
6.00	0.298	0.0885

EXTREMA OF Is-CURVE

Nc = 20.0

time t	max(Se)	Is(Se)
1.00	0.834	0.696
2.00	0.590	0.348
3.00	0.482	0.232
4.00	0.417	0.174
5.00	0.373	0.139
6.00	0.341	0.116

EXTREMA OF Is-CURVE

Nc = 30.0

time t	max(Se)	Is(Se)
1.00	0.782	0.611
2.00	0.553	0.306
3.00	0.451	0.204
4.00	0.391	0.153
5.00	0.350	0.122
6.00	0.319	0.102

Table 6-4 Extrema of Is-curves

7. Change from similarity solution to saturation

7.1 Introduction

We have seen a number of physical properties for two phase flow in porous media by means of the similarity solution (see sect. 4, 5, 6). Here we show explicitly the saturation S . On the basis of $f(\xi)$, the similarity solution (sect. 4.6), we obtain by a suitable transformation $S(\hat{x}, \hat{t})$, a function of \hat{x}, \hat{t} . We note that we use, for simplicity (if not otherwise stated) \hat{x}, \hat{t} , the dimensionless coordinates.

7.2 The transformation of the similarity solution

Based on the similarity transformations as given in equations (4-29), (4-30) and the similarity solution, as given in equations (4-37)-(4-41) the saturation can be evaluated as follows.

$$= \hat{x} \hat{t}^{-1/2} \tag{7-1}$$

with

ξ similarity variable
 \hat{x}, \hat{t} dimensionless coordinates.

And also

$$S(\hat{x}, \hat{t}) = \hat{t}^{-1/2} * f(\xi) \tag{7-2}$$

with

$S(\hat{x}, \hat{t})$ saturation
 $f(\xi)$ similarity solution.

Now we substitute the dimensionless variables \hat{x}, \hat{t} into the similarity solution obtained from (4-41) and obtain with (7-2) (7-3)

$$f(\xi) = \frac{\exp(- (1/4) * Nc * \xi^2)}{(\gamma * Nc)^{1/2} * \left[(1 / (\tanh((1/2) * Nc) - \operatorname{erf}((Nc/2) * \xi)) \right)} \tag{7-3}$$

Using (7-1) and (7-2) we obtain $S(\hat{x}, \hat{t})$.

$S(\hat{x}, \hat{t}) =$

$$\hat{t}^{-1/2} \frac{\exp(- (1/4) * Nc * \hat{x}^2 * (\hat{t})^{-1})}{(\pi * Nc)^{1/2} * \left((1/\tanh((1/2) * Nce) - \operatorname{erf}((Nc/2) * \hat{x} * \hat{t}^{-1/2})) \right)} \quad (7-4)$$

As can be seen in Appendix A5, this transform is introduced in the GAUSS-program, which gives explicitly the values for $S(\hat{x}, \hat{t})$. For saturation $S(\hat{x}, \hat{t})$ various diagrams are given in sect. 7.3.

7.3 Figures and Tables for saturation $S(x, t)$

We present the following diagrams, also noting the parameters. Here two things should be noted;

- (1) All coordinates \hat{x}, \hat{t} are dimensionless coordinates. Thus S-values differ by a constant factor from calculations which could be made with dimensioned variables such as x, t .
- (2) As can be seen, also parameters like Nc have been changed. Clearly, here variations, similar to the variations shown in sect. 4, 5, 6 will occur. See also sect. 7.4 regarding the short time behavior of the similarity solution.

We have the following types of figures:

- (a) Here $S(\hat{x}, \hat{t})$ is shown in 3-D diagrams.
- (b) Here the projection of lines for constant $S(x, t)$ are shown in the \hat{x}, \hat{t} -plane (isosaturation lines)
- (c) $S(\hat{x})$ for varying \hat{x} and fixed \hat{t}
 $S(\hat{t})$ for varying \hat{t} and fixed \hat{x}

Here $(i, j) = (1, 1)$ denotes \hat{x} low, \hat{t} low,
 and $(i, j) = (25, 25)$ denotes \hat{x} high, \hat{t} high.

Note:

It can be seen, that the curves $S(\hat{x}), S(\hat{t})$ are obtained from the 3-D diagrams, fixing \hat{t} and fixing \hat{x} respectively.

Now the Figures, showing the results are listed in more detail.

Nc	(a)	(b)	(c)	
	3D	proj.	\hat{x} -axis	\hat{t} -axis
0.5	Fig.7-1	Fig.7-2	Fig.7-3 Fig.7-5	Fig.7-4 Fig.7-6
1.0	: Fig.7-7	Fig.7-8	Fig.9-9 Fig.7-11	Fig.7-10 Fig.7-12
2.0	Fig.7-13	Fig.7-14	Fig.7-15 Fig.7-17	Fig.7-16 Fig.7-18
4.0	Fig.7-19	Fig.7-20	Fig.7-21 Fig.7-23	Fig.7-22 Fig.7-24

Table 7-1 Figures for different types for $S(\hat{x}, \hat{t})$

Note:

In Appendix A5 the program used for the calculations is shown in detail, see also [GAUSS] for information on the program system.

7.4 Limits of similarity solution (short time behavior)

It has to be noted as can be seen from (7-4), that for $t \rightarrow 0$ the solution $S(x, t)$ has a singularity. It can be seen solution (7-4) does not generally represent the behavior of the two-phase system (see also [Pistiner1]). For longer times the solution (7-4) approaches the real solution of the problem. It may be noted, that for some exponents, m, n , (introduced in (4-18) and (4-20), if not $m = n$ holds, this singularity does not exist. It is out of the scope of this research to discuss the type of convergence of the usual similarity solution.

In figures of section 7 the singularity is not graphically shown, which would give a serious distortion of the long-time behavior.

Saturation S

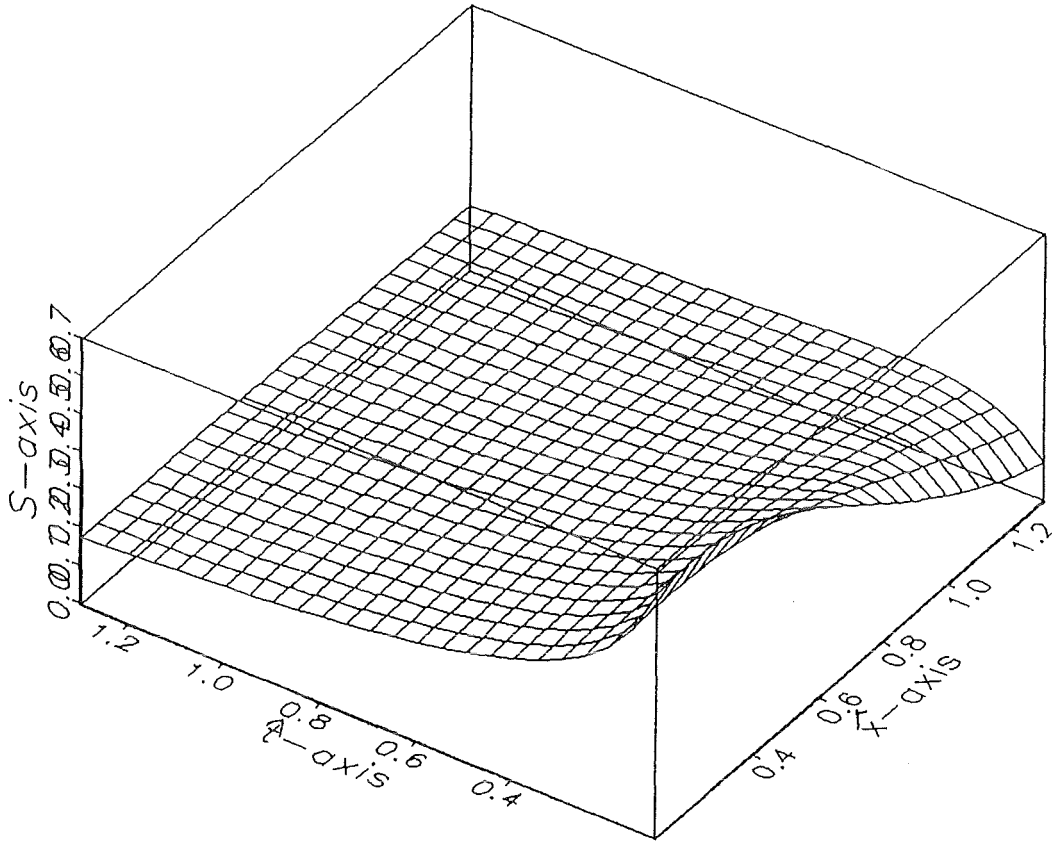


Fig. 7-1 Saturation $S(\hat{x}, \hat{t})$ in 3-D, $Nc = 0.5$

S on \hat{x}, \hat{t} -plane

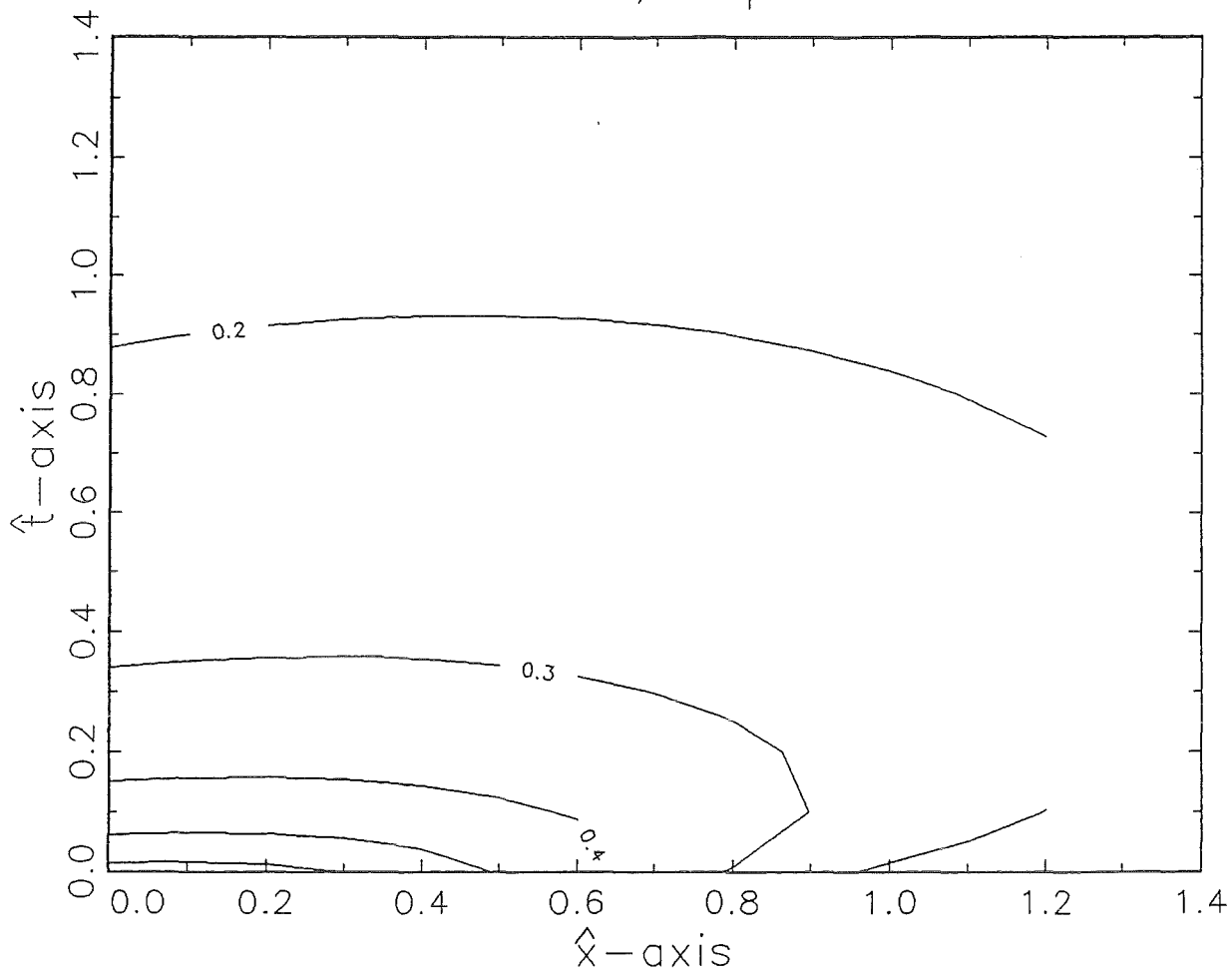


Fig. 7-2 Projection of $s(\hat{x}, \hat{t})$ on \hat{x} - \hat{t} -plane

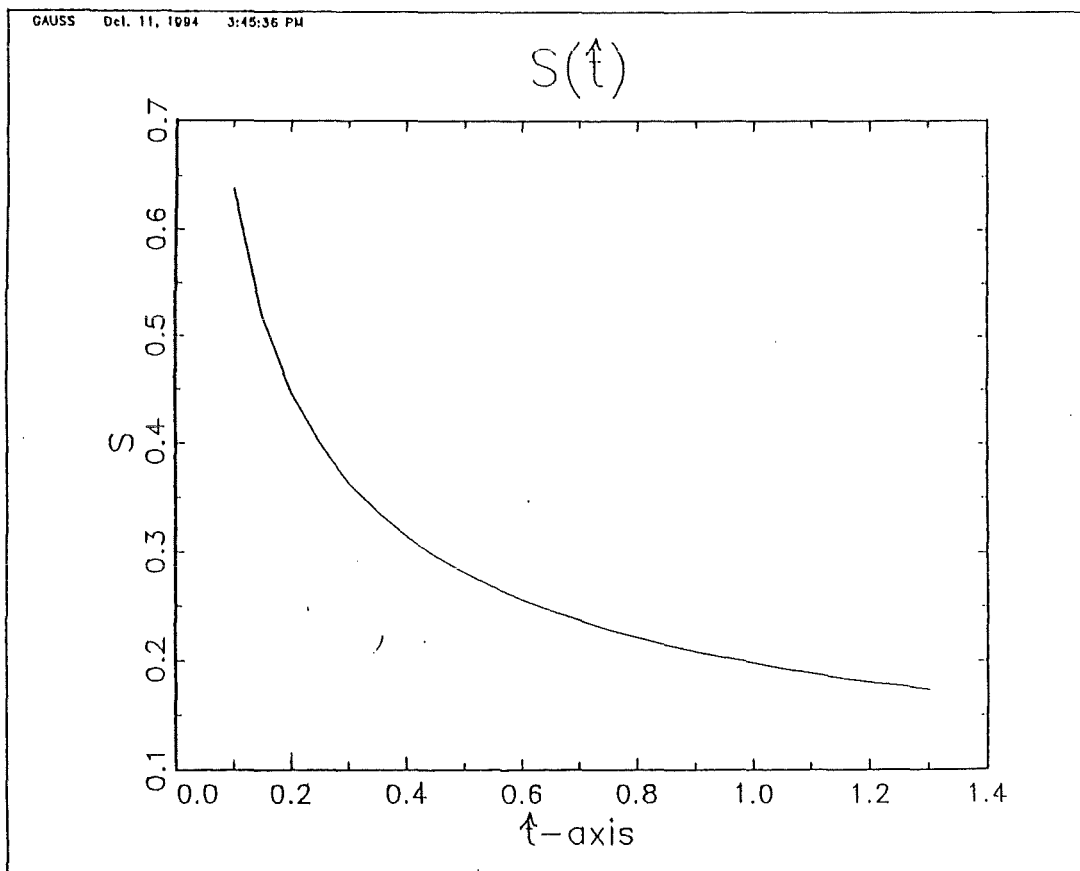
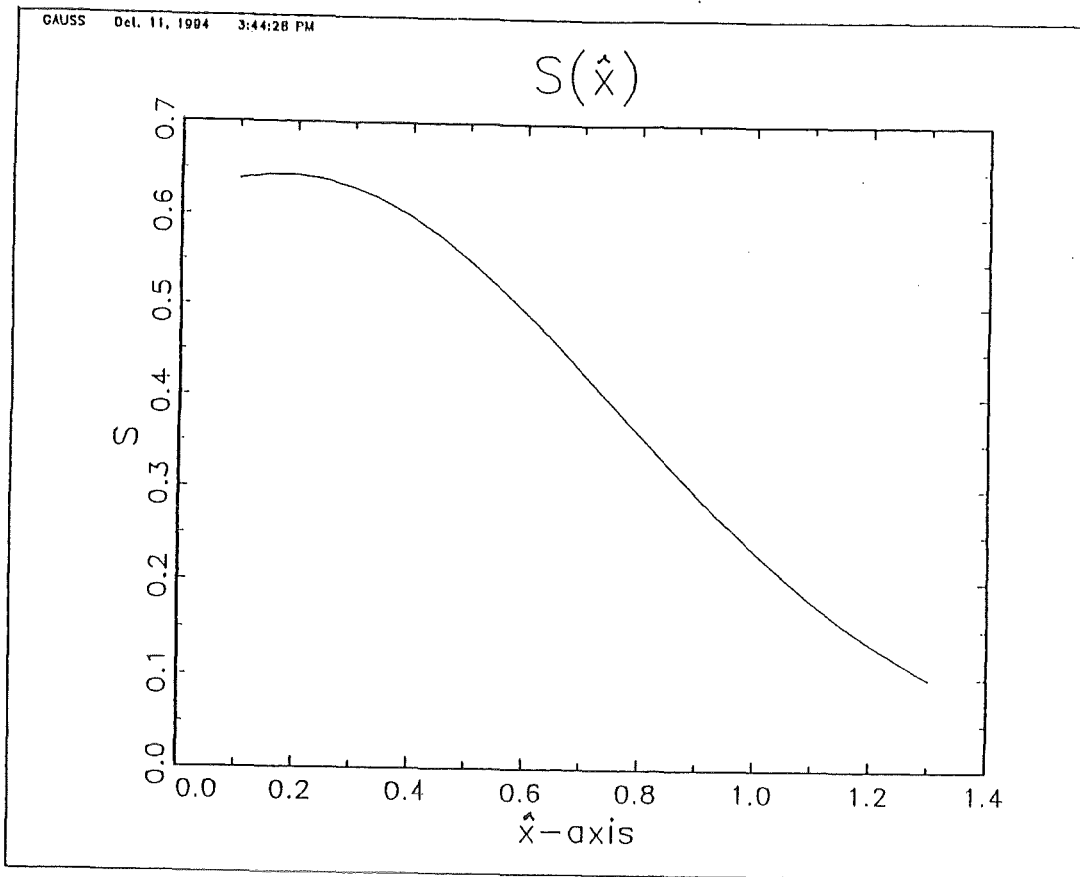


Fig. 7-3 $S(\hat{x}, \hat{t})$ on \hat{x} -axis | $Nc = 0.5$
----- | $(i, j) = (1, 1)$
Fig. 7-4 $S(\hat{x}, \hat{t})$ on \hat{t} -axis

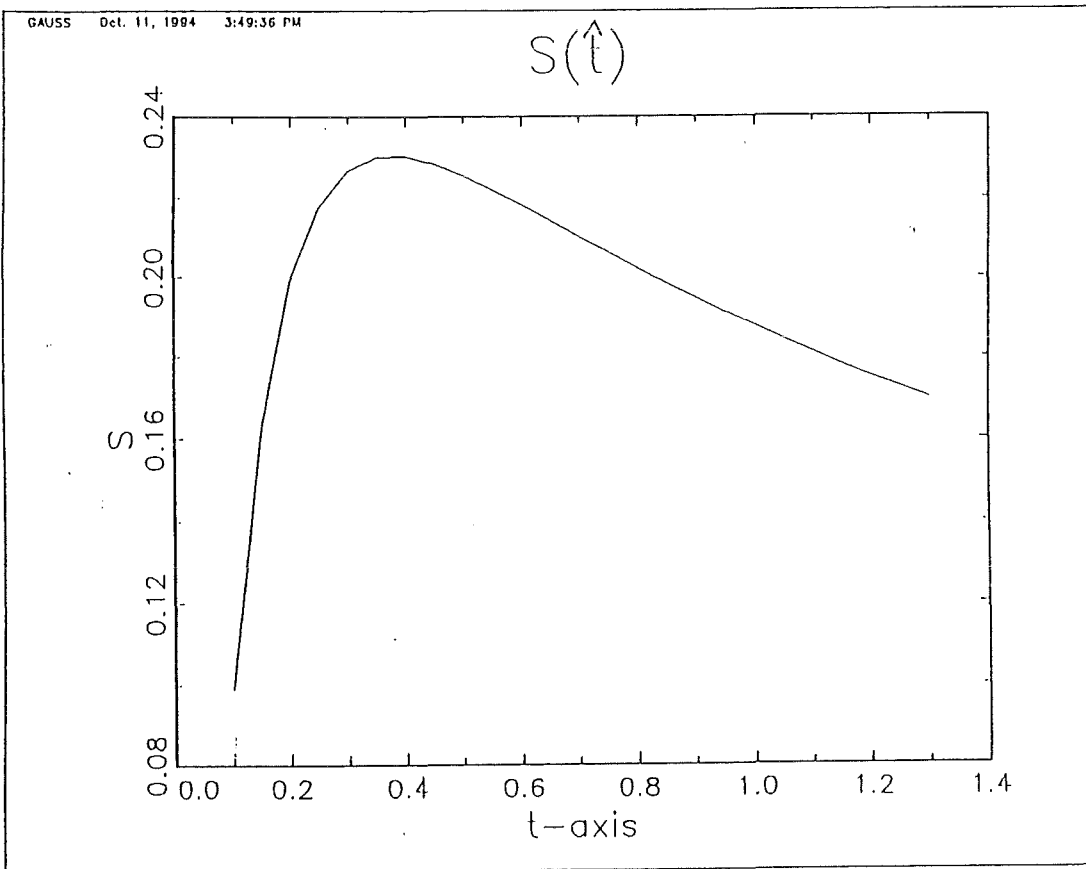
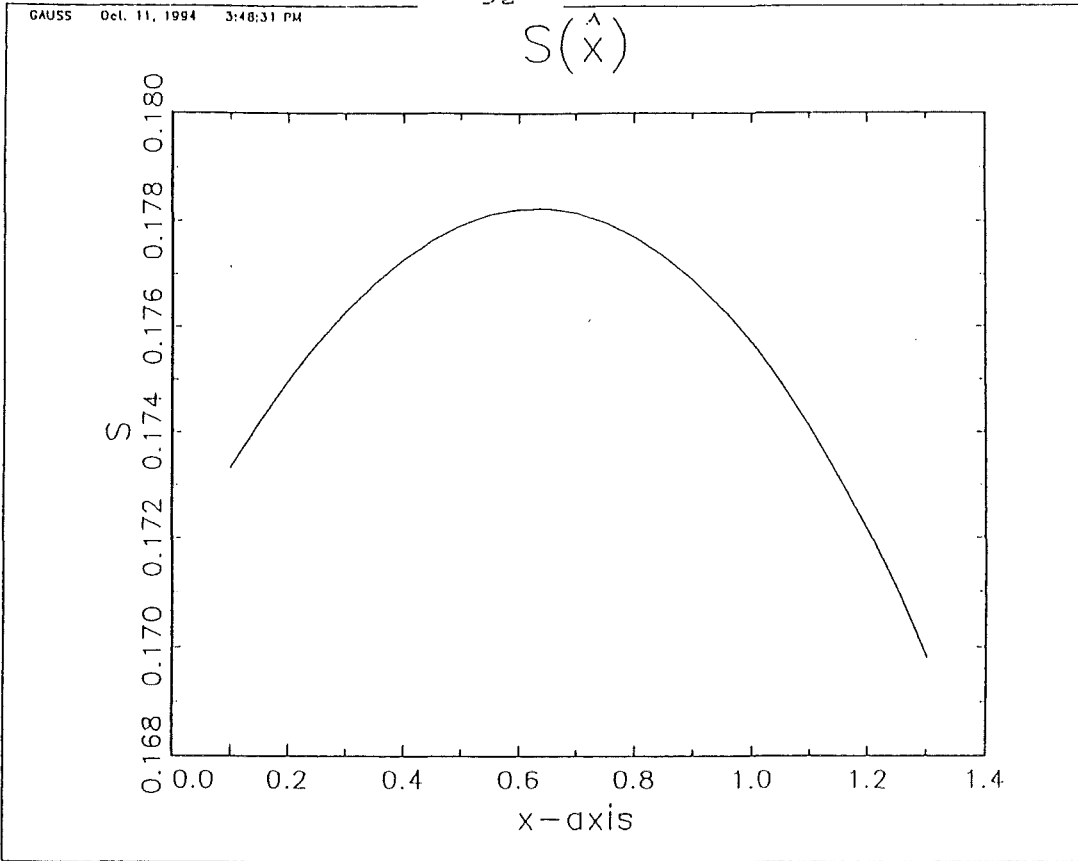


Fig. 7-5 $S(\hat{x}, \hat{t})$ on \hat{x} -axis | $Nc = 0.5$
----- | $(i, j) = (25, 25)$
Fig. 7-6 $S(\hat{x}, \hat{t})$ on \hat{t} -axis |

Saturation S

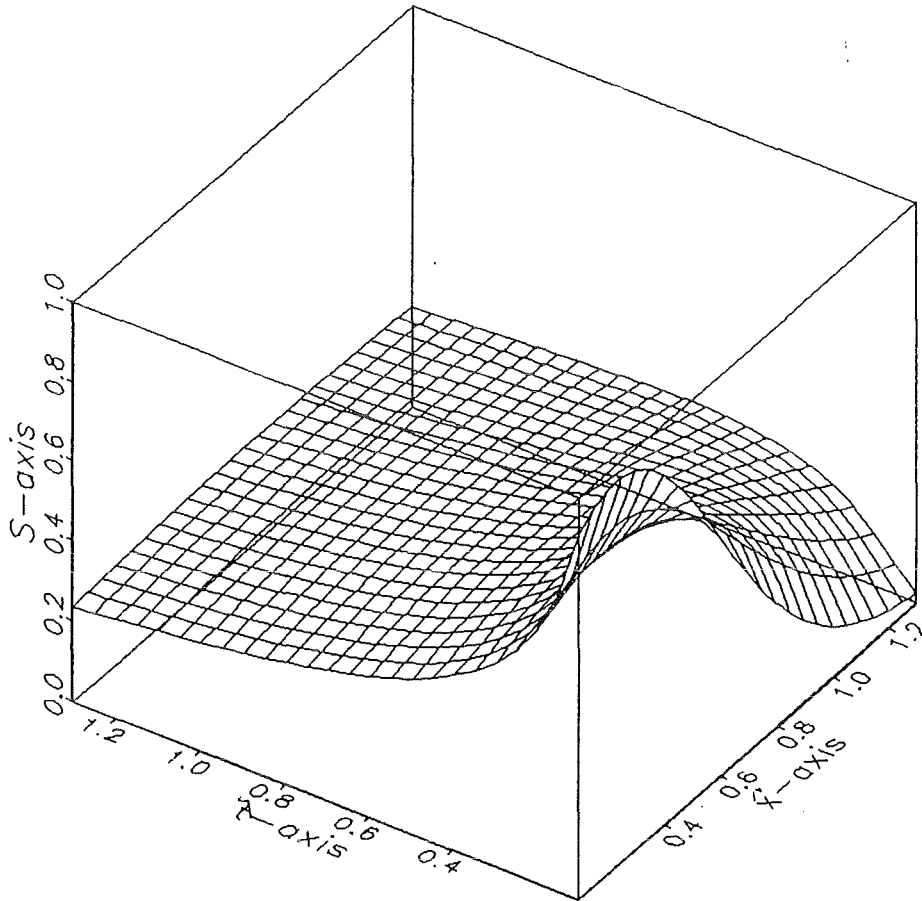


Fig. 7-7 Saturation $S(\hat{x}, \hat{t})$ in 3-D, $N_c = 1.0$

S on \hat{x}, \hat{t} -plane

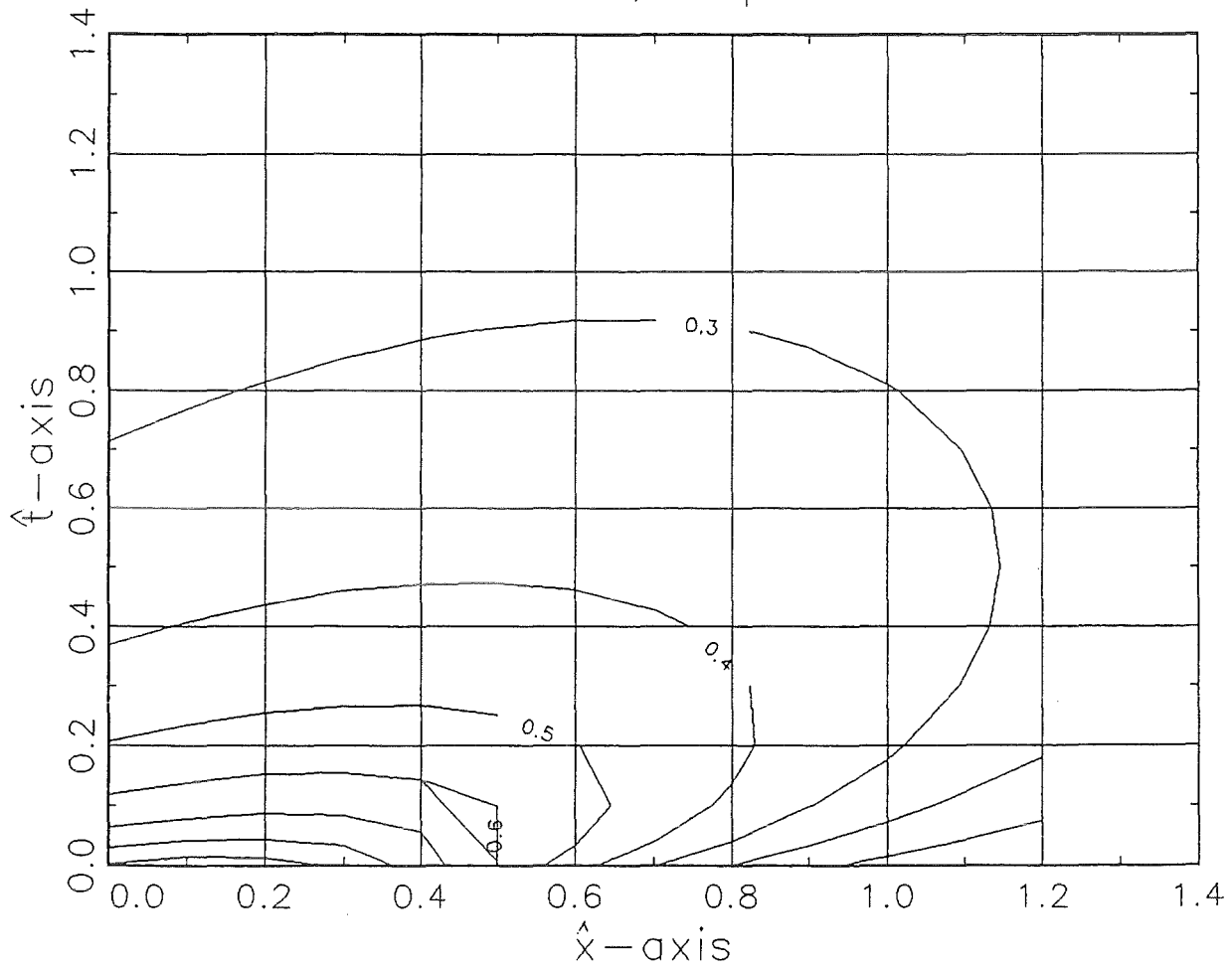


Fig. 7-8 Projection of $S(\hat{x}, \hat{t})$ on $\hat{x}-\hat{t}$ -plane

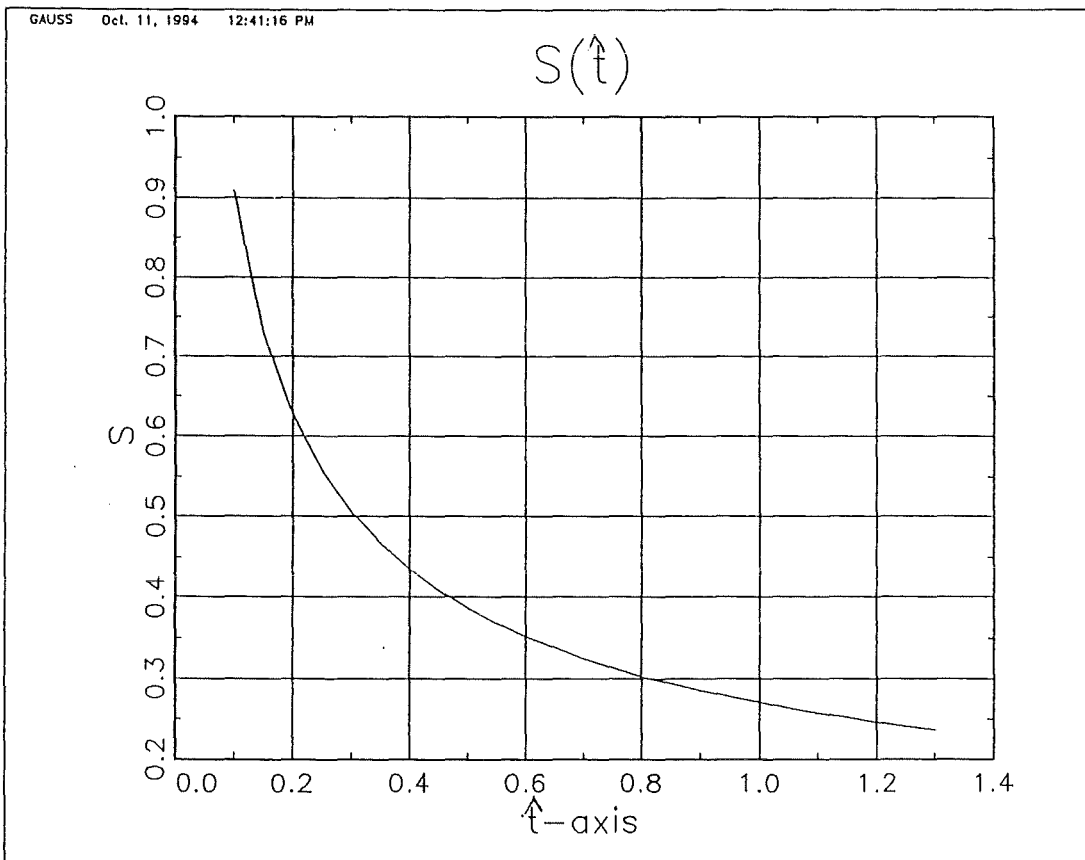
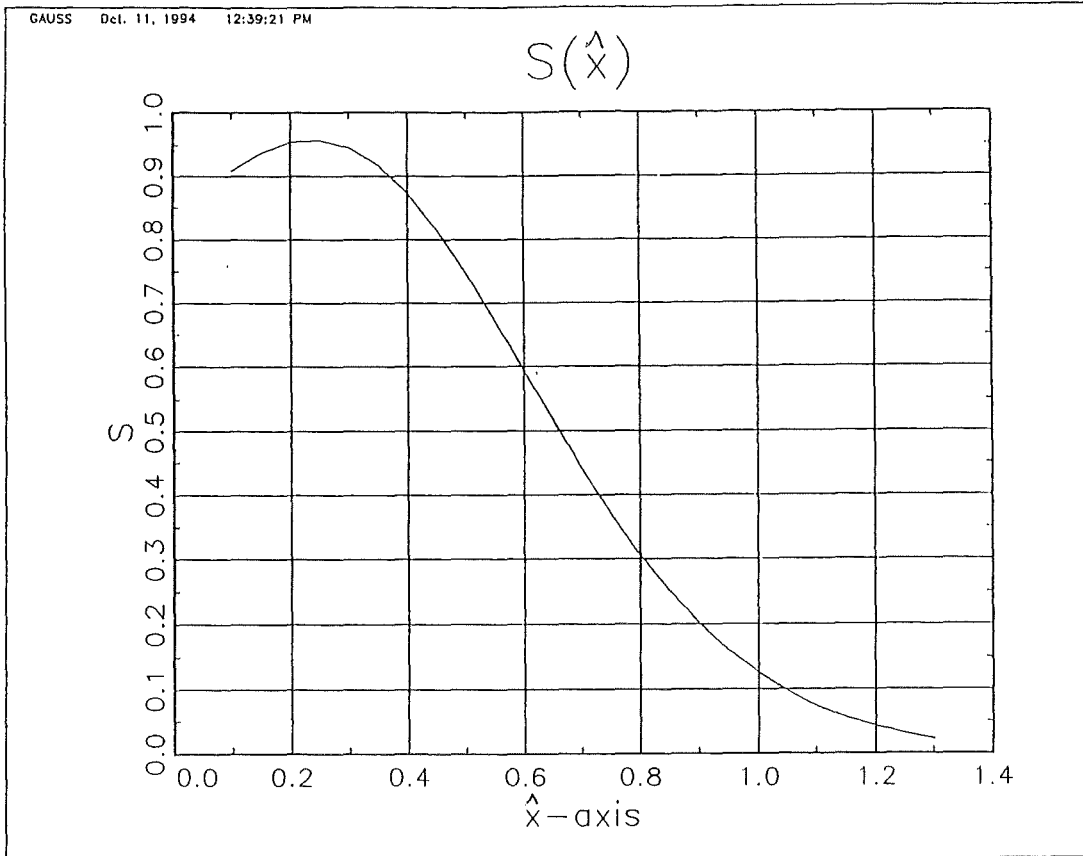


Fig. 7-9 $S(\hat{x}, \hat{t})$ on \hat{x} -axis | $Nc = 1.0$

Fig. 7-10 $S(\hat{x}, \hat{t})$ on \hat{t} -axis | $(i, j) = (1, 1)$

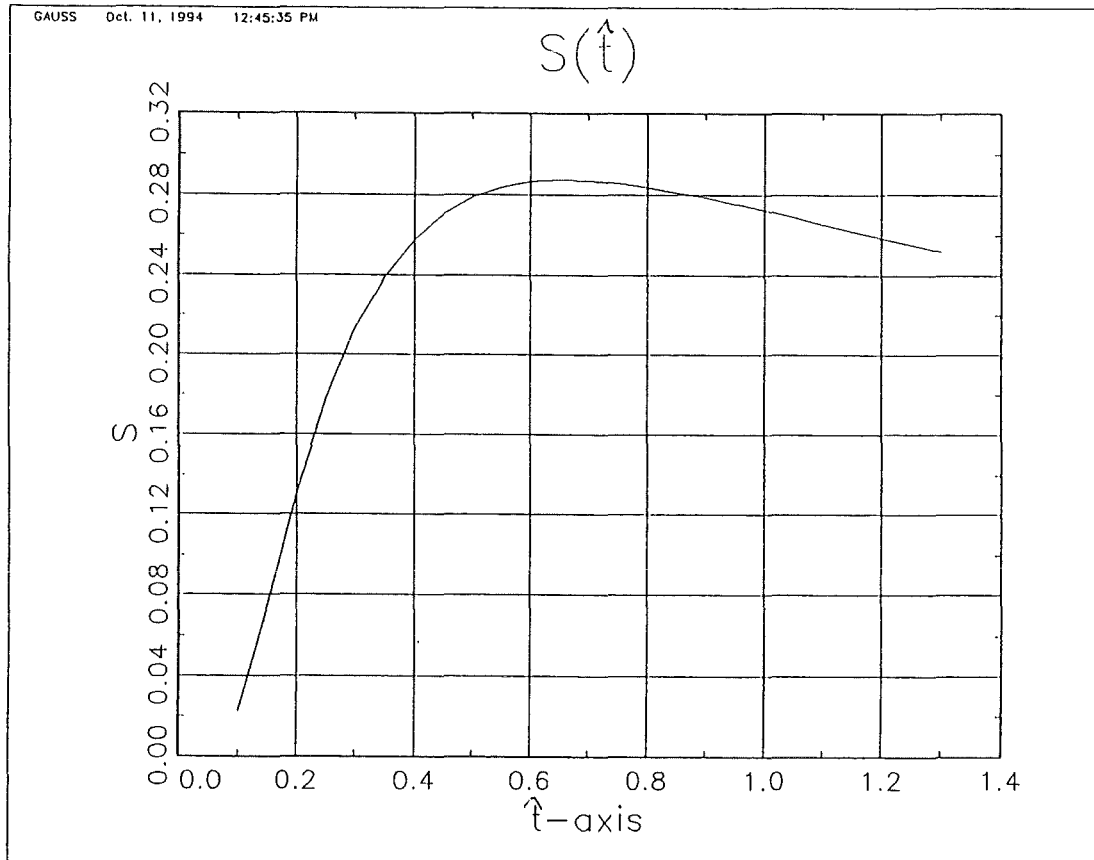
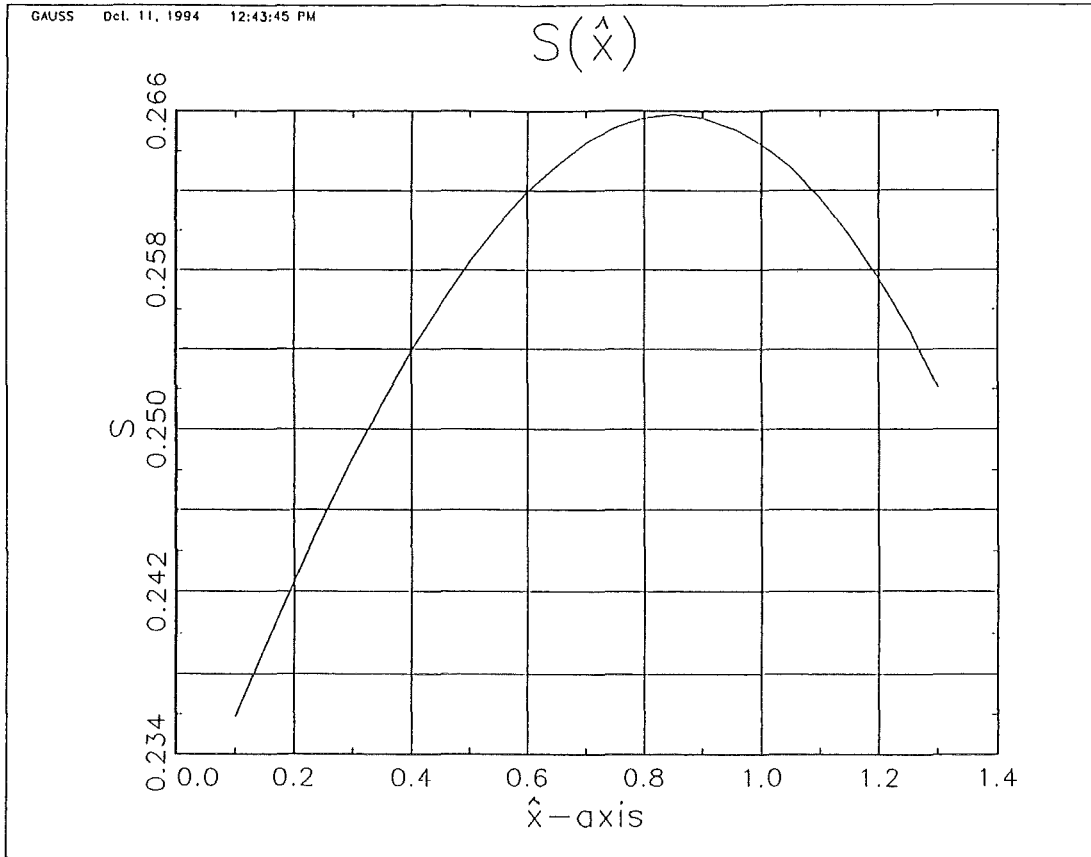


Fig. 7-11 $S(\hat{x}, \hat{t})$ on \hat{x} -axis | $N_c = 1.0$
----- | $(i, j) = (25, 25)$
Fig. 7-12 $S(\hat{x}, \hat{t})$ on \hat{t} -axis

Saturation S

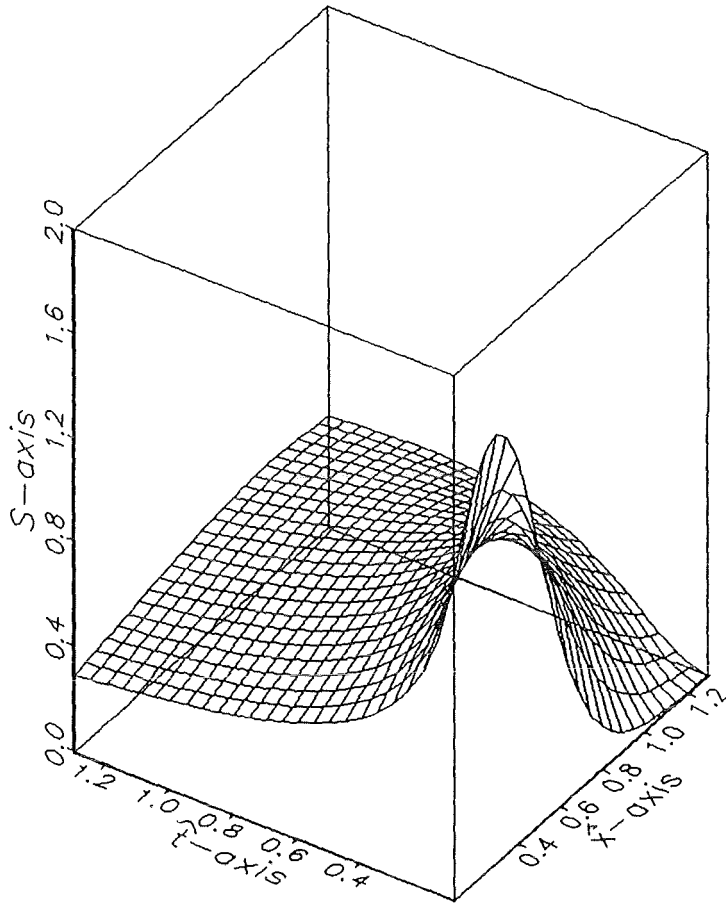


Fig. 7-13 Saturation $S(\hat{x}, \hat{t})$ in 3-D, $N_c = 2.0$

S on \hat{x}, \hat{t} -plane

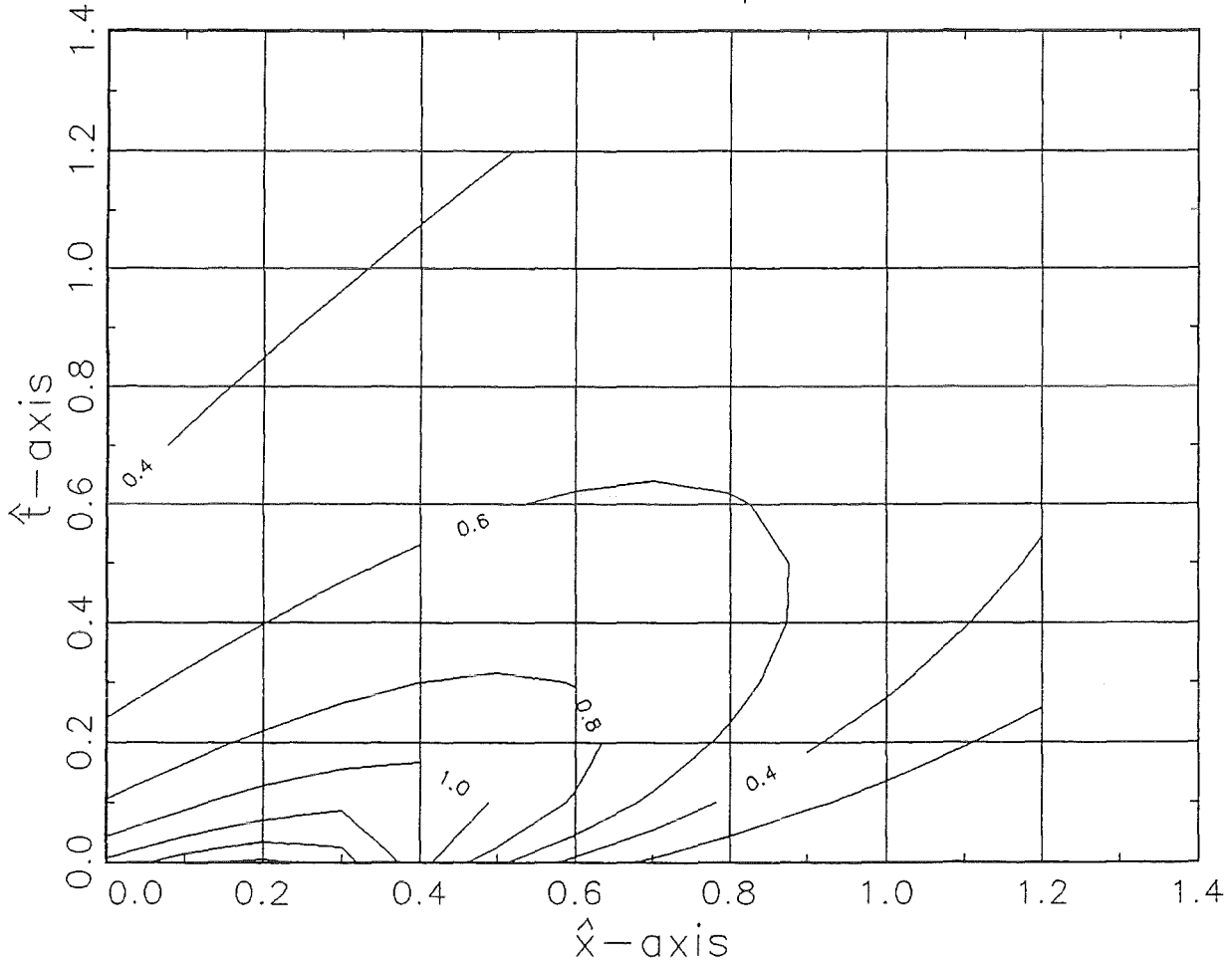


Fig. 7-14 Projection of $S(\hat{x}, \hat{t})$ on \hat{x} - \hat{t} -plane

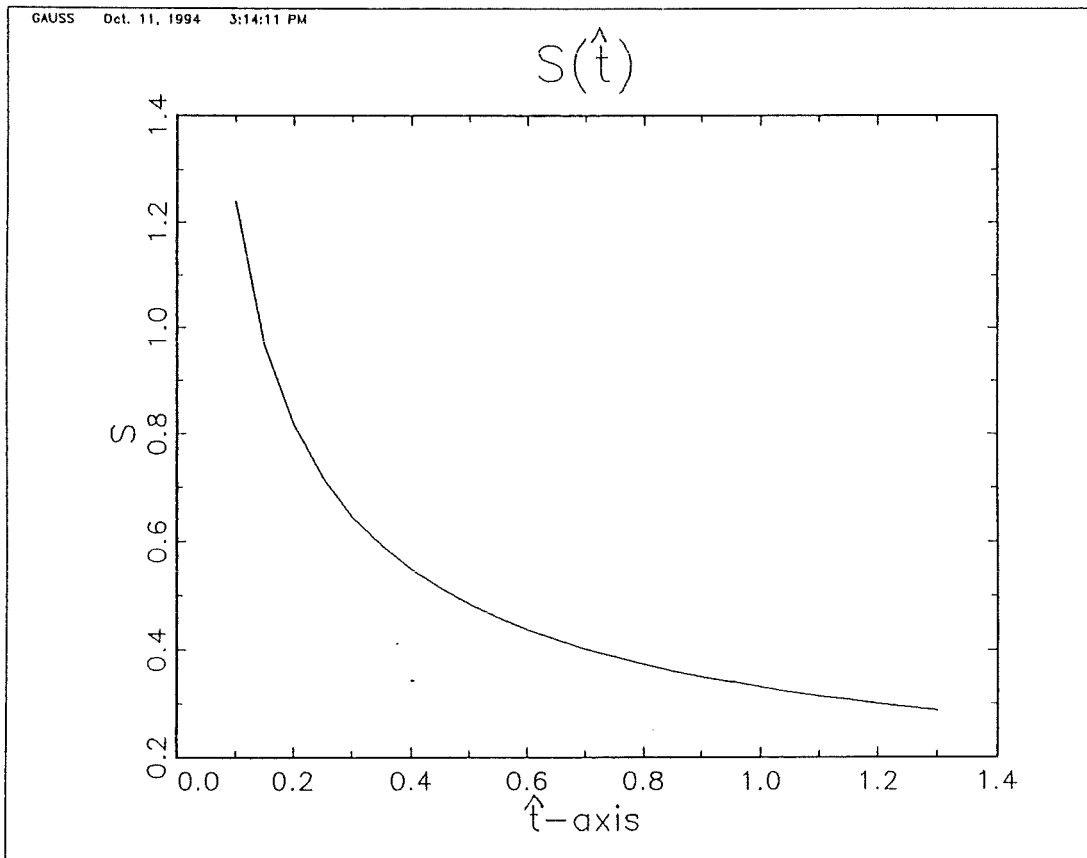
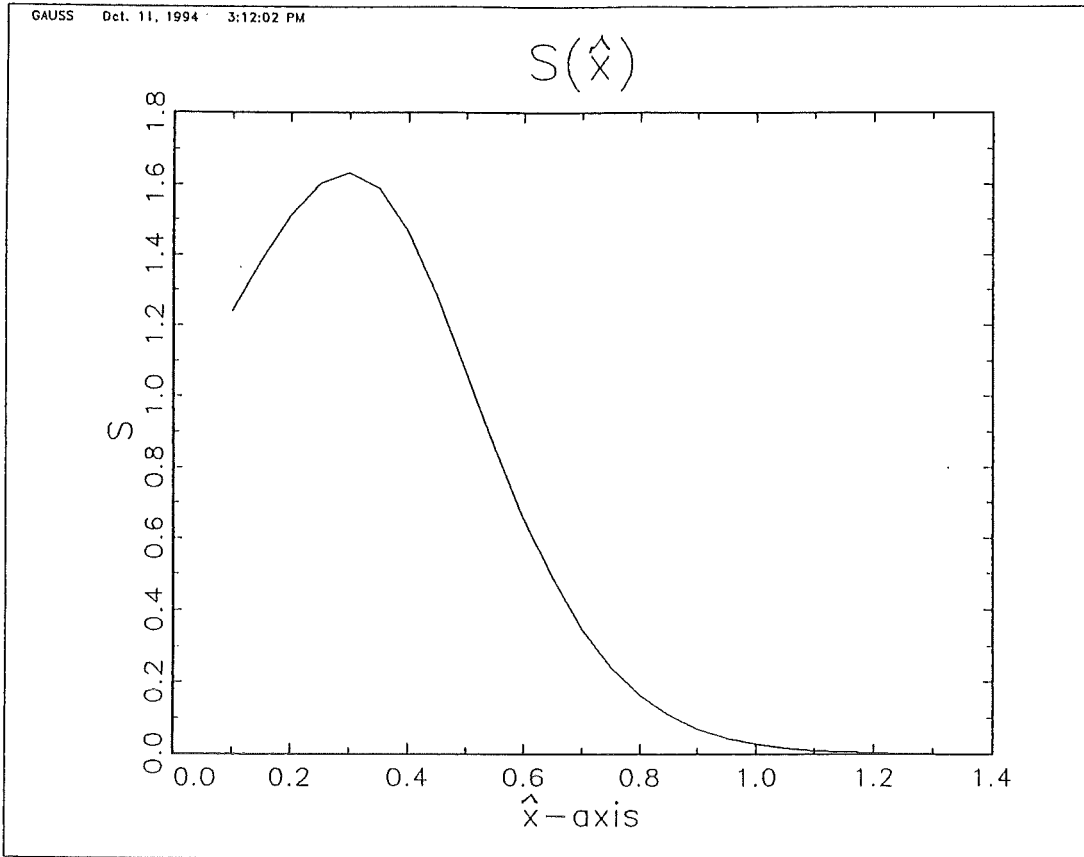


Fig. 7-15 $S(\hat{x}, \hat{t})$ on \hat{x} -axis | $N_c = 2.0$

Fig. 7-16 $S(\hat{x}, \hat{t})$ on \hat{t} -axis | $(i, j) = (1, 1)$

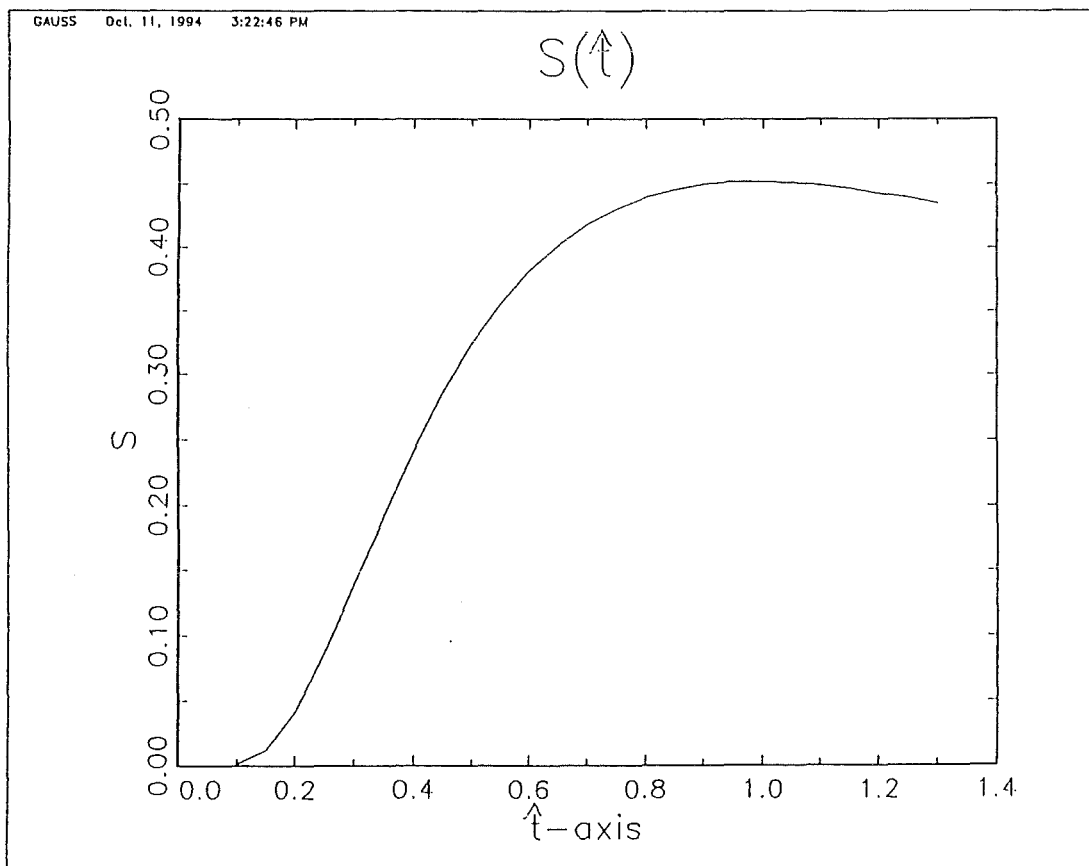
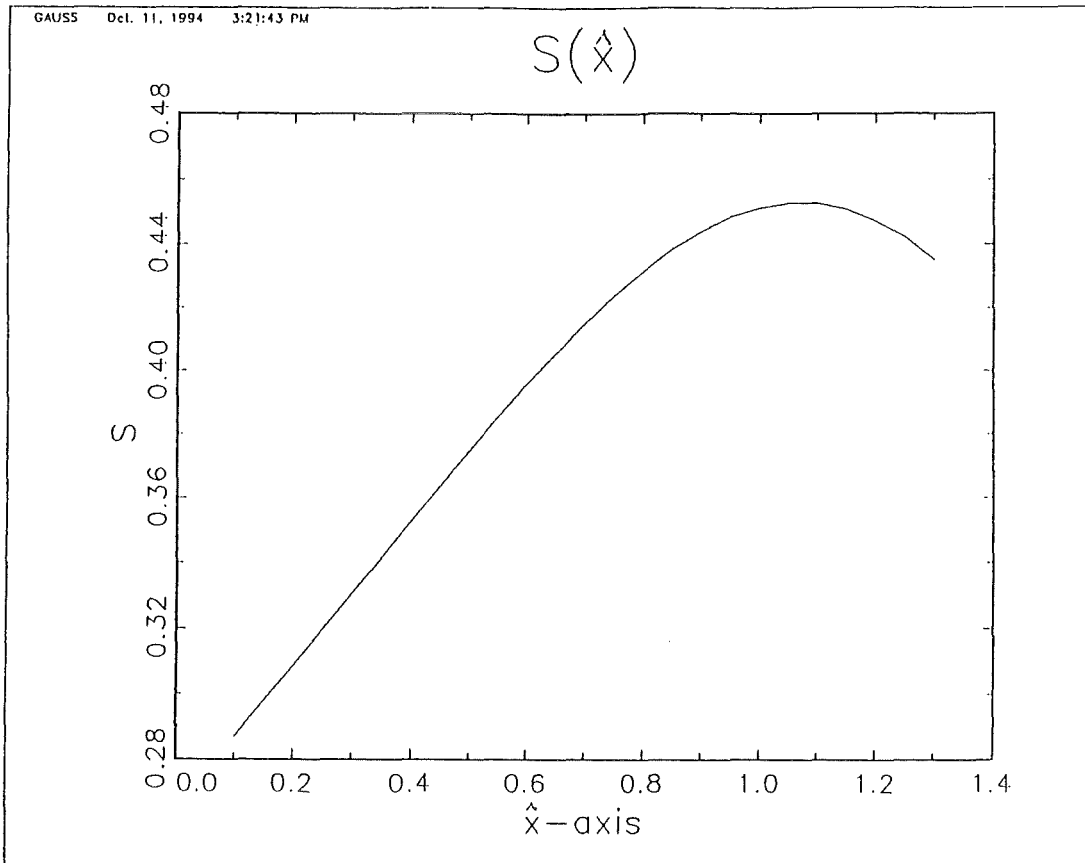


Fig. 7-17 $S(\hat{x}, \hat{t})$ on \hat{x} -axis | $N_c = 2, 0$

Fig. 7-18 $S(\hat{x}, \hat{t})$ on \hat{t} -axis | $(i, j) = (25, 25)$

Saturation S

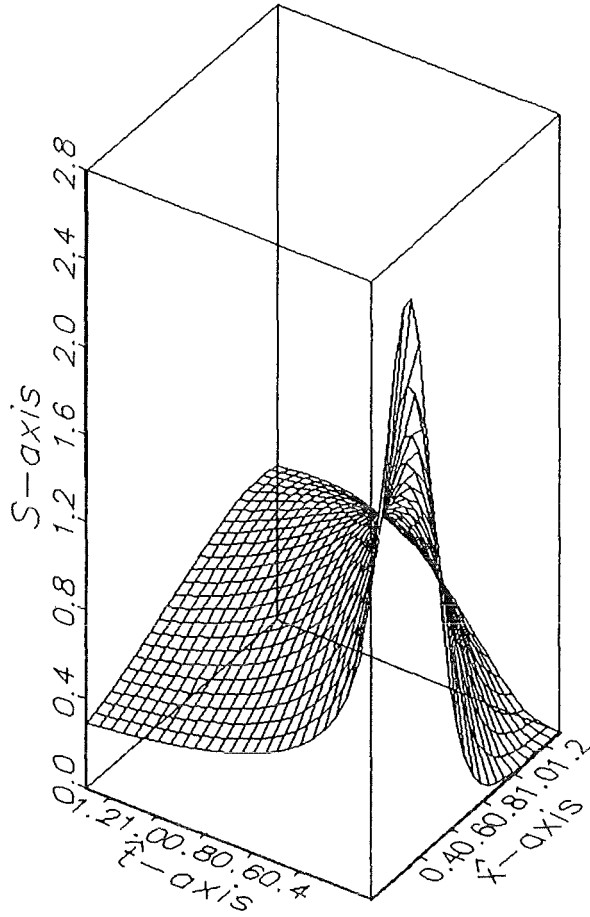


Fig. 7-19 Saturation $S(\hat{x}, \hat{t})$ in 3-D, $N_c = 4.0$

S on \hat{x}, \hat{t} -plane

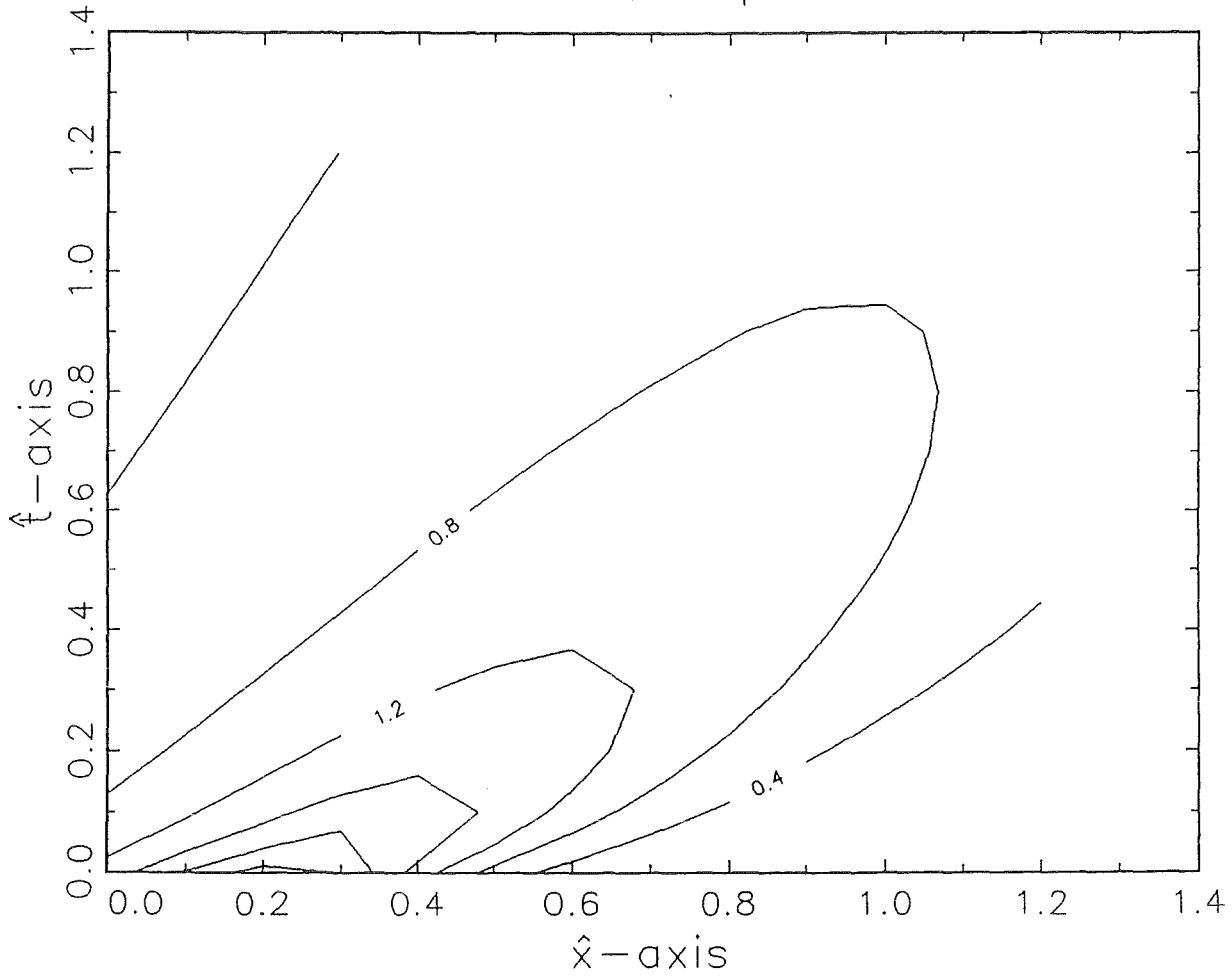


Fig. 7-20 Projection of $s(\hat{x}, \hat{t})$ on \hat{x} - \hat{t} -pane

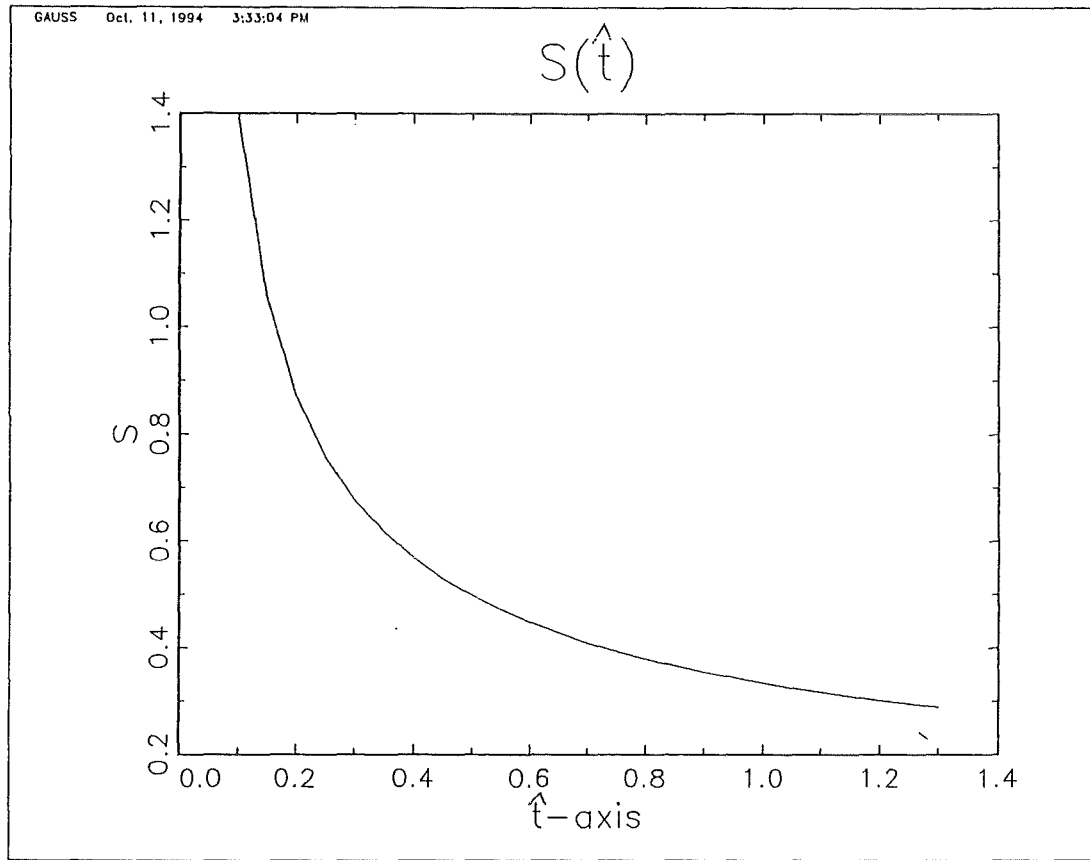
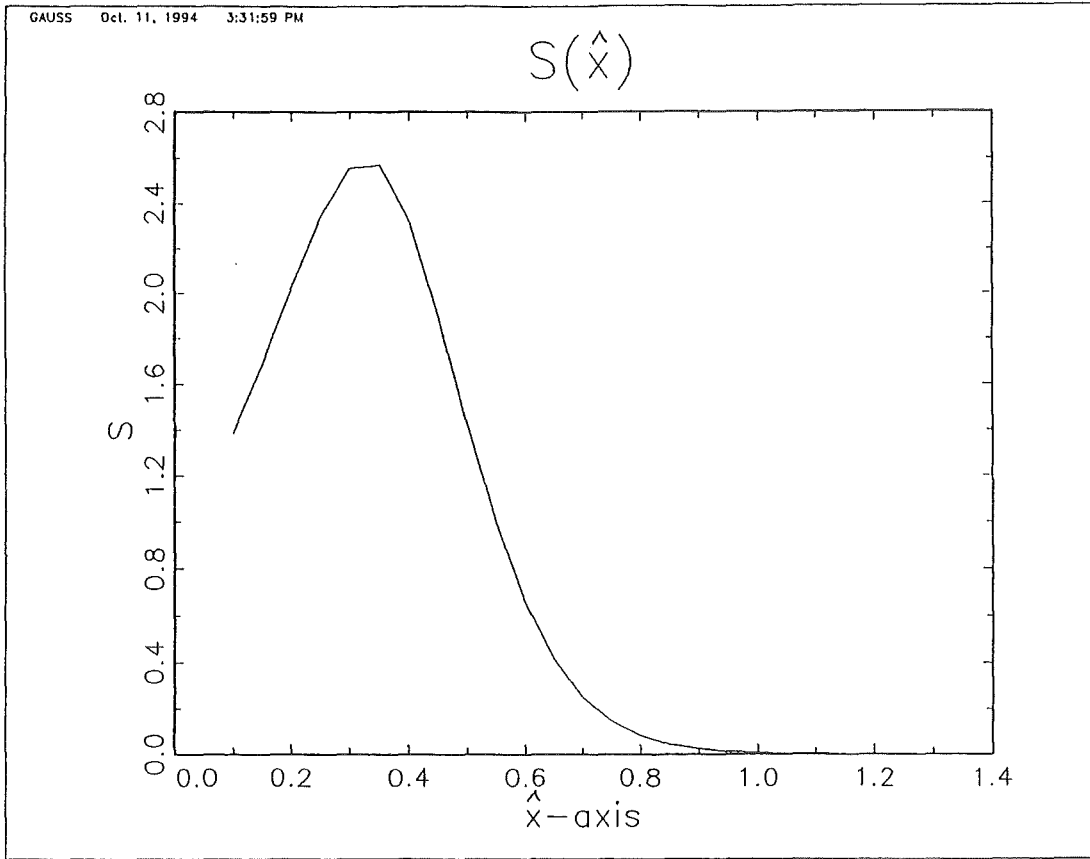


Fig. 7-21 $S(\hat{x}, \hat{t})$ on \hat{x} -axis | $N_c = 4.0$
----- | $(i, j) = (1, 1)$
Fig. 7-22 $S(\hat{x}, \hat{t})$ on \hat{t} -axis |

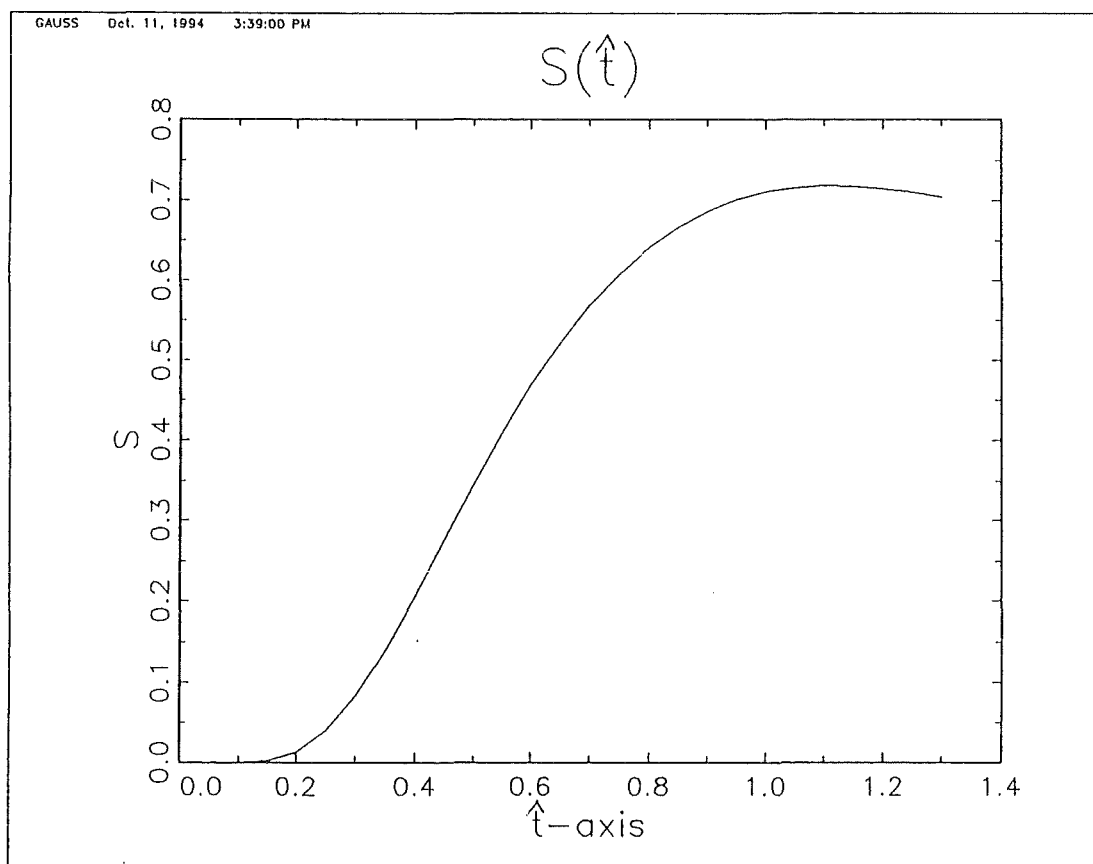
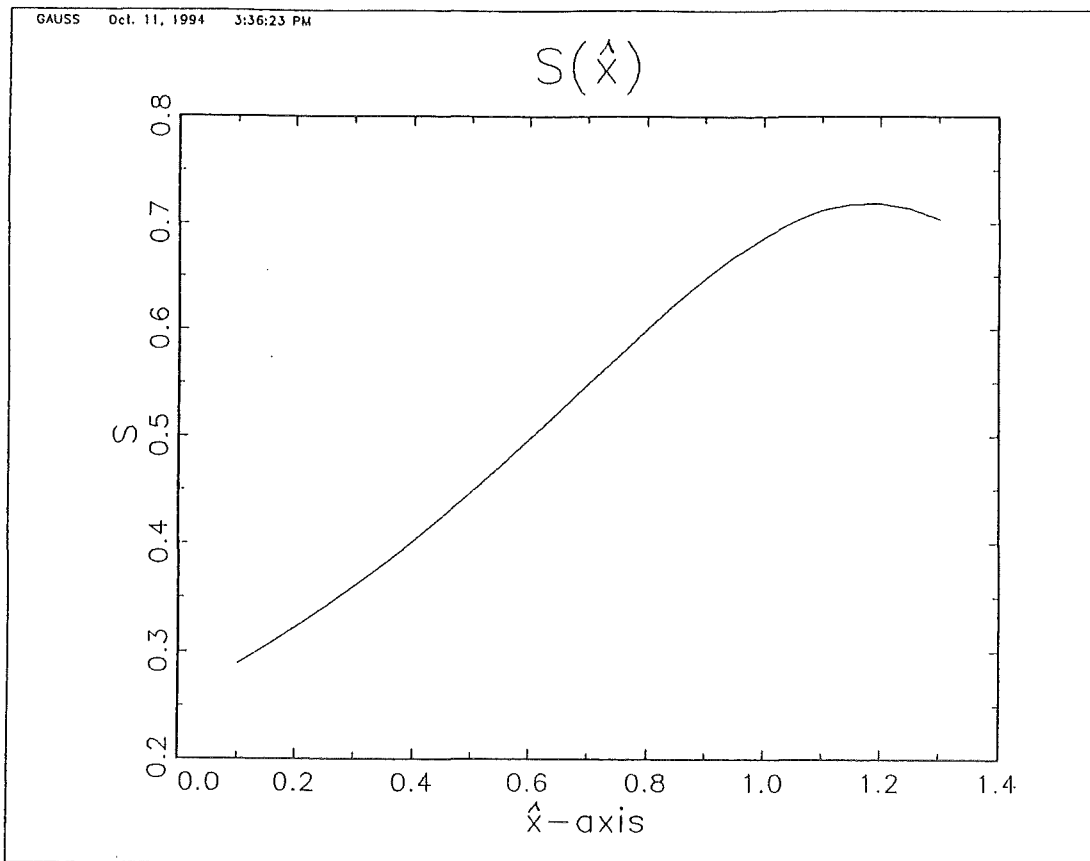


Fig. 7-23 $s(\hat{x}, \hat{t})$ on \hat{x} -axis | $Nc = 4.0$
----- | $(i, j) = (25, 25)$
Fig. 7-24 $s(\hat{x}, \hat{t})$ on \hat{t} -axis

Nc	x	Smax(x)
0.10	0.250000	0.0892738165
0.20	0.350000	0.1265386591
0.30	0.425000	0.1555608087
0.40	0.500000	0.1805685617
0.50	0.550000	0.2032302626
0.60	0.600000	0.2244267202
0.70	0.650000	0.2446936341
0.80	0.675000	0.2643973328
0.90	0.725000	0.2837949587
1.00	0.750000	0.3031003858
2.00	0.950000	0.5162286029
3.00	1.025000	0.8200895435
4.00	1.100000	1.2917354470
5.00	1.150000	2.0387377665
6.00	1.175000	3.2371430294
7.00	1.200000	5.1612333725
8.00	1.225000	8.2536617260
9.00	1.225000	13.2579576751
10.0	1.250000	21.3586296377

INPUT VALUES

Initial value x_0 = 0.100
initial value t_0 = 1.000
length of steps = 0.025
Number of steps n = 80.00

Table 7-2 Maxima for $S(x)$ with different Nc

8. Solutions for different parameters

8.1 Introduction

As has been shown in sect. 4.7 an ODE is the final step of the similarity solution, based on the transport equation (convection equation) introduced in sect. 4.3. We recall this ODE here:

$$f' = Nc * (f^n - b * \xi^{1+m-n} * g) \quad (4-46)$$

This equation gives, due to different values for exponents m, n, different solutions. The most interesting of them will be given in the following sections.

8.2 Exponents m, n larger than 1

Here we have the conditions

$$m = n \quad \text{and} \quad m, n > 1 \quad (8-1)$$

It may be noted that the case

$$m = n \quad \text{and} \quad m = 2, n = 2 \quad (8-2)$$

which is related to the Riccatti-equation has been discussed in detail in sects. 4 to 7.

For conditions (8-1) we have the following similarity solution:

$$f(\xi) = \frac{\exp(- (Nc/4) * \xi^2)}{[f(0) - \sqrt{(\pi * Nc * (n-1))} * \operatorname{erf}((1/2) * (Nc * (n-1)) * \xi)]^{1/(n-1)}} \quad (8-3)$$

Examples of (8-3) are shown in the following Tables and Figures:

In Tables 8-1, 8-2, 8-3

we show

- the maximum of f(ξ) (similarity solution for saturation) for various exponents n
- the coordinates of horizontal and vertical tangent for the flux Js, (see also "group velocity", sect. 6.2, interpretation of flux curve)

In Figs. 8-1 to 8-6

we show

- the similarity solution f(ξ) (transformed saturation)
- the shape of the flux Js.

Results

	n = 2	4	6	8
Nc =				
1	Fig. 8-1	8-2	-	-
2	Fig. 8-3	8-4	8-5	8-6

Interpretation

- (a) $f(\xi)$: For increasing N_c there is for the curves shown here, an increase of the maximum of $f(\xi)$, similar to the property of the solutions shown for the case $n = 2$.
- (b) $f(\xi)$: For increasing exponent n there is a decrease of the maximum of $f(\xi)$.
- (c) J_s : For increasing n there is a considerable change in the shape of J_s (flux).
- (d) J_s : For increasing n there is a considerable increase in the maximum of J_s .

It has to be noted, that for some regions of N_c where $N_c \ll 1$, the same relation clearly holds (increasing max. with increasing N_c). But there are also regions, where $N_c \gg 4$, where the relation becomes more complicated, where no monotonicity exists.

8.3 Exponents m, n smaller than 1

Here we have for (4-46) also the following conditions

$$m = n \quad \text{and} \quad m < 1, \quad n < 1 \quad (8-4)$$

It can be shown that the results for region (8-4) are different from the results of sect. 8.2:

$$f(\xi) = (f(0) \cdot \exp(-\eta^2) + 2 \cdot \sqrt{(1-n)} \cdot D(\eta)) \quad (8-5)$$

We note the following conventions:

$$\eta = \frac{Nc*(1-n)}{2} * \xi \quad (8-6)$$

where again ξ is the similarity variable. We also note, that $D(\eta)$, which is usually called Dawsons Integral (see[Abramowitz]).

$$D(\eta) = \exp(-\eta^2) * \int_0^\eta \exp(\eta'^2) * d\eta' \quad (8-7)$$

$D(\eta)$ is closely related to the error function, multiplied with an term which will cause that $D(\eta) \rightarrow 0$ for $\eta \rightarrow \infty$.

In Table 8-4 and Figs. 8-7 ff.

we show some properties of the similarity solution $f(\xi)$.

Results

	n = -4	-1	0	0.5
Nc = 1,2,3,4, 5,6,7,8	Fig. 8-7	8-8	8-9	8-10

Interpretation

- (a) $f(\xi)$: The maximum of $f(\xi)$ remains almost constant with changing Nc.
- (b) $f(\xi)$: For increasing Nc the abszissa of the maximum is shifting to the left.
- (c) $F(\xi)$: For increasing n the Maximum of $f(\xi)$ is decreasing.

8.4 Considerations for parameters

We do not discuss here other possibilities for the parameters, e.g. cases where $m > n$, or $m < n$ holds. For more details on the relations between exponents and the type of percolation, see Appendix A4.

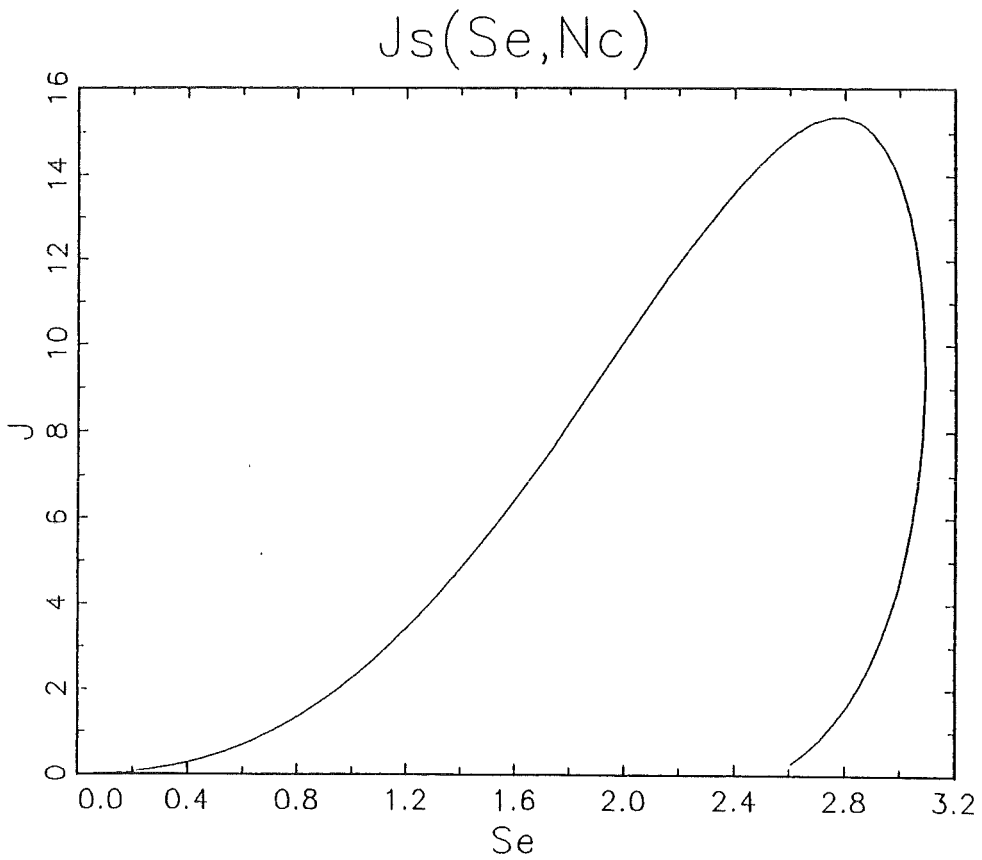
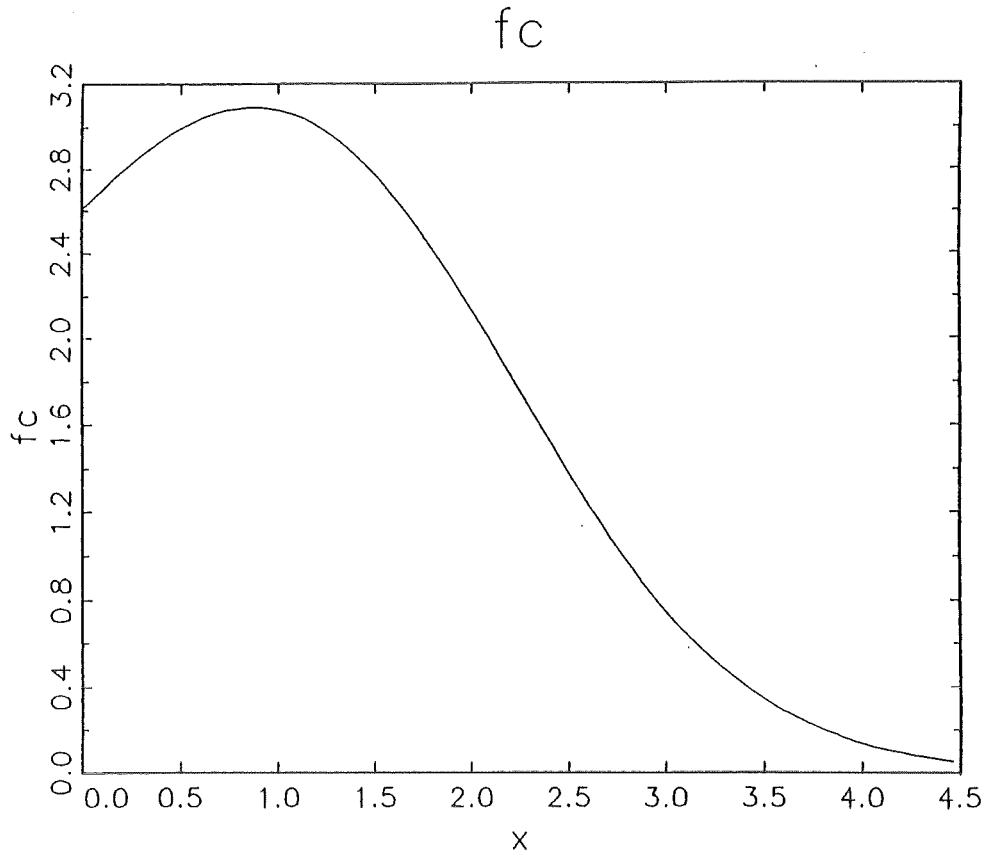
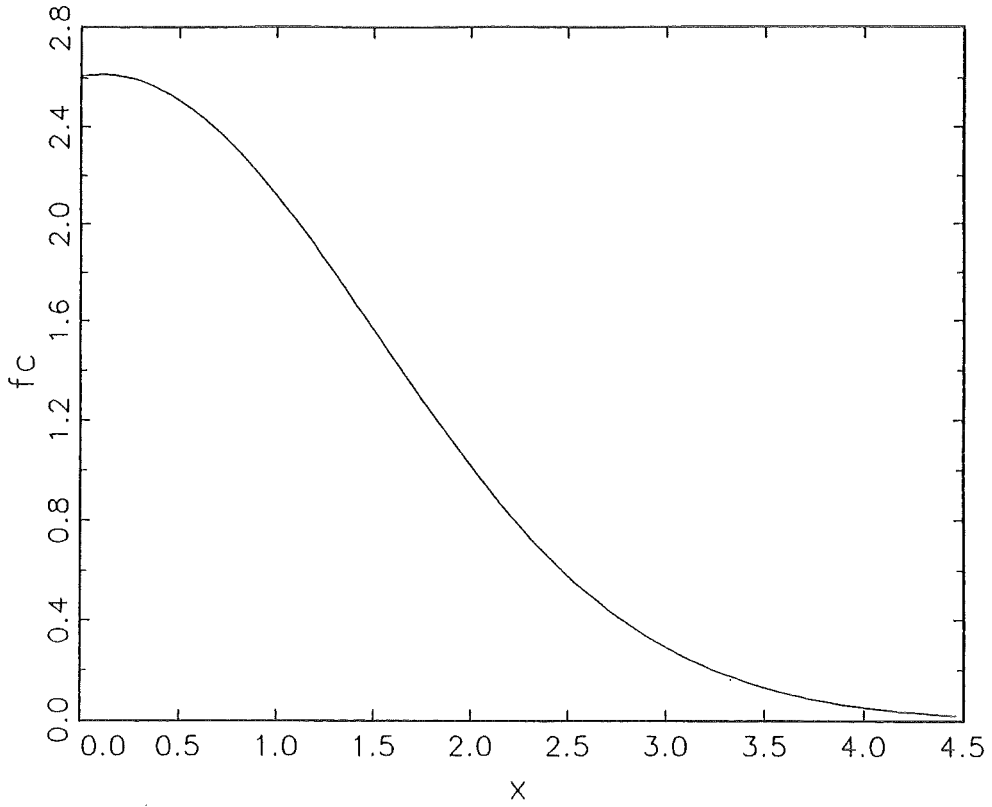


Fig. 8-1 For given n: (a) $f(\xi)$, reduced saturation

(b) saturation flux

fc



$J_s(Se, Nc)$

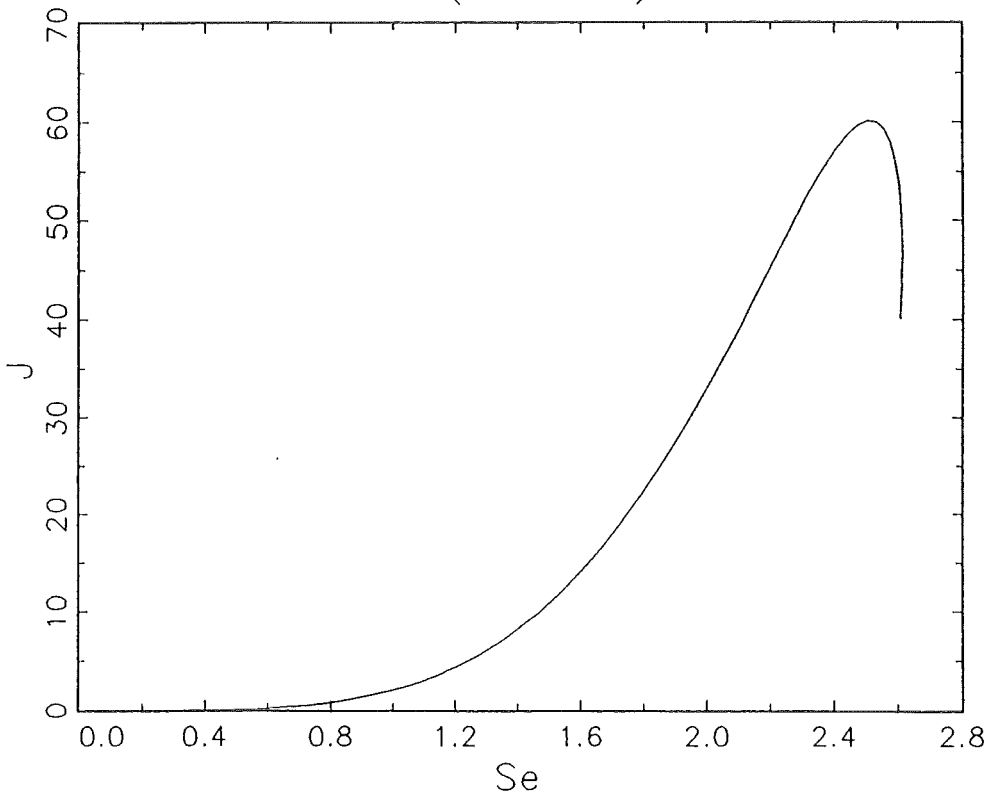


Fig. 8-2 For given n : (a) $f(\xi)$, reduced saturation

(b) saturation flux

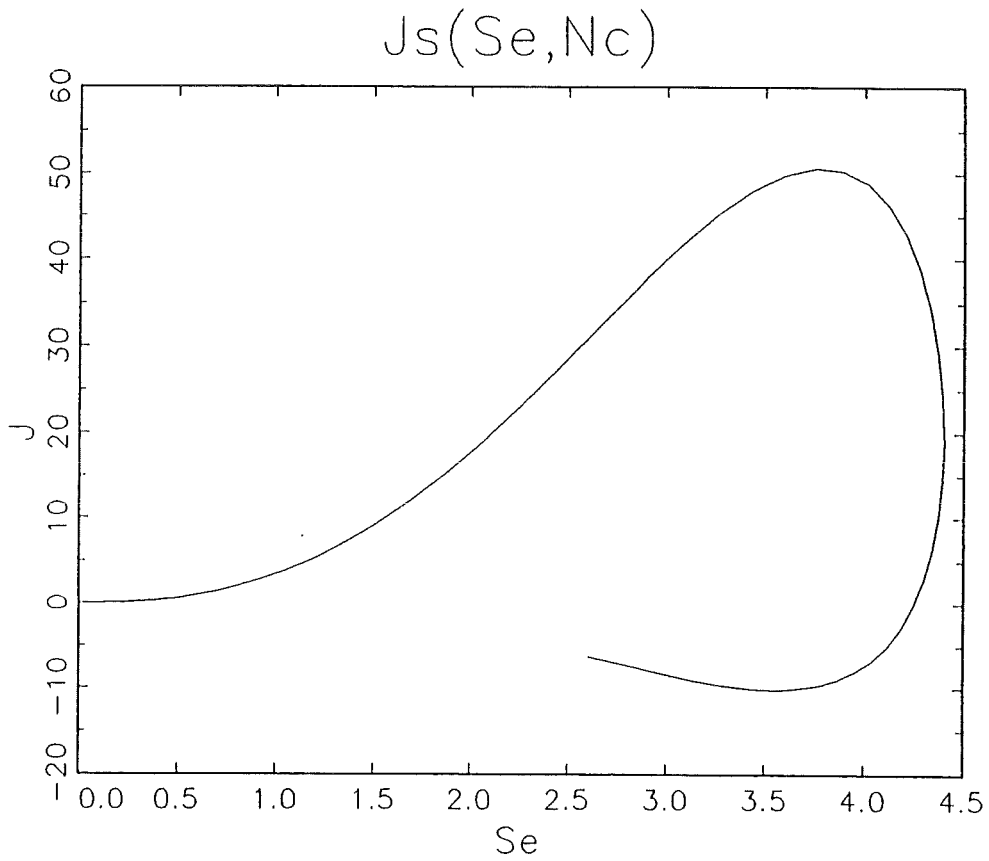
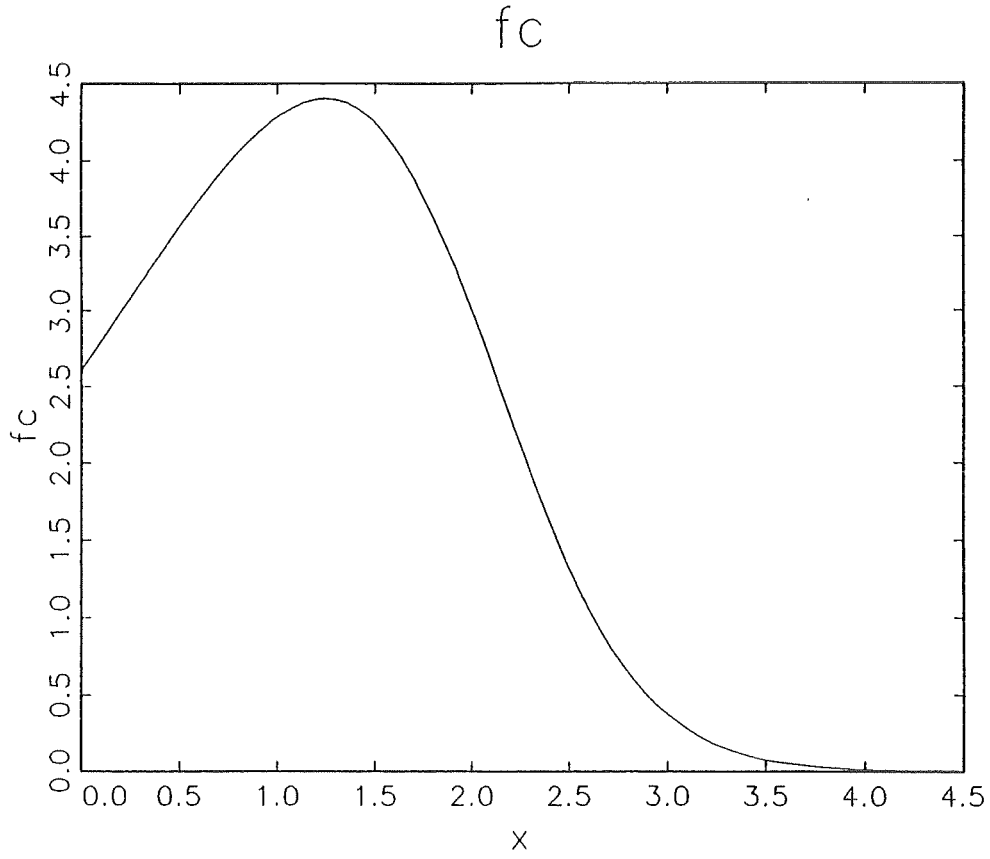
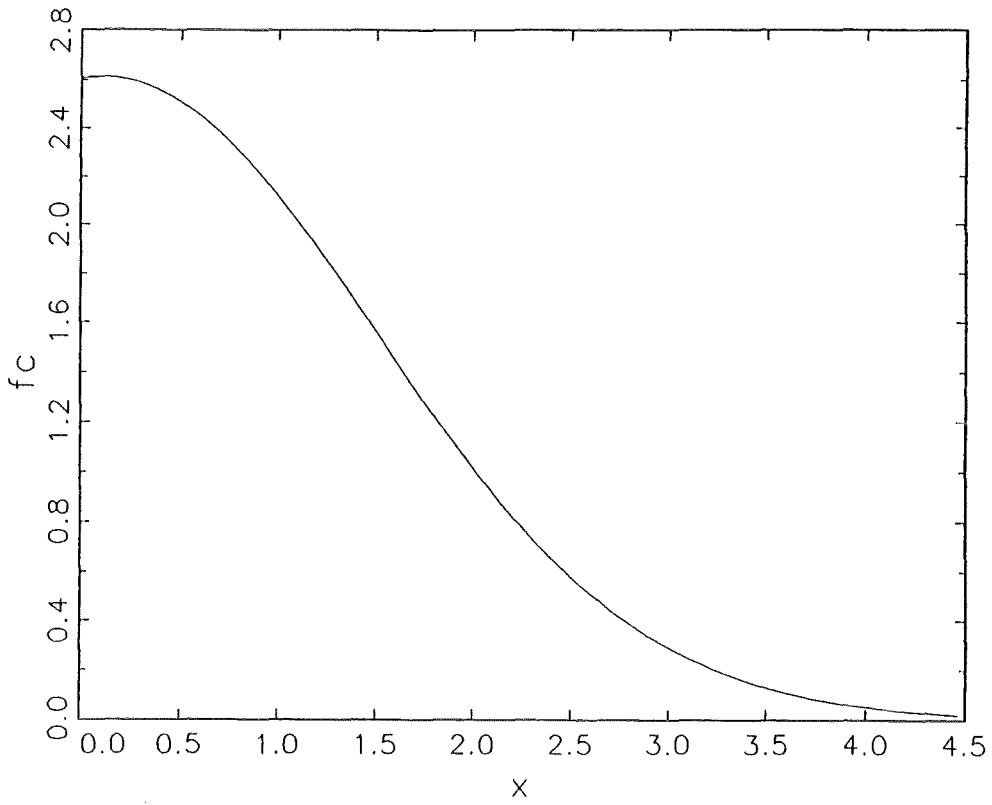


Fig. 8-3 For given n : (a) $f(\xi)$, reduced saturation

(b) saturation flux

fc



$J_s(S_e, N_c)$

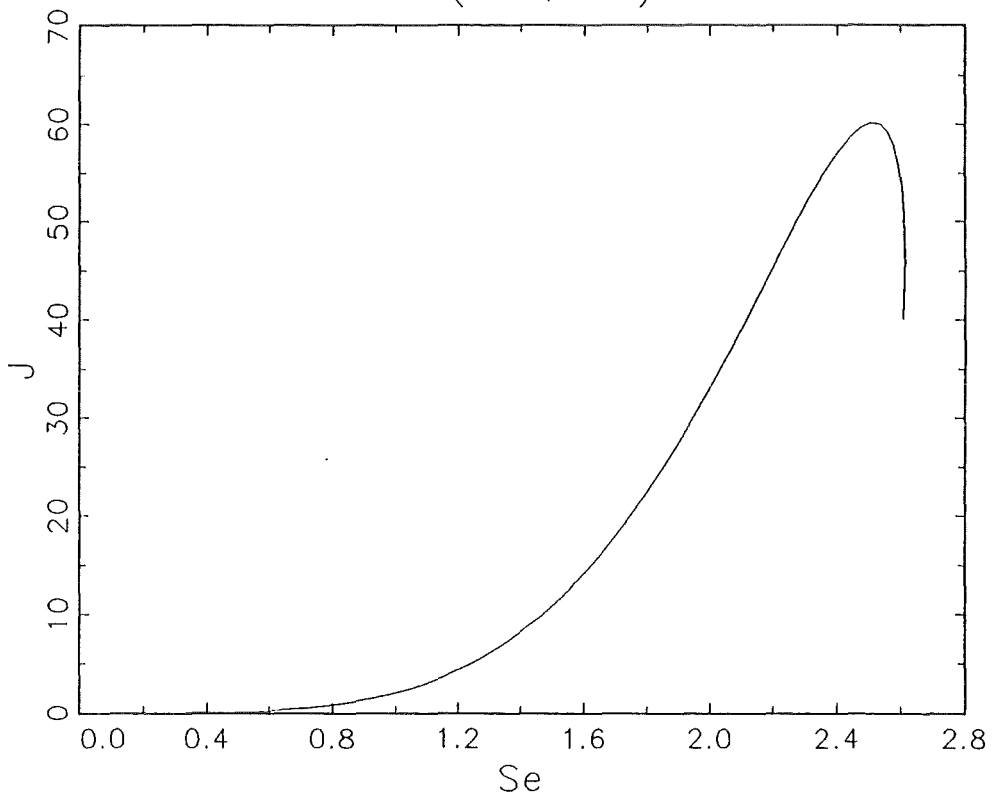


Fig. 8-4 For given n : (a) $f(\xi)$, reduced saturation

(b) saturation flux

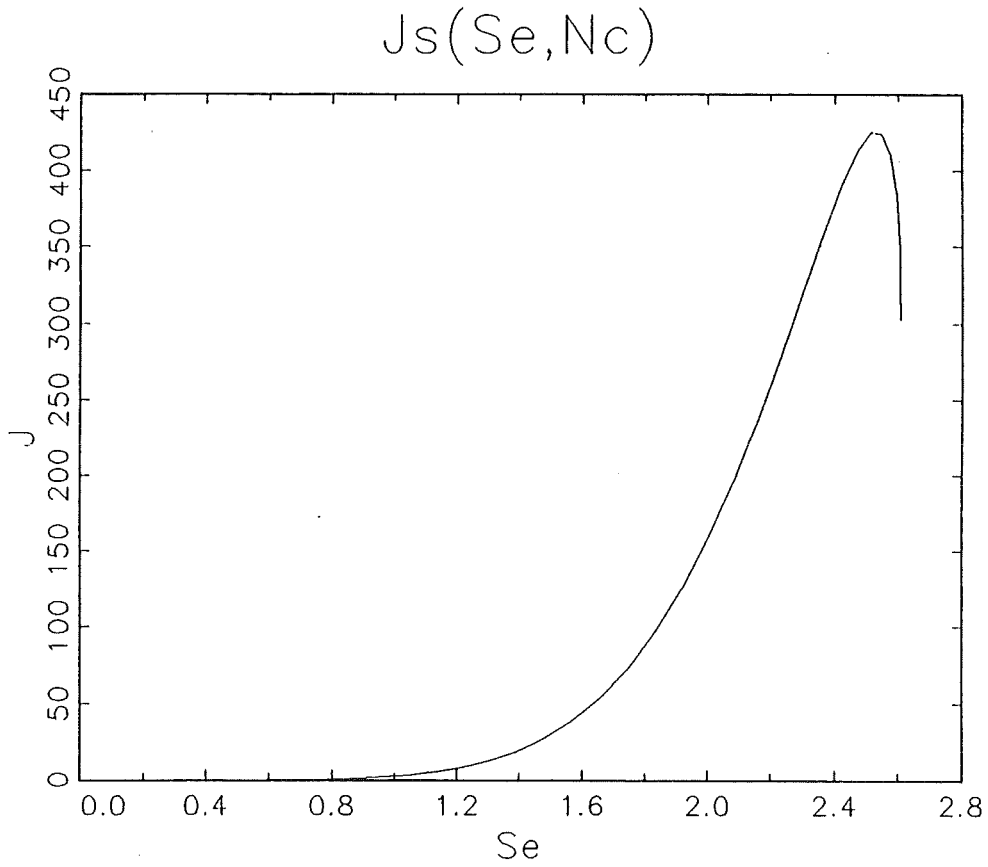
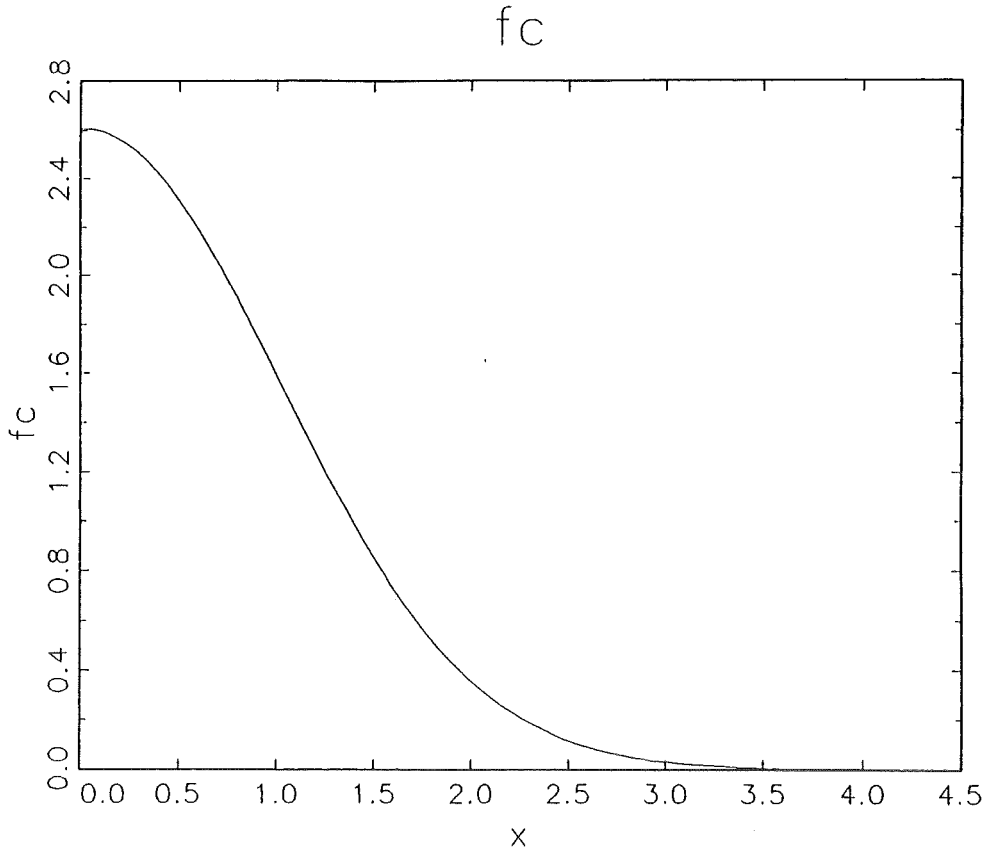


Fig. 8-5 For given n: (a) $f(\xi)$, reduced saturation

(b) saturation flux

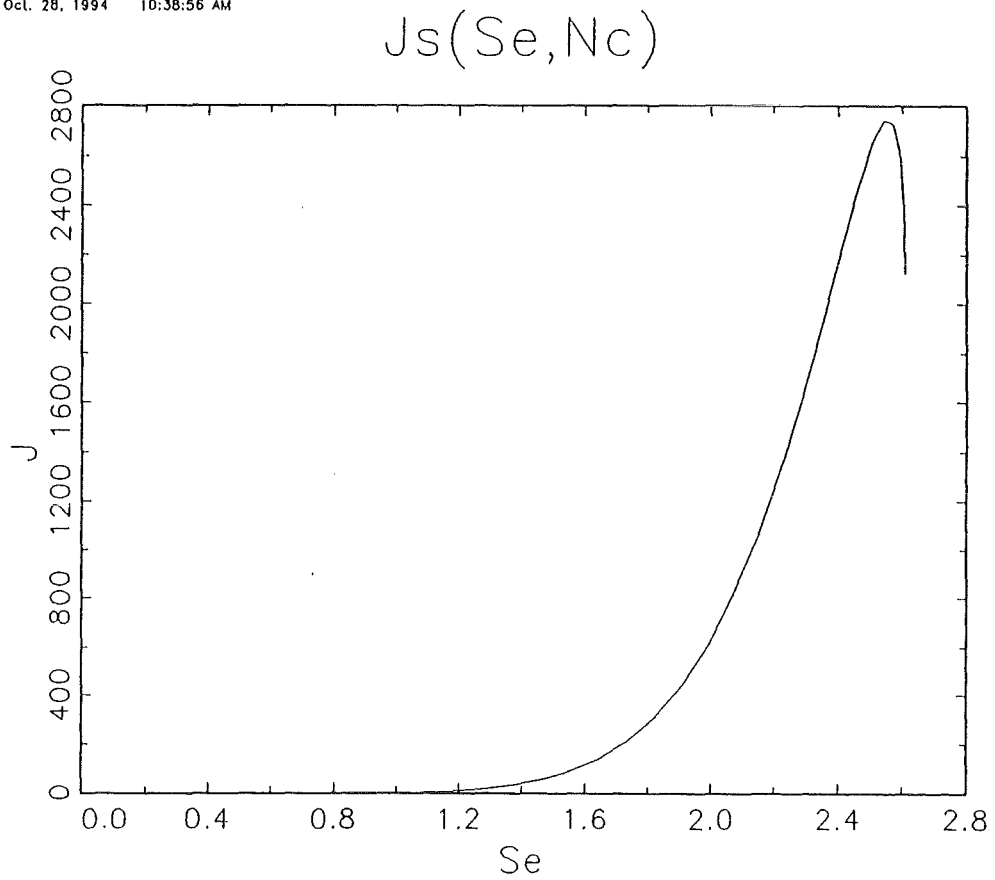
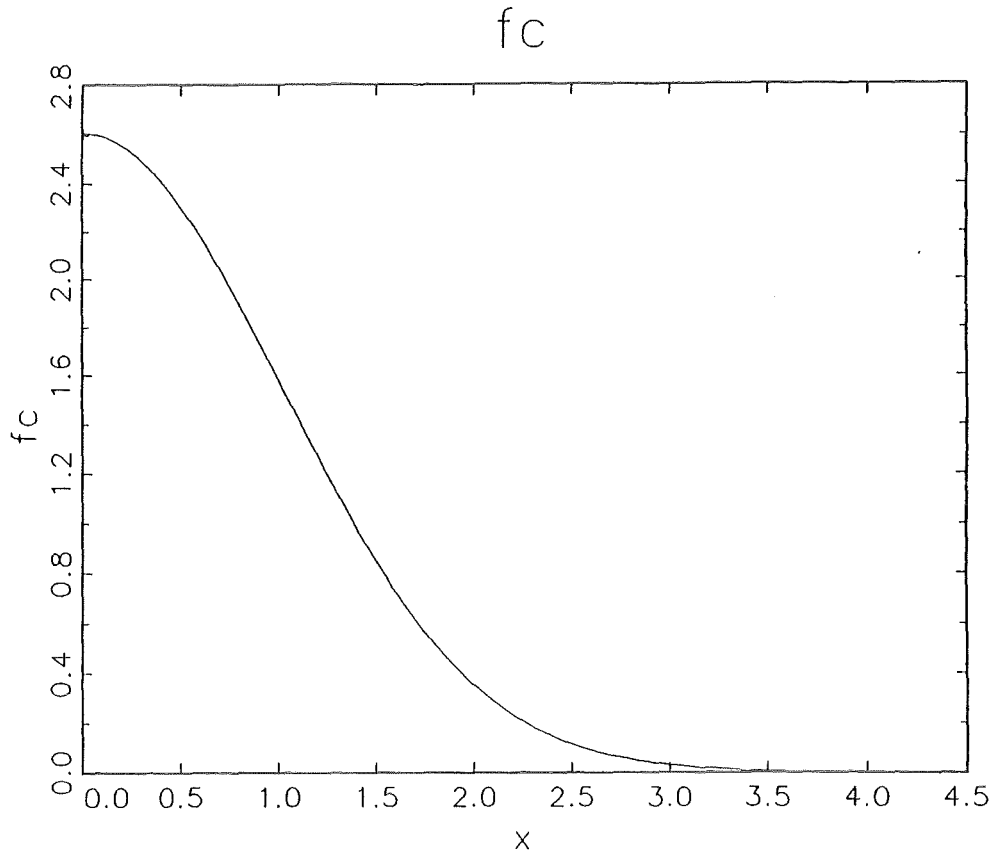
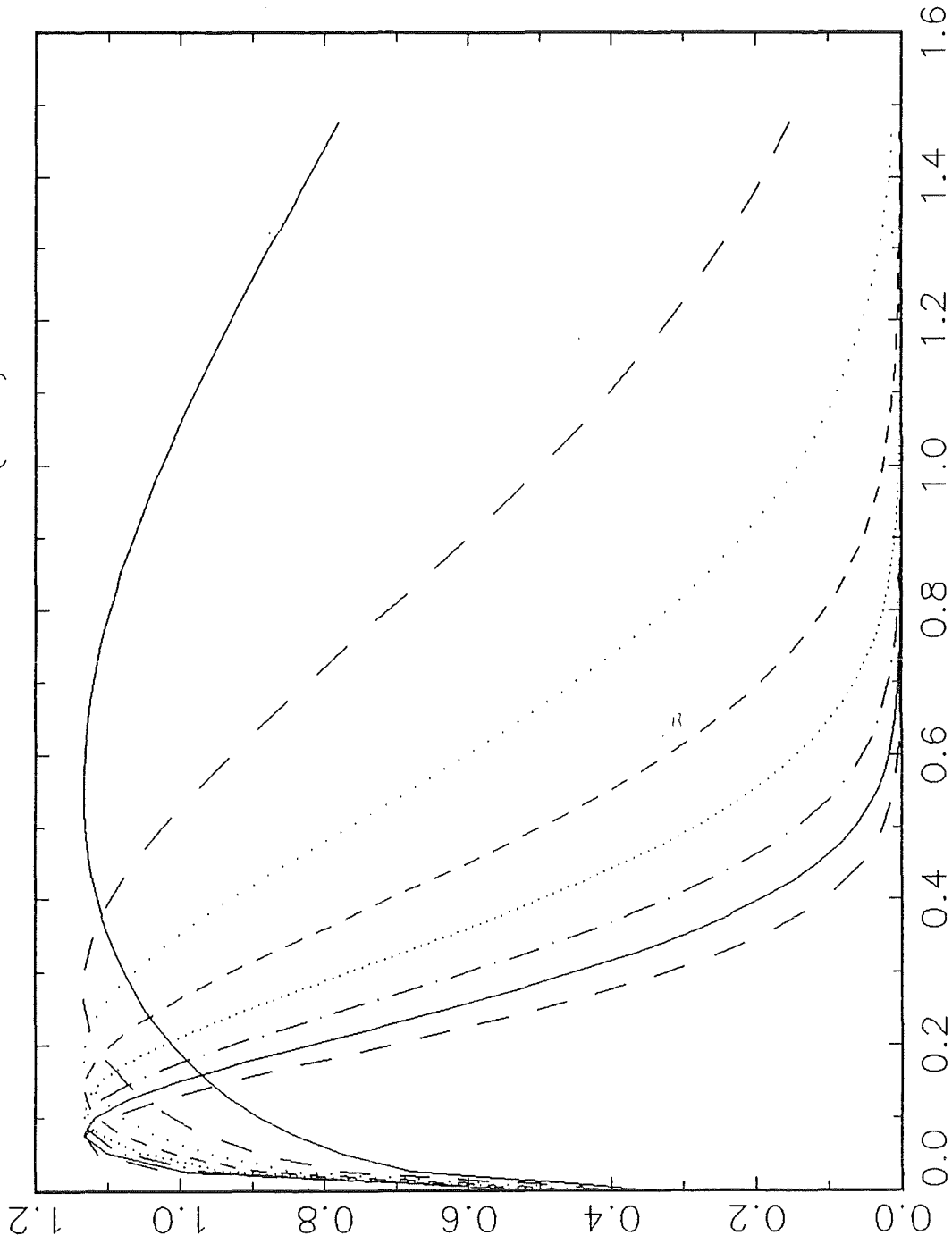


Fig. 8-6 For given n: (a) $f(\xi)$, reduced saturation

(b) saturation flux

*b128W

function $f(\xi)$

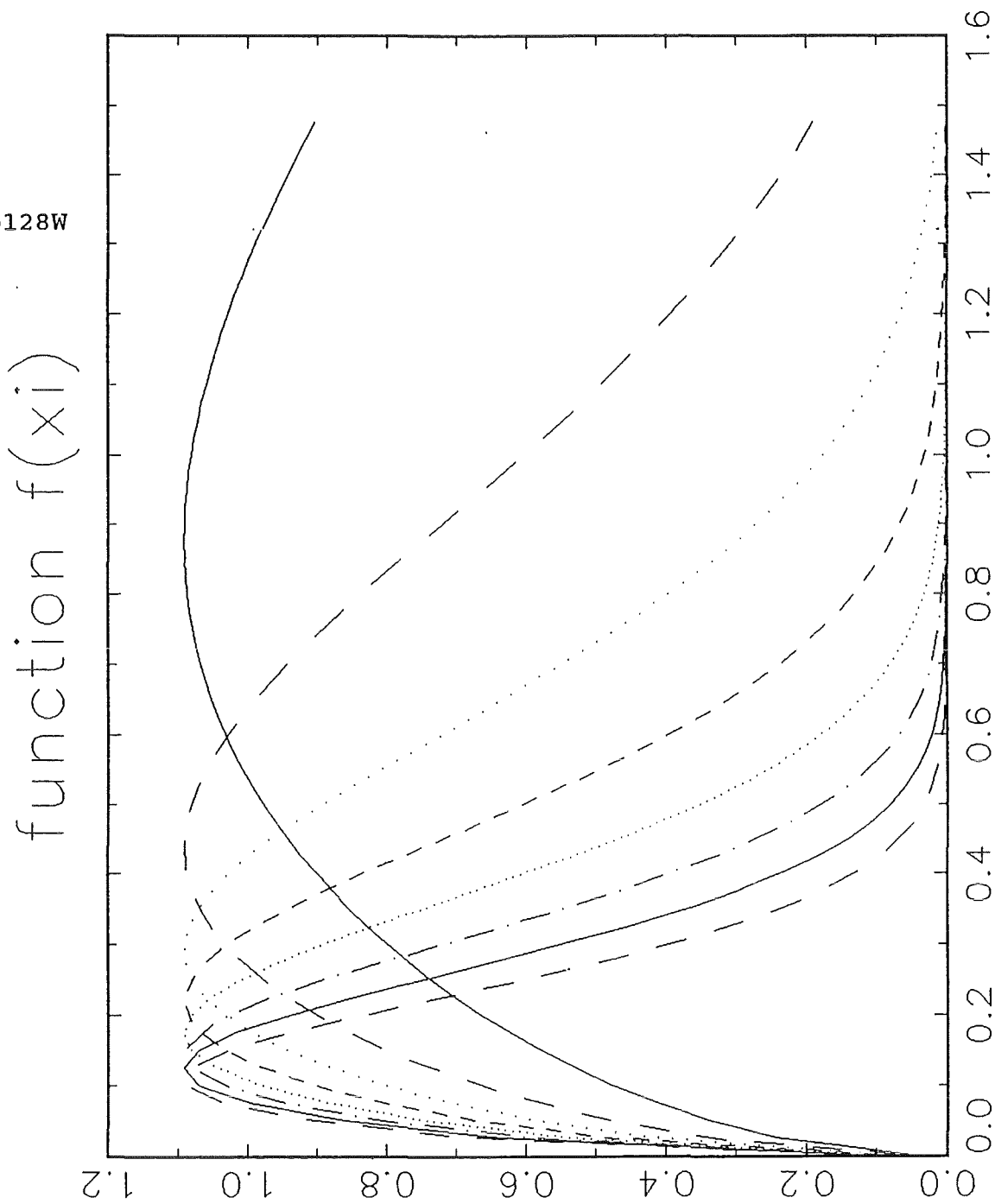


GAUSS Oct. 27. 1994 10:29:11 AM

Fig. 8-7 For given $n < 1$:

 $f(\xi)$, reduced saturation
($n = -4.0$)

*b128W



GAUSS Oct. 27, 1994 10:24:05 AM

Fig. 8-8 For given $n < 1$:

 $f(\xi)$, reduced saturation
($n = -1$)

GAUSS Oct. 27, 1994 11:41:37 AM

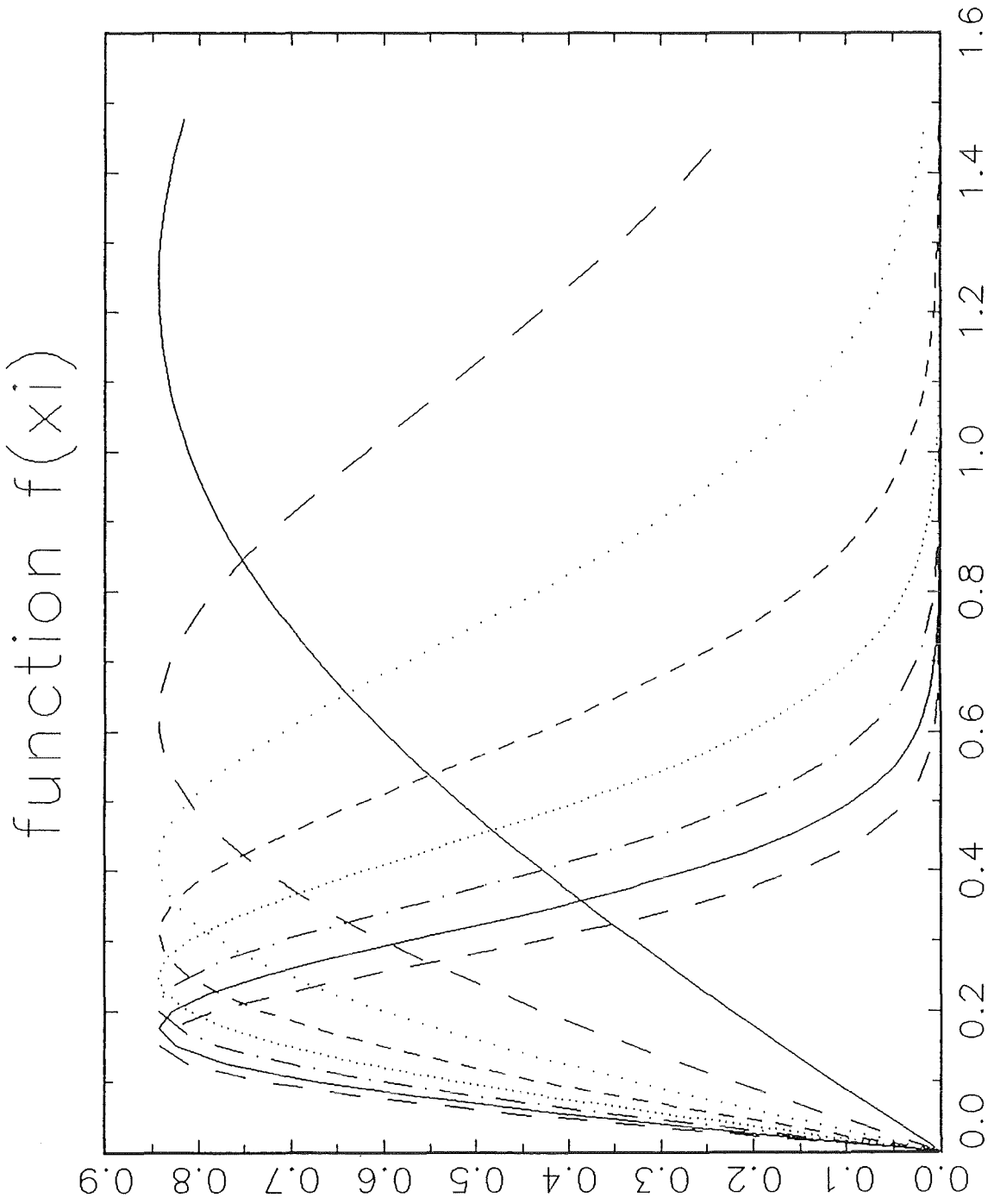
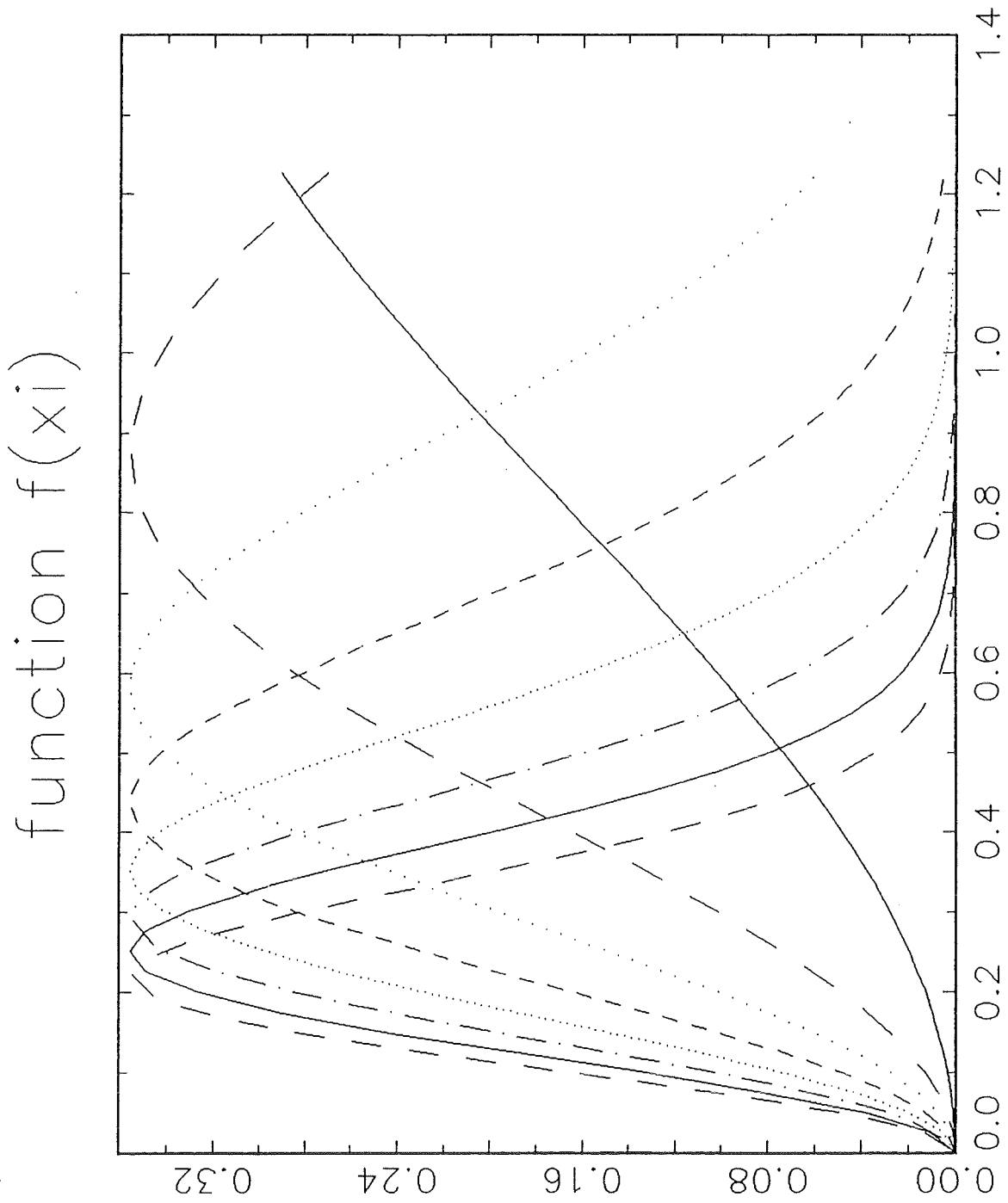


Fig. 8-9 For given $n < 1$:

 $f(\xi)$, reduced saturation
($n = 0.0$)



GAUSS Oct. 27, 1994 11:14:04 AM

Fig. 8-10 For given $n < 1$:

 $f(\xi)$, reduced saturation
($n = 0.5$)

EXPONENT	RESULTS
n = 2.0 m = n	Nc = 1.0
	EXTREME VALUE (A) for f(xi) (reduced saturation) max of f(xi) = 3.0895 (B) for Is(Se) (saturation flux) max of Is(Se) = 15.3427 max of Se = 3.0895 (same number as for (A))
n = 4.0 m = n	Nc = 1.0
	EXTREME VALUE (A) for f(xi) (reduced saturation) max of f(xi) = 2.6137 (B) for Is(Se) (saturation flux) max of Is(Se) = 60.1139 max of Se = 2.6137 (same number as for (A))

Table 8-1 Solution (8-3): Reduced saturation and saturation flux for different parameters n (See also Figs. 8-1 and 8-2)

EXPONENT	RESULTS
$n = 2.0$ $m = n$	$N_c = 2.0$
	<p>EXTREME VALUE</p> <p>(A) for $f(x_i)$ (reduced saturation) max of $f(x_i) = 4.4033$</p> <p>(B) for $I_s(Se)$ (saturation flux) max of $I_s(Se) = 50.7146$ max of $Se = 4.4033$ (same number as for (A))</p>
$n = 4.0$ $m = n$	$N_c = 2.0$
	<p>EXTREME VALUE</p> <p>(A) for $f(x_i)$ (reduced saturation) max of $f(x_i) = 2.6202$</p> <p>(B) for $I_s(Se)$ (saturation flux) max of $I_s(Se) = 69.9632$ max of $Se = 2.6202$ (same number as for (A))</p>

Table 8-2 Solution (8-3): Reduced saturation and saturation flux for different parameters n (See also Figs. 8-3 and 8-4)

EXPONENT	RESULTS
$n = 6.0$ $m = n$	$Nc = 2.0$
	<p>EXTREME VALUE</p> <p>(A) for $f(x_i)$ (reduced saturation) max of $f(x_i) = 2.6072$</p> <p>(B) for $Is(Se)$ (saturation flux) max of $Is(Se) = 425.9975$</p> <p>max of $Se = 2.6072$ (same number as for (A))</p>
$n = 8.0$ $m = n$	$Nc = 2.0$
	<p>EXTREME VALUE</p> <p>(A) for $f(x_i)$ (reduced saturation) max of $f(x_i) = 2.6072$</p> <p>(B) for $Is(Se)$ (saturation flux) max of $Is(Se) = 2749.1319$</p> <p>max of $Se = 2.6072$ (same number as for (A))</p>

Table 8-3 Solution (8-3): Reduced saturation and
saturation flux for different parameters n
(See also Figs. 8-5 and 8-6)

EXPONENT	RESULTS	
n = - 4.0 m = n < 1	Nc	Max. for f(xi;Nc)
	1.0	1.1353
	2.0	1.1353
	3.0	1.1348
	4.0	1.1336
	5.0	1.1335
	6.0	1.1335
	7.0	1.1350
	8.0	1.1333
	first, last xm value 0.5750 0.1000	
n = -1.0 m = n < 1		
	1.0	1.0922
	2.0	1.0917
	3.0	1.0917
	4.0	1.0917
	5.0	1.0922
	6.0	1.0916
	7.0	1.0921
	8.0	1.0888
	first, last xm value 0.9000 0.1250	

Table 8-4 Solutions from (8-5) (exponents n < 1)

 Similarity solution (red.saturation for
 different n, Nc (see Fig. 8-7 and 8-8).

CONCLUSION

 The main topic of the research presented here, was a better understanding of the behavior of a system of two immiscible phases in a porous medium. A model, based on Darcy's law as used for two phases and on the corresponding continuity equation, leading to a transport equation (PDE) has been used for this study. Applying a similarity transformation reducing the nonlinear PDE to an ODE was the main step in our analytic approach. It is important to recall some of our results which are closely related to mechanisms of displacement and flow (see Table 1 of this conclusion). It can be seen, that the following conditions are of importance to these mechanisms:

- (a) Different regions of the saturation, a quantity defining the percentage of one phase in relation to another phase.
- (b) Ratio of viscosities of two phases.
- (c) N_c , the capillary number, characterizing the ratio of capillary forces and viscous forces.
- (d) Different types of power laws, describing mechanisms which are typical for different types of percolation.

Now these influences are shown in Table 1:

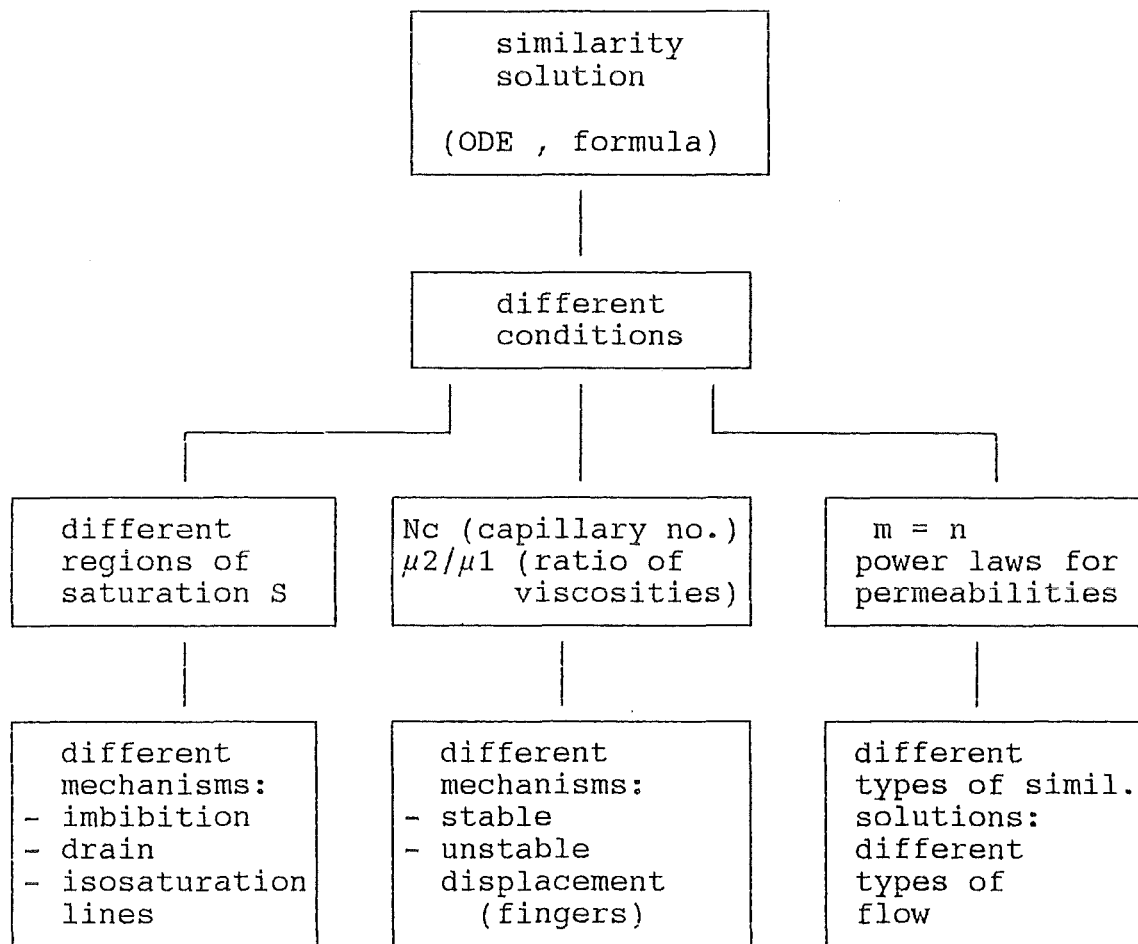


Table Different conditions for similarity solution

As can be seen, these conditions are relevant for different levels (such as large scale/small scale behavior). It also should be noted, that these influences are not always independent. But it seems to be out of the scope of this research, to study this type of dependencies in more detail. We also note, that a more general approach such as

- a discussion of more combinations of the parameters m , n relating different power laws to permeabilities,
- a generalization to a movement which is no longer horizontal,
- or the use of a 2- or 3-dimensional model

will be of considerable interest. Clearly, as a first step, the approach taken here is unavoidable.

A1 Similarity Methods for Partial Differential Equations

A1.1 Introduction

It is possible to obtain for partial differential equations (PDE), by some methods a solution, or simplification:

- It is possible, to apply Fourier- or Laplace- transforms
- it is possible to simplify PDE by Bäcklund-transforms [Rogers].
- it is useful, to apply a transform of a PDE into a ODE, while still holding certain invariant properties, as is done with the "similarity solutions" (see [Bluman], [Dresner], [Barenblatt]).

Using similarity methods it is either possible

- to find for ODE an integrating factor,
- to reduce a PDE of 2nd order (or of higher order) by one variable. This is our problem here.

A1.2 Similarity method

We assume a partial differential equation (PDE), e.g. with two independent variables x, t, and one dependent variable, u.

$$u_t = (x^m * u^n * u)_{xx} \tag{A1-1}$$

For a given PDE. Now transformations for (A1-1) are applied, where a group of transformations with group invariants is obtained which reduces PDE (A1-1) to an ODE. This type of a solution is also called "similarity solution", because here the following property exists: The profiles of u (dependent variable) versus z (independent variable) at various values of t (independent variable) are geometrically similar, and can be obtained by suitably stretching the abszissa and the ordinate. This similarity allows, to answer some physical questions already on the level of the similarity solution, as is shown in detail in sects. 4, 5, 6.

Boundary conditions

Boundary conditions must also be invariant to the group introduced for similarity solutions, which is discussed in more detail in sect. 4.

A1.3 Steps for similarity solution

We consider now a linear diffusion equation to make the steps for similarity solution evident.

$$u_t - u_{zz} = 0 \tag{A1-2}$$

It can be shown that (A1-2) is invariant under the following group of transformations:

$$\begin{aligned} u^* &= \lambda^* u \\ t^* &= \lambda^{*2} t \\ z^* &= \lambda^* z \end{aligned} \tag{A1-3}$$

where $0 < \lambda < \infty$,
 and α is any real number.
 Now, any solution for (A1-2), $u = f(z,t)$, is also a solution of the PDE which has been transformed by (A1-3). If this solution is the same, then the solution is called invariant with regard to (A1-3). To obtain this, for the parameters in (A1-3) the following requirements are necessary:

$$\lambda^{*2} f(z,t) = f(\lambda^* z, \lambda^{*2} t) \tag{A1-4}$$

Note;
 Equ.(A1-4) is equivalent to saying that in a point (z,t,u) for an integral surface S , i.e. where $u = f(z,t)$ holds, there also exists an image (z',t',u') , which also lies on the integral surface S , i.e. where $u' = f(z',t')$ holds. Then from (A1-3) we have

$$\lambda^{*\alpha} u = f(\lambda^* z, \lambda^{*2} t).$$

Now replacing z by $f(z,t)$ we obtain (A1-4). Differentiating (A1-4) with respect to λ , and also setting $\lambda = 1$, we obtain the auxiliary equation:

$$z^* f_z + 2^* t^* f_t = \alpha^* f \tag{A1-5}$$

Here the following characteristic equations associated to (A1-5) can be obtained (see e.g. [Bluman]):

$$\frac{dz}{z} = \frac{dt}{2^* t} = \frac{df}{\alpha^* f} \tag{A1-6}$$

From (A1-6) two independent integrals are obtained,

$$I_1 = z^* t^{-1/2} \tag{A1-7a}$$

$$I_2 = f^* t^{-1/2} \tag{A1-7b}$$

From this, the most general form, f can take under the invariance conditions is (based on (A1-7a,b), if

$$\zeta = z^*t^{-1/2}$$

$$f = t^{\alpha/2} * y(\zeta) \tag{A1-8}$$

Since this function is invariant, from (A1-8) we obtain, especially using the function y from (A1-8) the following substitutions

$$u_t = f_t = t^{(\alpha/2)-1} * \left(-\frac{\alpha}{2} * y - \frac{1}{2} * z^*t^{-1/2} * \frac{dy}{dx} \right) \tag{A1-9a}$$

$$u_z = t^{(\alpha/2-1)/2} * \frac{dy}{dx} \tag{A1-9b}$$

$$u_{zz} = t^{(\alpha/2)-1} * \frac{d^2y}{dx^2} \tag{A1-9c}$$

and with the assumption that $x = z^*t^{-1/2} = \zeta$, we can rewrite the differential equation (A1-2):

$$\frac{d^2y}{dx^2} = (\alpha/2) * y - (1/2) * y * \frac{dy}{dx} \tag{A1-10}$$

This is the basic way to obtain the similarity solution. Note: This method is to a large extent also typical for many cases of nonlinear PDEs. It also is useful for the diffusion equation (with nonlinearity) as shown in A2.

A2 From continuity equation to similarity solution

A2.1 Introduction

Based on some results of A1 (Methods for nonlinear partial differential equations) we discuss here in more detail the steps from a generalized interpretation of fractional flow (A2.2) over a continuity equation (A2.3) to an ordinary differential equation (A2.4), which is part of the similarity solution (4.5).

A2.2 A generalized interpretation of fractional flow

We recall, the concept of fractional flow which is used for 2-phase flow (sect. 4.3):

$$\text{fractional flow of fuel} = \frac{\text{flow of fuel}}{\text{total flow}} \quad (\text{A2-1})$$

We write (using the generalized Darcy-law (4-10), (4-11)):

$$F(S_f) = \frac{K_{rf}/\mu_f}{K_{rf}/\mu_f + K_{rw}/\mu_w} \quad (\text{A2-2})$$

Here S_f is the saturation of fuel. This formula is without capillary pressure. But in the presence of capillary pressure, P_c we obtain

$$P_c = P_f + P_w \quad (\text{A2-3})$$

where

P_f pressure of fuel
 P_w pressure of water.

For pressures P_f , P_w , we can write (analogous to the Darcy formulas) for the velocities U_w , U_f of the water phase, and fuel phase:

$$U_w = - \frac{k \cdot K_{rw}}{\mu_w} * \frac{\partial P_w}{\partial x} \quad (\text{A2-4a})$$

$$U_f = - \frac{k \cdot K_{rf}}{\mu_f} * \frac{\partial P_f}{\partial x} \quad (\text{A2-4b})$$

It can be shown, that a type of fractional flow $G(S_f)$ is also obtained dependent on capillary pressures alone:

$$G(Sf) = \frac{k \cdot Kr_f \cdot K_{ro}}{\phi \cdot (K_{rw} \cdot \mu_f + K_{rf} \cdot \mu_w)} * \frac{\partial Pc}{\partial Sf} \quad (A2-5)$$

With (A2-1)-(A2-5) we define the fractional flow F_m , which applies for viscous and capillary forces :

$$F_m(Sf) = F(Sf) + (A \cdot \phi / Q) \cdot G(Sf) * \frac{\partial Sf}{\partial x} \quad (A2-6)$$

Now $F_m(Sf)$ can be expressed using the following concepts:

- dimensionless variables, such as introduced for x, t (4-23),
- definition of $F(Sf), G(Sf)$ by polynomial expressions (4-18), (4-20).

This way we obtain the following quantity, also called in the following "Saturation Flux I_s ":

$$I_s = q_e(t) \cdot S^n + (1/N_c) \cdot S^{n-m} * \frac{\partial S}{\partial \hat{x}} \quad (A2-7)$$

Note that the saturation flux I_s is a fractional flow (based on viscous and capillary forces, taking into account dimensionless variables, and explicit use of polynomial expressions (A4).

A2.3 Transformation of the continuity equation

We recall the continuity equation (4-24):

$$\frac{\partial S}{\partial \hat{t}} + \frac{\partial I_s}{\partial \hat{x}} = 0 \quad (A2-8)$$

where I_s has been defined as a polynomial (4-25) and (A2-7). Using a new variable, ξ , (A2-8) may be rewritten:

$$\frac{\partial S}{\partial \xi} * \frac{\partial \xi}{\partial \hat{t}} + \frac{\partial I_s}{\partial \xi} * \frac{\partial \xi}{\partial \hat{x}} = 0 \quad (A2-9)$$

From A1 we see how the similarity variable ξ and similarity solution $f(\xi)$ can be related to x and t :

$$\xi = \hat{x} \cdot \hat{t}^{-1/2} \quad (A2-10a)$$

$$S = f(\xi) \cdot \hat{t}^{-1/2} \quad (A2-10b)$$

Noting, in addition to (A2-10a,b) also the definition of saturation flux I_s :

$$I_s = g(\xi) \cdot t^{\hat{-1}} \quad (A2-11)$$

where $f(\xi)$ and $g(\xi)$ are functions of ξ , to be determined in the following differential equation:

$$(g(\xi) - b \cdot \xi \cdot f(\xi))' = 0 \quad (A2-12)$$

Here ' denotes differentiation with regard to variable ξ . On the basis of (A2-7), the polynomial representation of F_s and G (see (4-18), (4-20)) we rewrite (A2-12):

$$g(\xi) = f^n - \frac{1}{Nc} \cdot f' \quad (A2-13)$$

This leads us to the following differential equation for f :

$$f' = Nc \cdot (f^n - (1/2) \cdot f \cdot \xi) \quad (A2-14)$$

From continuity equation (A2-8) we obtained a differential equation for f which clearly is equivalent to the similarity solution (4-32), (4-37) and (4-41).

A3 Transitions between different mechanisms

A3.1 Basic considerations for transitions

For different mechanisms it was important to define the respective models and parameters. In relation to a phase diagram (sect.3.3) different mechanisms have been located:

- DLA (diffusion limited aggregation)
- IP (invasion percolation)
- anti-DLA (stable displacement).

It may be also interesting to see how these transitions can be characterized quantitatively. Let us first introduce some concepts from percolation. It is known (e.g. from [Wilkinson], [Pietronero], [Weber]) that invasion percolation is at least to some extent related to classical percolation. We first introduce notations used for our phase diagram (sect. 3.3). Then we recall a few concepts from percolation theory and then make some considerations regarding the transitions between mechanisms.

A3.2 A classification of transitions

As is shown in Fig. A3-1, there are the following boundaries:

Boundaries for invasion percolation domain

- (a1) injecting the more viscous fluid ($\mu_2 > \mu_1$),
boundary characterized by Ca^*
- (a2) injecting the less viscous fluid ($\mu_2 < \mu_1$),
boundary characterized by Ca^*

Boundaries for DLA domain

- (b1) viscous limit, boundary characterized by M^*
- (b2) capillary limit, boundary characterized by Ca^*

Boundaries for anti-DLA domain

- (c1) capillary limit, boundary characterized by Ca^*
- (c2) viscous limit, boundary characterized by M^*

All these transitions are shown in Fig. A3-1. But quantitative descriptions of the transitions will be given in sects. A3.3 to A3-5.

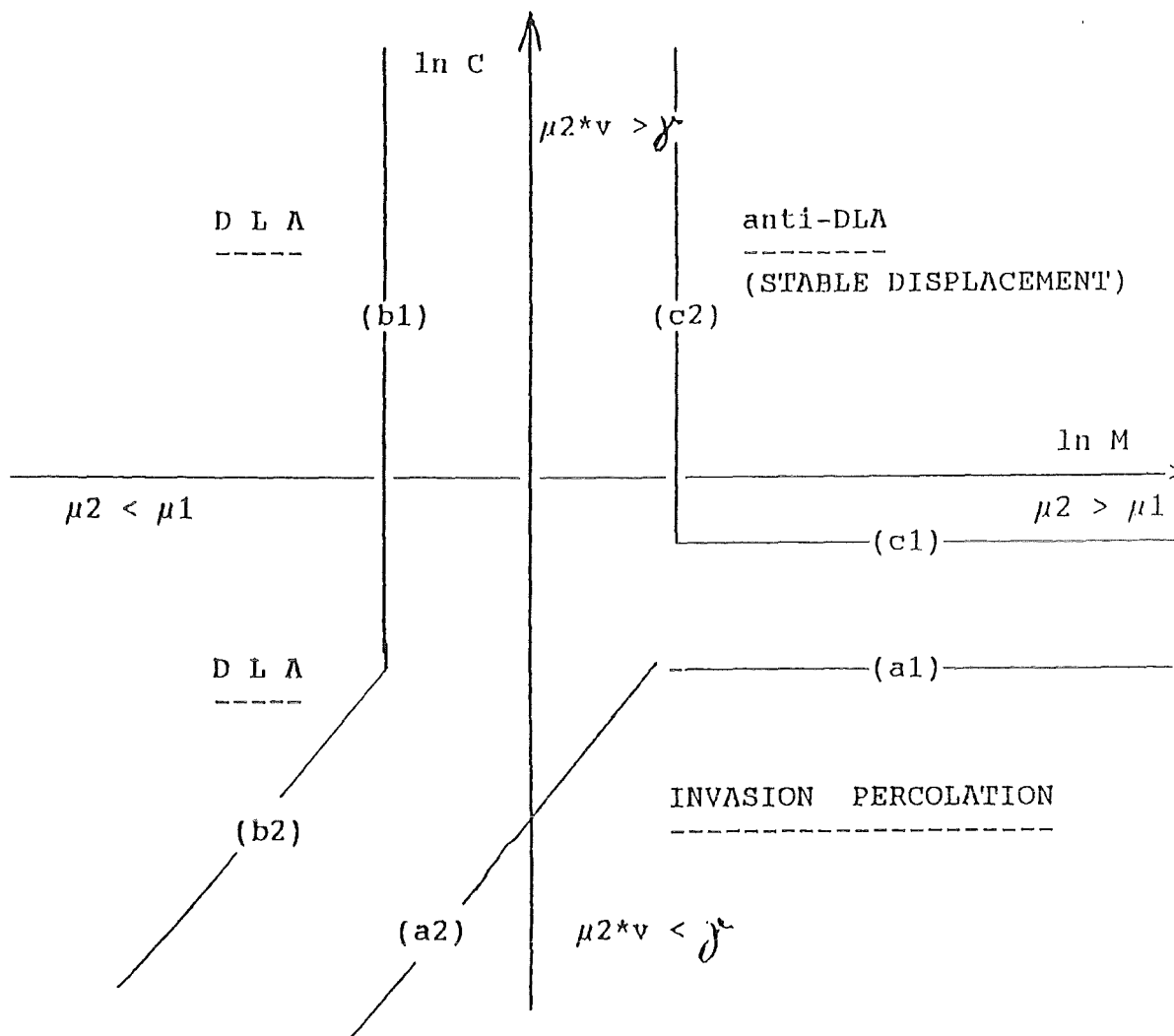


Fig.A3-1 Phase-Diagram, showing 3 different mechanisms

For Fig. 3-1 the following notations are used:

C capillary number

$$M = \frac{\mu_2}{\mu_1}$$

where

- 2 injected fluid
- 1 displaced fluid

A3.3 Critical exponents for percolation

We note that the following considerations are related to some concepts and properties of invasion percolation as well as conventional percolation [Wilkinson], [Lenormand]. The occupation probability p (of sites or bonds) in percolation theory has a role comparable to temperature in thermal critical phenomena. For percolation there exists a critical concentration p_c such that

- (a) for $p < p_c$ only finite clusters exist, with "size" (i.e. number of sites), whereas
- (b) for $p > p_c$ an infinite cluster exists, but also finite clusters.

Here we define $n_s(p)$ as the average number of finite sites with size s . We note, that usually $n_s(p)$ is related to random physical quantities. Here we have a scaling theory (see e.g. [Nakayama]) which states that there exist parameters, characteristic for this system, which diverge at $p = p_c$. This means that we can make for $n_s(p)$ the following Ansatz, with a parameter $\tau(p)$:

$$n_s(p) = s^{-\tau} F(s/s(p)) \quad (A3-1)$$

We note that $F(x)$ is an unknown function. But we will come to certain regions where this function is greatly simplified, if $s(p)$ is close to p_c . Here we can write as is well known the following relation:

$$s(p) \sim |p - p_c|^{-1/\tau} \quad (A3-2)$$

This is usually called a power law. We will have, for $p \rightarrow p_c$, the limit $s \rightarrow \infty$ (s is diverging). Close to this critical point, we can write:

$$n_s(p) = s^{-\tau} F((p - p_c) * s^\eta) \quad (A3-3)$$

where $s(p)$ is replaced by s^η . This is also called a scaling form, where quantities like this can be obtained for various physical quantities in regions close to the critical value, p_c . This will be applied to several quantities of interest, such as the correlation length.

A3.4 Introduction of correlation length

We now illustrate the concept of correlation length ξ as used for a percolation network (Fig. A3-2a, b). Here two types of a network are shown:

- (a) Case of $p < p_c$

Here only finite clusters exist. In Fig. A3-2a the following things are shown:

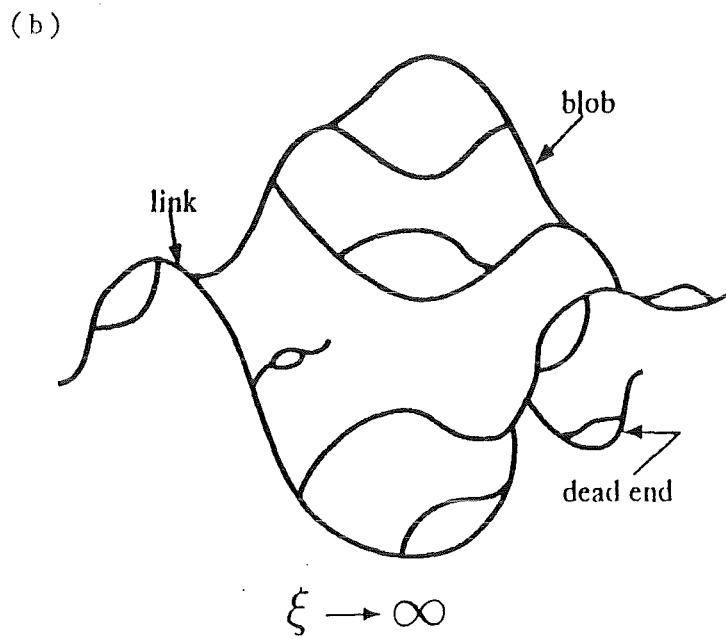
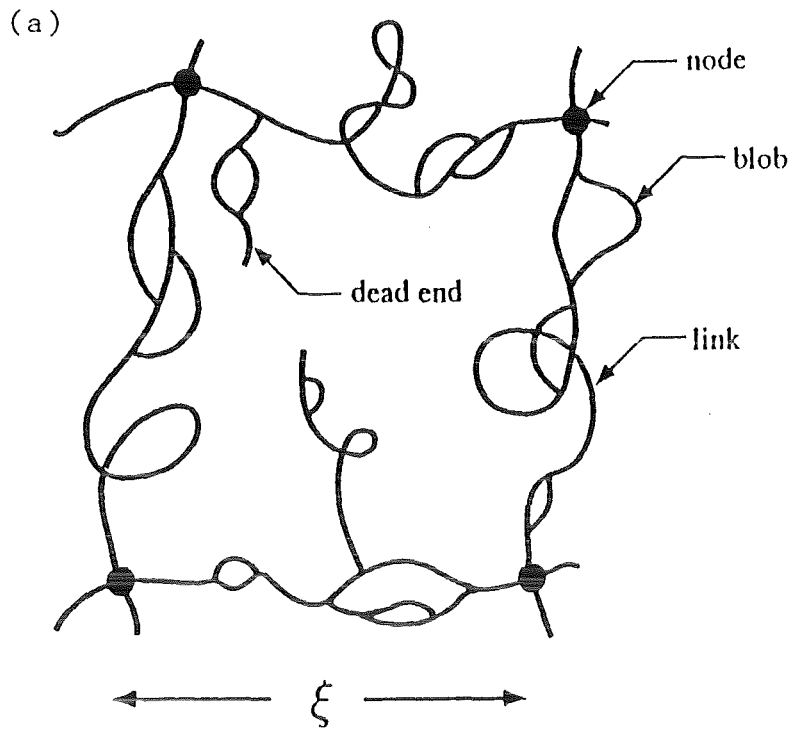


Fig. A3-2 (a) Network with nodes (ξ finite)
(b) Network with links ($\xi \rightarrow \infty$)

- nodes (shown as heavy circles),
- links (if a link is cut, no flow between two nodes is possible),
- blobs (a blob contains several parallel paths for flow),
- dead ends (dead ends can be cut without any consequence for flow).

Note that the distance between two nodes is of the order of ξ (the basic elements of correlation length). but the type of evaluation is discussed in A3.5.

(b) Case of $p > p_c$

Here an infinite cluster (leading from input to output) is available ($\xi \rightarrow \infty$). Then correlation length diverges.

A3.5 Calculation of correlation length

The diameter of finite clusters below p_c is characterized by (p) and called correlation length. (p) is defined as the root mean square distance between two sites i and j (nodes) in the same cluster, averaged over all finite clusters. Thus we can at first for a given cluster of size s write the average distance between two sites i and j :

$$R_s^2 = \frac{1}{2*s} \sum_{i,j} |r_i - r_j|^2 \quad (A3-4)$$

Now the number of ways connecting two sites in a given cluster of size s is s^2 , thus $s^2 * n_s$ becomes the number of ways connecting two sites in clusters of the same size s . Thus the correlation length (p) is R_s , averaged by the probability

$$\frac{s^2 n_s}{s^2 n_s}$$

This means

$$\xi^2(p) = \frac{\sum R_s^2 * s^2 * n_s}{\sum s^2 * n_s} \quad (A3-5)$$

Now we can assume that the same scaling function is possible as already mentioned in (A3-3), and obtain

$$R_s = s^w H((p - p_c) * s^\eta) \quad (A3-6)$$

and we can write

$$\xi(p) = X_0 * |p - p_c|^{-\nu} \quad (A3-7)$$

where X_0 is a constant factor which can be evaluated only in some cases, mostly approximately. We have $\gamma = \omega / \eta$. We note here, that the correlation length represents

- the characteristic size of the clusters (for $p < p_c$) and
- the characteristic size of the voids (for $p > p_c$).

A3.6 A line which includes the cluster, the hull

Next an exponent is introduced which will be very useful for some of the following considerations for the transition between some mechanisms. Assume a finite cluster of percolation as shown in Fig. A3-3a. In Fig. A3-3b the cluster is shown with a "hull" (heavy curve). As can be seen, the following empty sites are connected by a line which follow these conditions:

- (a) they are adjacent to cluster sites and
- (b) can be connected to infinity via a chain of empty sites, using next neighbors and nearest to next neighbors only.

This type of line encloses the cluster (see Fig. A3-3b). There exists a measure for the "length" of this hull, L_h :

$$L_h \sim a^{d_h} \tag{A3-8}$$

where a is the average size of the cluster, and d_h the hull exponent (see [Isichenko]).

It could be shown, that for d_h the following holds:

$$d_h = \frac{\gamma + 1}{\gamma} = 7/4 \tag{A3-9}$$

if $\gamma = 4/3$ and $d = 2$ (2-dimensional model of percolation). This could be estimated using simulation (see [Sapoval] and could be demonstrated using rigorous results of statistical mechanics [Saleur]. We also note, that the percolation hull exponents could be used for different purposes, especially for modelling the fronts of diffusion limited aggregation (DLA) as has been shown by Meakin and Family (see [Meakin]).

It is important to note, that (A3-8), (A3-9) also hold for many finite systems (see [Isichenko]).

A3.7 Some considerations of porous media

We need a few concepts for an easy formulation of boundaries to certain mechanisms.

Saturation as a function of M and Ca

Assume we have the fraction of invading fluid (saturation S) at breakthrough as a function of M (shown in network simulations of the three processes (see [Lenormand])). This function is shown

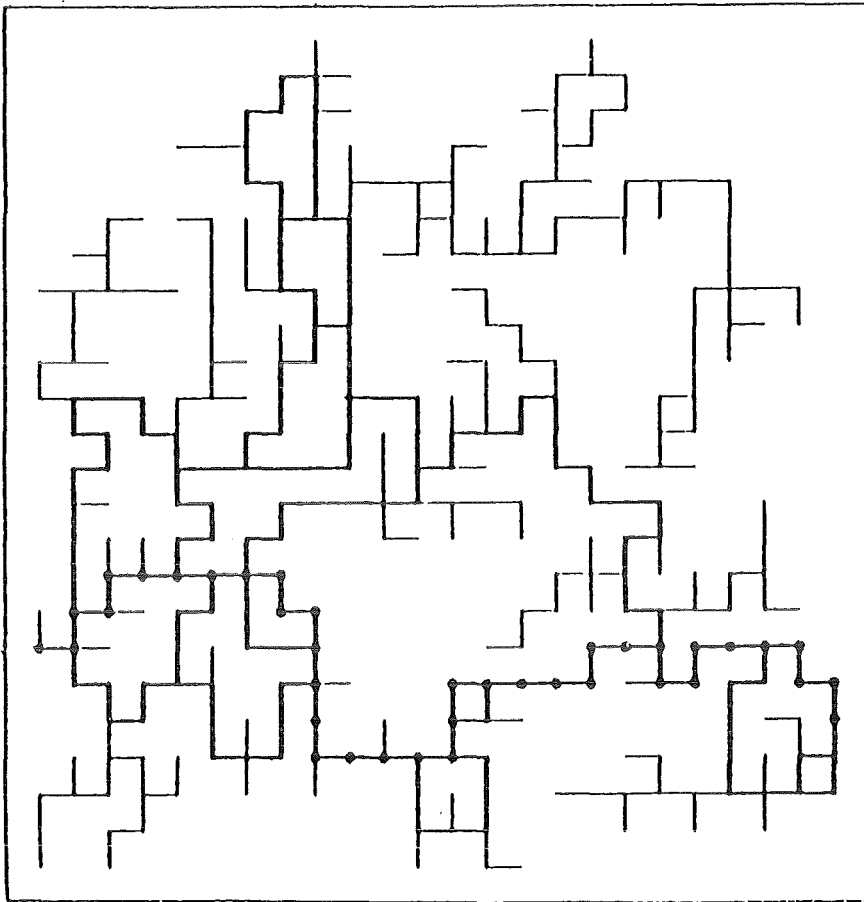


Fig. A3-3a Cluster

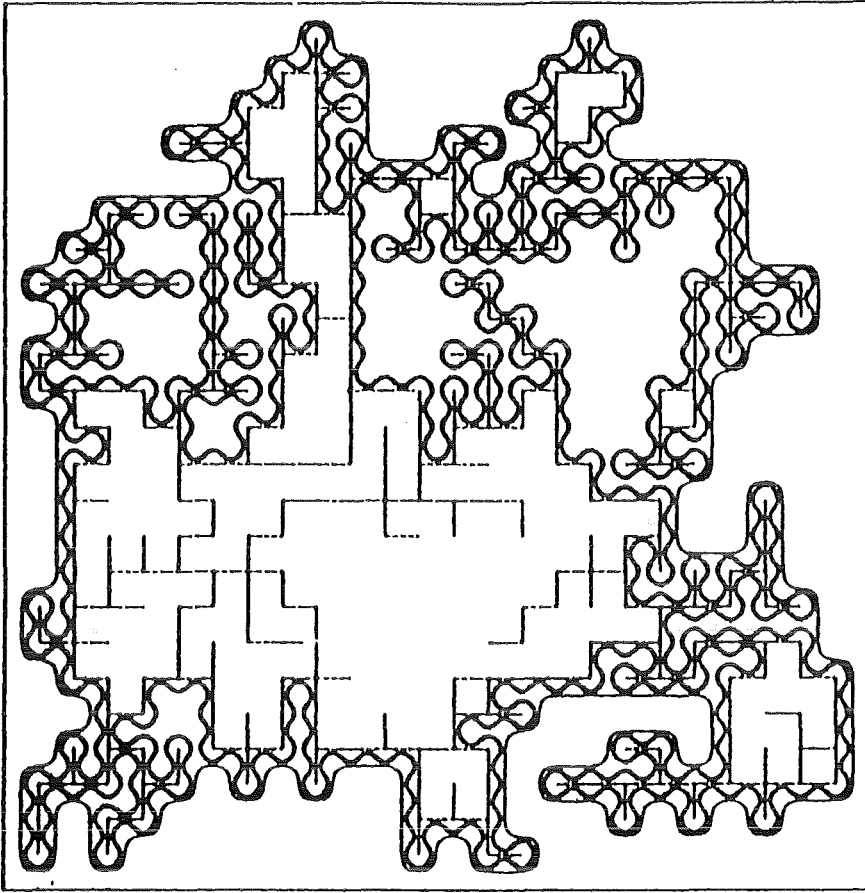


Fig A3-3b Same cluster, with "hull"

in Fig. A3-4. In this process S can reach a maximum (called also plateau). Already at a somewhat lower value of M, called M*, the limit of M will be reached, characterizing the change of mechanisms. The distance

$$| S(M^*) - S(\text{plateau}) | = \epsilon \quad (\text{A3-10})$$

will be called ϵ . This quantity can be estimated from Simulation [Lenormand].

A similar consideration also applies for S as function of Ca (where Ca* is the limit value of the capillary number Ca). This will not be derived in detail, but see [Lenormand].

Geometrical properties of a porous medium

The porous medium is a two dimensional network, interconnected with capillaries (Fig. A3-5). The capillaries have a radius R, which varies in the following interval:

$$[(1 - \delta) * R_0, (1 + \delta) * R_0] \quad (\text{A3-11})$$

We note that the size of the network is L x L, the mesh size is a.

Relation to Darcys law

For a flow where only one phase is present, we use the following version of Darcys law:

$$\frac{q}{\Sigma} = \frac{k}{\mu} * \frac{\Delta P}{x} \quad (\text{A3-12})$$

q	flow	
Σ	area for flow	
k	permeability	
μ	viscosity	
$\frac{\Delta P}{x}$	approximation for pressure gradient	(A3-13)

We also note that for two phases a more general form for Darcys law is required.

For resistance to flow we can write the mean conductance g_0 of a single channel, based on Poiseuilles law):

$$g_0 = (1/8) * \pi * \frac{R_0^4}{a * \mu} \quad (\text{A3-14})$$

and also, using $R_0 = a^2$, $x = a$ we can write again

$$k = (1/8) * \pi * \frac{R_0^2}{a} \quad (\text{A3-15})$$

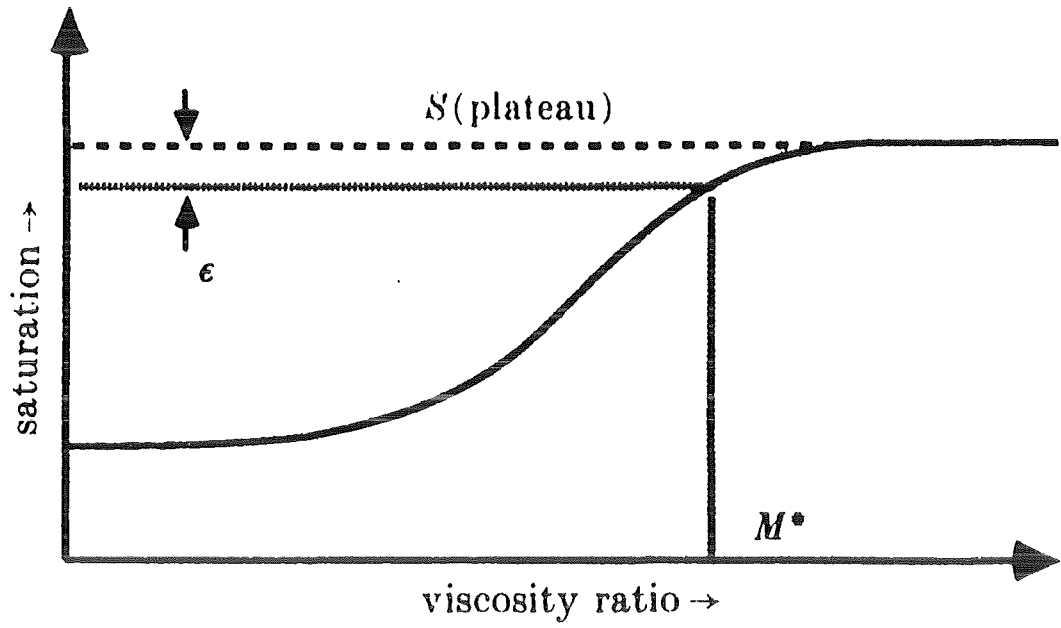


Fig A3-4 Function characterizing invading fluid (saturation), with variable M

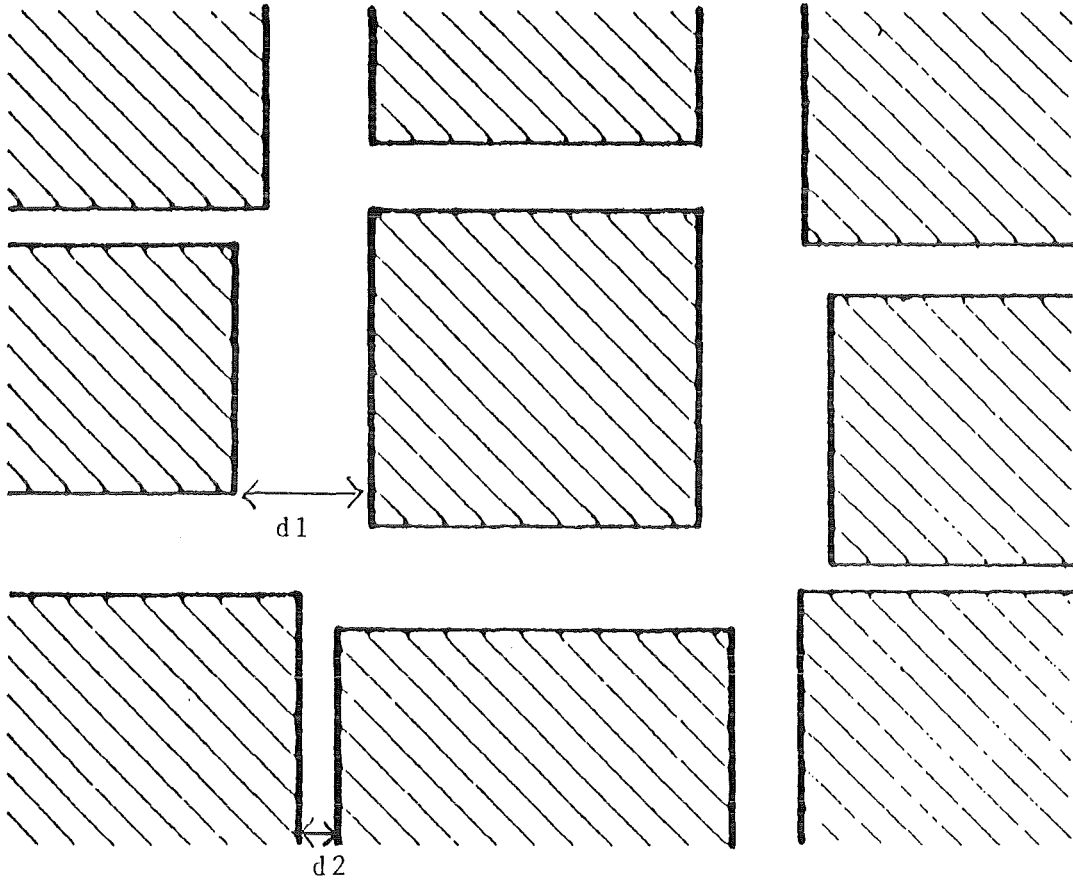


Fig. A3-5 Porous medium, with capillaries of variable diameters:

$$d1 = 2*(1 + \epsilon) * R_o \quad (\text{maximum})$$

$$d2 = 2*(1 - \epsilon) * R_o \quad (\text{minimum})$$

This can be used to formulate the limits for the mechanisms.

A3.8 Boundaries for mechanisms

With a few considerations, relating a number of considerations due to percolation theory and due to some formulas of A3.7 we can write the following formulas.

Boundaries for invasion percolation domain

(a1) Injecting the more viscous fluid

As can be seen, the this boundary is a horizontal line, which is given as follows:

$$Ca^* = A * \epsilon * \zeta (L/a)^\tau * (Ro/a)^3 \quad (A3-16)$$

where

A a constant (empirical factor due to simulations),

ϵ difference of $S(M^*)$ and $S(\text{plateau})$, (see (A3-10))
which is also due to simulations,

ζ is a variation parameter due to pore geometry,
see (A3-11),

a mesh size of percolation network

L size of percolation network

$$\tau = (t + 1 + \nu) / \nu$$

this exponent is related to the following exponents:
 ν exponent for correlation length (A3-7),
t exponent for conductivity.

Since $t = 1.3$ and $\nu = 4/3$ holds, we can approximately write

$$t \cong \nu = 4/3$$

and also

$$\tau = -2.75 = -11/4$$

Here also seems to be a certain relation to the "hull exponent" (A3-9). Of course, such a statement has to be taken with care. It seems to us, that for the exponent assumptions, similar to A3.6 apply (we have also a finite system with a network where $L \gg a$ applies. We have $L = 100$, $a = 1$.

(a2) injecting the less viscous fluid

As can be seen, this is anyway a monotonously increasing function of M , in a certain range, it is a linear function of M .

We can write for this limit:

$$Ca^* = B * \xi * \zeta * (L/a)^{ah} * (Ro/a)^* M \tag{A3-17}$$

Here most variables used remain the same as for (A3-16) unless explicitly stated:

B is an empirical numerical factor, obtained by simulation, but of a different value.

$ah = (\nu + 1)/\nu = 7/4$ is the exponent clearly used as hull exponent (see A3.6). This means, that (L/a) scales with the ah exponent (defining the hull). It has to be noted, that the exponent ah , used in (A2-17) applies for all networks where $L \gg a$, (see [Isichenko]), we have $L = 100$, $a = 1$.

Boundary for DLA domain

(b1) viscous limit M^*

$$M^* = \xi * (L/a) \tag{A3-18}$$

We note that in (b1) as well as in (b2), and in (c1), (c2) we have no critical exponent for this evaluation.

(b2) Capillary limit Ca^*

$$Ca^* = C * \xi * \zeta * (a/L)^3 * (Ro/a)^* M \tag{A3-19}$$

C is also a constant, but of a different value. Here we also have a linear function of M , as has been discussed for (a2). This is parallel to the transition show in (A3-17).

Boundaries of anti-DLA domain

(c1) capillary limit Ca^*

$$Ca^* = D * \xi * \epsilon^3 * (Ro/a) \quad (A3-20)$$

We have here $D = 80$, a constant due to simulation.
Here we also have a horizontal line.

(c2) viscous limit M^*

$$M^* = E * \xi \quad (A3-21)$$

We have here $E = 1000$, a constant due to simulation.
Here we have again a vertical line.

A3.9 Evaluation

We give a graphic representation, showing all the boundaries of these mechanisms (Fig. A3-5):

- invasion percolation (IP), (a1), (a2)
- diffusion limited aggregation (DLA), (b1), (b2)
- anti-DLA, (c1), (c2).

In Table A3-1 all parameters used in this model are listed. Now Fig. (A3-1) is quantified, giving Fig. A3-5. Here all the coefficients and parameters, mentioned in the model of A3 and shown in Table A3-1 have been used. For a generalization of this model, and some of its limits. see sect. A3.10.

A3.9 Generalization and some limits of the model

We assume, that only L (size of the network) is changed, all other parameters are kept fixed (Table A3-1). Then obtain for increasing (decreasing) values of L the following changes for the boundaries.

A few examples of these changes are given in Tables A3-1a,b:

A3-1a : increasing L

A3-1b : decreasing L .

We assume that always $L \gg a$ (network dimension \gg mesh size) holds.

We obtain (compare Fig. A3-1 and Fig. A3-5) the following changes for boundaries (in $(\log M, \log Ca)$ -plot):

IF L IS INCREASING (Table A3-2a),

(a1), (c1)

- both boundaries remain horizontal
- distance between boundaries increases
- c1 stays fixed, a1 moves downward

(b1), (c2)

- both boundaries remain vertical
- distance between boundaries increases
- c2 stays fixed, b1 moves to the left

(a2), (b2)

- both boundaries keep the direction (45° to ln M-axis)
- distance between boundaries increases
- a2 moves downwards, b2 moves downwards

We also note, that for DECREASING L (Table A3-2b), distances are decreasing, the movements indicated in the case of increasing L have to be reversed.

Limitations of this model

Having no results from other simulated grids, the model used here for $L > 100$ ($L < 100$) is only of a limited precision, but stays at least qualitatively the same.

In addition to the mechanisms which relate to capillary number Ca and to viscosity ratio M (as discussed here in detail), there are also some considerations referring to a parameter called "crossover length", which means this: Sometimes the types of mechanisms also strongly depend on the scale of observation, i.e. whether mechanisms are observed in a scale significantly larger than a certain length scale (crossover length) or below this length scale [Fernandez].

This way, mechanisms sometimes may depend (in addition to Ca and M) also on a third physical quantity. It is out of the scope of this report to include also these considerations in detail.

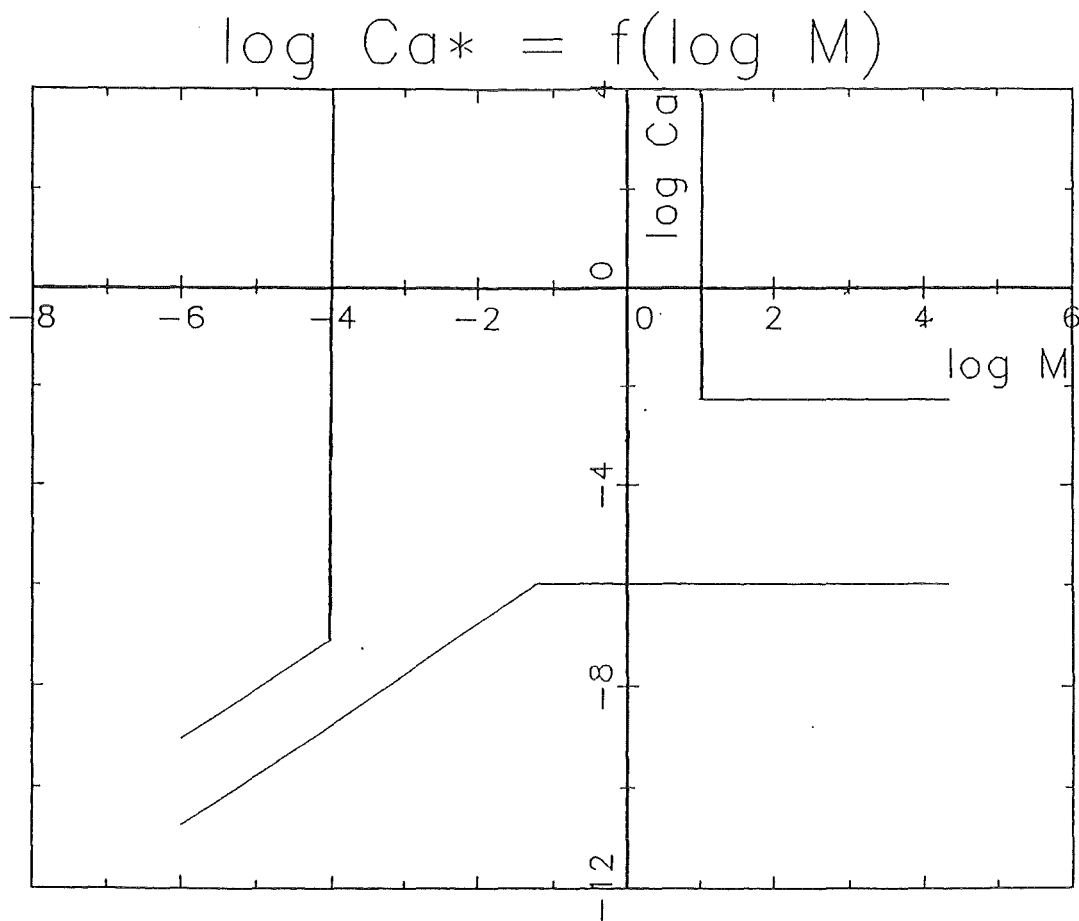


Fig. A3-6 Quantitative representation

 of the phase diagram introduced in Fig. A3-1
 using parameters given in Table A3-1

Parameters for the model	
(1) General parameters	(2) Exponents
$\epsilon = 0.01$	$ah = 7/4$
$\sigma = 0.56$	$\tau = 2.75$
$L = 100$	
$a = 1.0$	
$Ro = 0.23$	
(3) Special coefficients for boundaries	
$A = 5000$ (a1)	
$B = 800$ (a2)	
-- (b1)	(no special coefficient)
$C = 1300$ (b2)	
$D = 80$ (c1)	
$E = 1000$ (c2)	

TABLE A3-1 Listing of all coefficients for model

RESULTS

varying L and coordinates for boundary
 (1)log Ca*-values,(2) log M*-values,(3) typical log Ca*-values

(1)	L:	dist.(a1),(c1):	coo. (c1):	coo.(a1):
	100.00000	3.7041200	-2.2635385	-5.9676585
	200.00000	4.5319525	-2.2635385	-6.7954909
	300.00000	5.0162034	-2.2635385	-7.2797419
	400.00000	5.3597850	-2.2635385	-7.6233234
	500.00000	5.6262875	-2.2635385	-7.8898260
(2)	L:	dist.(b1),(c2):	coo. (c2):	coo.(b1):
	100.00000	5.0000000	1.0000000	-4.0000000
	200.00000	5.3010300	1.0000000	-4.3010300
	300.00000	5.4771213	1.0000000	-4.4771213
	400.00000	5.6020600	1.0000000	-4.6020600
	500.00000	5.6989700	1.0000000	-4.6989700
(3)	L:	dist.(a2),(b2):	coo. (b2):	coo.(a2):
	100.00000	1.7108534	-8.0526851	-9.7635385
	200.00000	2.2376559	-8.3537151	-10.290341
	300.00000	2.5458156	-8.5298064	-10.598501
	400.00000	2.7644584	-8.6547451	-10.817143
	500.00000	2.9340509	-8.7516551	-10.986736

RESULTS

varying L and coordinates for boundary
 (1)log Ca*-values,(2) log M*-values,(3) typical log Ca*-values

(1)	L:	dist.(a1),(c1):	coo. (c1):	coo.(a1):
	100.00000	3.7041200	-2.2635385	-5.9676585
	90.000000	3.5782869	-2.2635385	-5.8418254
	80.000000	3.4376174	-2.2635385	-5.7011559
	70.000000	3.2781396	-2.2635385	-5.5416781
	60.000000	3.0940359	-2.2635385	-5.3575744
(2)	L:	dist.(b1),(c2):	coo. (c2):	coo.(b1):
	100.00000	5.0000000	1.0000000	-4.0000000
	90.000000	4.9542425	1.0000000	-3.9542425
	80.000000	4.9030900	1.0000000	-3.9030900
	70.000000	4.8450980	1.0000000	-3.8450980
	60.000000	4.7781513	1.0000000	-3.7781513
(3)	L:	dist.(a2),(b2):	coo. (b2):	coo.(a2):
	100.00000	1.7108534	-8.0526851	-9.7635385
	90.000000	1.6307778	-8.3537151	-9.6834629
	80.000000	1.5412608	-8.5298064	-9.5939460
	70.000000	1.4397749	-8.6547451	-9.4924600
	60.000000	1.3226181	-8.7516551	-9.3753032

Table A3-2 Dependence of diferent characteristics

 (capillary number, ratio of viscosities)
 on the total length of the 2D-network

A4 Relations of permeability and saturation

A4.1 Introduction

Now in relation to section 4 (Evaluation of phase flow in a porous medium, 4.1 - 4.3) relations of permeability to saturation will be discussed. For this reason, first we recall some of the concepts used in A3 and introduce some more concepts.

A4.2 A few concepts from percolation

In a percolation network, some of the relevant quantities are percolation probability p and critical probability pc (also called critical concentration) as well as correlation length (see A3.4).

Also other quantities are needed for our considerations:

(1) Accessible fraction XA.

That is the fraction of occupied bonds, belonging to an (infinite) cluster.

(2) Backbone fraction XB.

That is the fraction of occupied bonds, belonging to an (infinite) cluster, which actually carry flow (or current), excluding the dead ends, which do not effectively contribute to flow.

It is to be noted, that the fractions (1), (2) are very relevant for various transport properties, giving measures for all transport paths. Here it will be interesting to ask if there exist some relations between permeability K and the quantities (1) and (2).

It has been shown (by theoretical considerations, simulations and by experiments) that quantities like ξ , XA, XB follow polynomial laws (see [Sahimi2], [Nakayama]). For illustration, see Fig. A3-1. It has been noted in section A3.4, that for the correlation length, a polynomial law exists.

$$\xi(p) \sim |p - pc|^{-\nu} \tag{A3-7}$$

We also state, that XA, XB follow polynomial laws.

$$X_A(p) \sim (p - pc)^{\beta_p} \tag{A4-1}$$

$$X_B(p) \sim (p - pc)^{\beta_B} \tag{A4-2}$$

Here we recall the concept of critical point (see also (A3-1)). At some well defined value of p, there must be a transition for the structure of the network, where the network obtains at least one connected cluster which spans the whole network. This transition probability is called "bond percolation threshold pc". Below pc there exists no sample spanning cluster. Now, β_p is a critical exponent related to the percolation probability P as follows:

$$P \sim (p - p_c)^{\beta_p} \quad (A4-3)$$

Similarly, β_B is related to the backbone fractal dimension. Thus we have for 2 dimensions:

$$\beta_p = 5/26 \quad (A4-4a)$$

$$\beta_B = 0.48 \quad (A4-4b)$$

A4.3 Mass and fractal dimension D_f

From (A3-6) we note, that

$$R_s \sim s^\omega \quad (A4-5)$$

holds, which is useful if we are sufficiently close to p_c , the critical point where percolation starts. This can be written, since s is the cluster size as

$$s \sim R_s^{1/\omega} \quad (A4-6a)$$

Using for $1/\omega$ the notation D_f , fractal dimension (or Hausdorff dimension) we can write also

$$s(R_s) \sim R_s^{D_f} \quad (A4-6b)$$

As is well known, for D_f the following relation holds

$$D_f = d - \beta/\nu \quad (A4-7)$$

D_f is usually smaller than the Euclidean dimension d . It can be seen that M , (number of all bonds of the sample spanning cluster) can be given as a power law of R_s (rel. to correlation length), where the exponent is D_f . The quantity D_f is important for percolation and also inversion percolation (see e.g. [Pietronero], [Weber]). It has to be noted that the so-called "mass" $M(R)$ of the cluster scales as

$$M(R) \sim R_s^{D_f} \quad (A4-8)$$

Also note, that p_c , the correlation length (sect. A3.4) is a threshold, up to which the cluster can be regarded as fractal. For $p > p_c$ and for length scales $L > \xi$ the percolation network can be regarded as homogeneous.

We thus can write as follows (for a quantity analogous to $M(R)$):

$$M(L) \sim \begin{cases} L^{\frac{Df}{L}} & \text{for } L \ll \xi \\ L^d & \text{for } L \gg \xi \end{cases} \quad (\text{A4-9})$$

where $d = 2$.

This change in polynomial behavior depending on the question, if L is small or large compared to a quantity, such as correlation length ξ , is called "cross over".

We also can relate to $M(L)$ - especially for two-phase fluid flow - quantities like saturation S . This will be discussed in detail.

A4.4 Saturation and polynomial laws

We consider a porous medium with volume $V_v = \phi > \phi_c$ (ϕ porosity, ϕ_c critical porosity, below ϕ_c the original fluid is separated in different parts. Assume that the entire pore space of this medium is at the beginning filled with a non-wetting (nw) fluid (see [Larson]). Now the nw-fluid is removed beginning with some pores and is now replaced by a second phase, the wetting fluid. We usually assume, that the wetting fluid (w-fluid) remains still randomly distributed, but anyway will prefer smaller pores due to capillary forces. (see 3.2 criteria for different mechanisms). Let V_{nw} be the volume of the nw-fluid, being distributed over the porous medium. For the nw-fluid, still randomly distributed, the fraction of accessible pores occupied by the nw-fluid, is called saturation S_{nw} . Until now, we have pores which are separated, i.e. do not belong to a backbone, (a cluster of pores which span the medium). Note that here for S_{nw} the equivalence to X_A , accessible fraction, is evident. We also have

$$V_{nw} = \phi * S_{nw} \quad (\text{A4-10})$$

If random replacement of the nw-fluid causes $V_{nw} = \phi * S_{nw}$ to drop below ϕ_c , then the nw-fluid is no longer continuous across the medium. Then the residual nw-saturation is called S_{rnw} , defined by

$$\phi S_{rnw} = \phi_c \quad (\text{A4-11})$$

Now since S_{nw} is closely related to X_A (A4-1) we can write for

- (a) drainage (a procedure, analogous to the procedure discussed above, where the non wetting fluid replaces the wetting fluid).
- (b) imbibition (exactly the procedure discussed above)

the following relations (similarly to (A4-1), (A4-2)):

(a) drainage

$$S_{nw} \sim (p - p_c)^{\beta p} \quad (A4-12)$$

(b) imbibition

$$S_{nw} - S_{rnw} \sim (p - p_c)^{1 + \beta p} \quad (A4-13)$$

A4.5 Relation to permeability

It is also known from experiments, simulation and theoretical considerations ([Larson], [Sahimi]) that for permeability K the following power law holds (similar to conductivity):

$$K \sim (p - p_0)^\mu \quad (A4-14)$$

We take into account, that for some quantities a cross over is taking place (as stated in relation to (A4-9)). This means, that we can use equations referring to (A4-4)-(A4-6) for a suitable scaling. Thus we obtain, for the relative permeability k_r the following equations (assuming $\xi \gg L$):

(a) during drainage

$$k_{rnw} \sim (S_{nw})^{\mu/\beta p} \quad (A4-15)$$

(b) during imbibition

$$k_{rnw} \sim (S_{nw} - S_{rnw})^{\mu/(1 + \beta p)} \quad (A4-16)$$

We see, that the two formulas are based on

- two variables, S_{nw} and $(S_{nw} - S_{rnw})$ and
- two exponents, $\mu/\beta p$ and $\mu/(1 + \beta p)$.

It can be seen that for (b) we have an increasing function, and for (a) a decreasing function. The respective angles of the two curves in relation to the abscissa are considerably different (as can be seen from (A4-15) and (A4-16)). This leads us to the statements of sects. 4.2 and 4.3.

A5. Remarks on Programs for analytic solution

A5.1 Introduction

In relation to the discussions in sections 4 to 8 a number of programs were required. Some of these programs are here shown in detail. They belong to the GAUSS-program system (see [GAUSS] for more details. We prefer two types for an illustration of the programs used in our research.

Similarity Solution

It is interesting to note, that for an analytic solution, i.e. for a similarity solution of the Riccati equation was used. We recall this differential equation, discussed in sect. 4.5:

$$f' = Nc * Nc (f^n - (1/2) * f * \xi) \quad (4-36)$$

For $n = 2$, we have a Riccati-equation. As solution we have

$$f(\xi) = \frac{\exp(-0.25 * Nc * \xi^2)}{(\pi * Nc)^{0.5} * (1/\tanh(0.5 * Nc * \xi) - \operatorname{erf}(0.5 * Nc * \xi))^{0.5}} \quad (4-41)$$

This is shown in sect A5.2.

Interpretation of a flux-curve

It may be noted, that an interesting criterions, do see if there are some mechanisms available (such as drain, imbibition, for different directions of the two liquids) (see Fig. 6-2) it is required, to evaluate the flux-curve as is given in sect. 6:

$$J = t^{-1/2} * S - (1/Nc) * \frac{\partial S}{\partial x} \quad (6-4)$$

This is shown in sect. A5.2.

It may be also noted, that it was possible, to use most programs in a version which was either suited to

- a quick representation or to
- a representation for publication quality.

A5.2 Similarity Solution and Flux Curve

With the equ. (4-41) and (6-4) a program for the GAUSS solution is given. For more information on this program see [GAUSS].

```
/*FLUXA-----*/  
/*Analytical solution for global fuel migration */  
/*FLUX of a phase, function of Saturation, Nc, t */  
/* Js(Se;Nc,t) */  
/*February 2, 1995 */  
/*-----*/
```

"fs(Se,Nc), as dimensionless function";

anf2:

```
/*qgraph-commands*/
```

```
library qgraph;  
graphset;  
setgmode(16);  
  _qmajor = 3;  
  _qminor = 3;
```

```
beggraph;
```

```
  r = 1;  
  c = 1;
```

```
setgmode(16);  
  _qnum = 1;  
  _qbox = 1;  
  _qdfmode = 0;
```

```
window(r,c);
```

```
"INPUT :";print;
```

```
"no. of curves m1 = ";m1 = con(1,1);  
"Nc = ";Nc = con(1,1);  
"times t = ";t = con(m1,1);  
"END of Input DATA";
```

```
/*"fixed parameters"*/
```

```
let inc = 0.05;  
let n1 = 80;
```

```
/*Evaluation*/
declare x ? = 0;
declare yma ? = 1;

ni = seqa(0,1,n1);
x = ni*inc + 0.001;

/*f(xi)-*/
n1 = exp(-0.25*x^2.*nc);
d11 = 1/tanh(0.5*nc) - erf(0.5*(nc^0.5)'*x);
d12 = (pi*nc)^0.5;
d1 = d12.*d11;

f = n1./d1; /*similarity solution f(xi)*/

/*diff(f(xi), x) = f'*/ /*see appendix A6.2*/
n2 = -0.5*(nc^0.5)*x.*exp(-0.25*nc*x^2);
d21 = 1/tanh(0.5*nc) - erf(0.5*(nc^0.5)*x);
d2 = pi^0.5*d21;

diffa = n2./d2;

n3 = (exp(-0.25*nc*x^2)).^2;
d31 = 1/tanh(0.5*nc) - erf(0.5*nc^0.5*x);
d3 = pi*d31^2;

diffb = n3./d3;

diff = (diffa + diffb);

g = f^2 - (1/Nc).*diff;
f2 = f^2;

Is = g./t'; /*flux Is(Se)*/
Se = f.*(t^(-1/2))'; /*saturation Se(xi)*/

Is1 = maxc(Is); Se1 = maxc(se);
xm1 = maxindc(is); f3 = (Se1)^2;
xm = xm1*inc;

wait;cls;
print;

anf1:

"xmin, xmax = ";;v1 = con(1,2 );
"ymin, ymax = ";;v2 = con(1,2);

scale(v1,v2);
```

```
/* |=====| */
/* | GRAPHIC OUTPUT | */;
/* |=====| */

    format 3,3;

    title("f(x)");
    xy(x,f);

    title("diffa and diffb");
    xy(x,diffa~diffb);

    title("diff");
    xy(x,diff);

    title("Is(Se)");
    xlabel("Se");
    ylabel("Is");
    xy(Se,Is);

wait;cls;

    OUTPUT FILE = typea ON;

    print;

    "EXTREMA OF Is-CURVE ";

    "Nc = ";;Nc;
    "-----";
    "time t      max(Se)      Is(Se) ";
    print t~sel~f3;
    "=====";
    OUTPUT OFF;

"use file typea, reseta";

"continue : ";;w2 = con(1,1);
    if w2 == 1;
        goto anf2;
    endif;

endgraph;

"reset <typea> with <run reseta>";

"END";
```

A6 Check of the behavior of the similarity solution

 We discuss here some of the applications of the symbolic computation with MAPLE (Version 3) for obtaining partial derivatives of $f(x_i, N_c)$. Note that most of the expressions shown here are automatically reproduced during a MAPLE-session.

A6.1 Analytical form of the similarity solution

 Here the formula $f(x, N_c)$ is written to obtain (using numerator $n1$ and denominator $d1$). Note that this can also be used for a 3D-representation.

$$> n1 := \exp(-0.25 \text{ nc } x^2);$$

$$\triangleright d11(x, nc) := 1/\tanh(0.5*nc) - \text{erf}(0.5*nc^{0.5}*x);$$

$$d11(x, nc) := \frac{1}{\tanh(.5 \text{ nc})} - \text{erf}(.5 \text{ nc}^{.5} x)$$

$$\triangleright d12(x, nc) := (\text{Pi}*nc)^{0.5};$$

$$d12(x, nc) := \text{Pi}^{.5} \text{ nc}^{.5}$$

$$\triangleright d1(x, nc) := d12(x, nc)*d11(x, nc);$$

$$d1(x, nc) := \text{Pi}^{.5} \text{ nc}^{.5} \left(\frac{1}{\tanh(.5 \text{ nc})} - \text{erf}(.5 \text{ nc}^{.5} x) \right)$$

The similarity solution $f(x, nc)$ is represented as follows (A6-1):

$$\triangleright f(x, nc) := n1(x, nc)/d1(x, nc);$$

$$f(x, nc) := \frac{\exp(-.25 \text{ nc } x^2)}{\text{Pi}^{.5} \text{ nc}^{.5} \left(\frac{1}{\tanh(.5 \text{ nc})} - \text{erf}(.5 \text{ nc}^{.5} x) \right)} \quad (\text{A6-1})$$

A6.2 Partial derivative with regard to x:

 We now make a partial derivative for f(x,Nc) with regard to x, showing the slope of f(x,Nc) with regard to x.

```
► f (x,nc) := diff(f(x,nc), x);
   x
```

$$f_x(x, nc) = - .50 \frac{nc^{.5} x \exp(-.25 nc x^2)}{\text{Pi} \left[\frac{1}{\tanh(.5 nc)} - \text{erf}(.5 nc^{.5} x) \right]} + \frac{\exp(-.25 nc x^2) \exp(-.25 nc x^2)}{\text{Pi} \left[\frac{1}{\tanh(.5 nc)} - \text{erf}(.5 nc^{.5} x) \right]^2} \quad (\text{A6-2})$$

A6.3 Partial derivative of f(x,nc) with regard to nc :

 We also make a partial derivative of f(x, Nc) with regard to Nc. It shows in more detail the behavior of the reduced saturation f(x,Nc) with regard to possible mechanisms.

```
► f (x,nc) := diff(f(x,nc), nc);
   nc
```

$$f_{nc}(x, nc) := - .25 \frac{x^2 \exp(-.25 nc x^2)}{\text{Pi} nc^{.5} t1} - .5 \frac{\exp(-.25 nc x^2)}{\text{Pi} nc^{1.5} t1} \quad (\text{A6-3})$$

(a)

(continued)

$$\begin{aligned}
 & \frac{\exp(-.25 \text{ nc } x^2) - \frac{.5 - .5 \tanh(.5 \text{ nc})^2}{\tanh(.5 \text{ nc})^2}}{\text{Pi nc}^{.5} t1} \\
 & + .5 \frac{\exp(-.25 \text{ nc } x^2)}{\text{Pi nc}^{.5} t1}
 \end{aligned}
 \tag{A6-3}$$

(b)

where t1 means

$$t1 := \frac{1}{\tanh(.5 \text{ nc})} - \text{erf}(.5 \text{ nc}^{.5} x)$$

This answers the questions of increasing and decreasing of the similarity solutions with regard to Nc.

REFERENCES

- [Abramowitz] Pocket Book of Mathematical Functions
Abridged edition of Handbook of Mathematical
Functions, M. Abramowitz, I.A.Stegun (Eds.)
Verlag Harri Deutsch, Thun-Frankfurt/Main, 1984
- [Barenblatt] G.I.Barenblatt
Similarity, Self-Similarity and Intermediate
Asymptotics
Consultant Bureau, New York and London, 1979
- [Bensimon] D.Bensimon, L.Kadanoff, S.Liang,
B.I.Shraiman, Ch.Teng
Viscous flow in two dimensions
Rev.Mod.Phys., Vol 58, pp.977-999, 1986
- [Bluman] G.W.Bluman, J.D.Cole
Similarity Methods for Differential Equations
(Applied Mathematical Sciences 13)
Springer Verlag, Berlin, 1974
- [Davis] H.T.Davis
Introduction to nonlinear differential and
integral equations
Dover Publications, Inc. New York, 1962
- [Dresner] L.Dresner
Similarity Solutions of Nonlinear Partial
Differential Equations
Pitman Advanced Publishing Program
Boston, London, Melbourne, 1983
- [Fernandez] J.F.Fernandez, R.Rangel, J.Rivero
Crossover Length from Invasion Percolation
to Diffusion Limited Aggregation in Porous
Media
Phys.Rev.Lett. 67, pp. 2958-2961, 1991
- [GAUSS] GAUSS
The GAUSS System Version 2.0
For IBM PC-XT-AT-PS2 & Compatibles
Aptech Systems Inc.
26250 196th Place S.E.
Kent, Washington 98042

- [Isichenko] M.B.Isichenko
Percolation, statistical topography, and transport
in random media
Rev.Mod.Phys. Vol.64, No.4, October 1992,
pp.961-1043
- [Kessler] D.E. Kessler
Pattern selection in fingered growth phenomena
Adv. in Phys. Vol. 37, 1988
- [Koza] Z.Koza
The Equivalence of the DLA and a Hydrodynamic
Model
J.Phys. A: Math. Gen., 24 (1991), pp. 4895-4905
- [Lamb] H.Lamb
Hydrodynamics
Cambridge University Press, Cambridge, 1932
- [Larson] R.G.Larson, H.T.Davis, L.e.Scriven
Displacement of residual nonwetting fluid
from porous media
Chem.Eng.Sci. Vol.36, pp.75-85, 1981
- [Lenormand] R.Lenormand
Flow through porous media: limits of fractal
patterns
Proc.R.Soc. London A 423, pp.159-168 (1989)
- [Meakin] P.Meakin, F.Family
Diverging length scales in diffusion-limited
aggregation
Phys.Rev. A 34, p.2558, 1986
- [Nakayama] T.Nakayama, K.Yakubo, R.L.Orbach
Dynamical properties of fractal networks: Scaling,
numerical simulations, and physical realizations
Rev.Mod.Phys. Vol.68, No.2, April 1994, pp. 381-443
- [Pietronero] L.Pietronero, W.R.Schneider
Viscous Percolation as a Fractal Growth Problem
Physica A, 170 (1990), pp.81-104

- [Pistiner1] A.Pistiner, M.Shapiro, H.R.Rubin
Analysis of Fuel Pollutant Migration in Water
Flow through Porous Media
Int.J.of Multiphase Flow, Vol.15, pp.135-154, 1989
- [Pistiner2] A.Pistiner, H.R.Rubin, M.Shapiro
Migration of an Immiscible Contaminant in a
Water Flow Through a Double Porosity Porous Medium
in [Rubin]
- [Pistiner3] A.Pistiner, M.Shapiro, H.R.Rubin
Self-Similar Analysis of Fuel Pollutant Migration
in Porous Media Including Gravity Segregation
in [Rubin]
- [Po-zen Wong] Po-zen Wong
The statistical physics of sedimentary rocks
Physics Today, December 1989
- [Rogers] C.Rogers, W.F.Shadwick
Bäcklund Transformations and their Applications
(Math.in Science and Engineering, Vol 161)
Academic Press, New York, 1982
- [Rubin] H.Rubin (Principal Investigator), E.Mechrez
Development of Methodologies for Restoring
Aquifers Contaminated by Oil Spills
Technion-Israel Institute of Technology
JOINT GERMAN ISRAELI RESEARCH PROJECTS
(Bundesministerium für Forschung und Technologie
(BMFT), Bonn,
Ministry of Science and Development, National
Council for Research and Development (NCRD))
Haifa and Kernforschungszentrum Karlsruhe
1987-1990
- [Sahimi1] M.Sahimi
Statistical and continuum models of fluid-solid
reactions in porous media
Chem.Eng.Sci. Vol.45, pp.1443-1502, 1990
- [Sahimi2] M.Sahimi
Flow phenomena in Rocks:
from continuum models to fractals, percolation,
cellular automata, and simulated annealing
Rev.Mod.Phys. Vol.65, pp.1395-1534, 1993

- [Sahimi3] M.Sahimi
Applications of Percolation Theory
Taylor & Francis, London 1994
- [Saleur] H.Saleur, B.Duplantier
Exact determination of the percolation hull
exponent in 2 dimension
Phys.Rev. Lett. 58, p. 2325
- [Sapoval] B.Sapoval, M.Rosso, J.F.Gouyet
The fractal nature of a diffusion front and
the relation to percolation
J.Phys.Lett., 46, L149
- [Sonin] A.A.Sonin
Viscous Fingers: from Simple Amorphous Forms
to Anisotropic Fractals
Riv. del Nuovo Cimento, Vol. 14, No. 10,
pp. 1-21, 1991
- [Weber] G.Weber
Unveröffentlichte Resultate
Kernforschungszentrum Karlsruhe, Juni 1992
- [Wilkinson] D.Wilkinson, J.F.Willemsen
Invasion Percolation: a new form of percolation
theory
J.Phys. A: Math.Gen., 16, pp. 3365-3376, 1983
- [Zhang] Yu Zhang
The Fractal Volume of the Two-Dimensional
Invasion Percolation Cluster
Commun. Mathematical Physics, Vol. 167,
pp. 237-258 (1995)